

# Engineering effective models with the cRPA

Masterarbeit

vorgelegt von

Michael SeiBinger,  
geboren am 03.01.1987 in Schweinfurt



Institut für Theoretische Physik und Astrophysik  
der Julius-Maximilians-Universität Würzburg

22.05.2012

Betreuer: Prof. Dr. Fakher Assaad



# Abstract

In this thesis, two constraint random phase approximation (cRPA) methods are presented and applied to a three-band model. The basic concept of the cRPA method is the reduction of a multi-band model to a low-energy effective model, where the influence of the high-energy bands is included on a RPA level via an additional energy-dependent interaction term. The first cRPA method is based on the localization of bands, but turns out to be inappropriate for the separation of high- and low-energy processes. In order to avoid these difficulties, we introduce a second cRPA method. We show that for this method only high-energy processes contribute to the effective interaction and relate the contributions to the band structure. Applying this cRPA method to the three-band model, the resulting effective low-energy model is a  $t$ - $V$  model with an additional interaction term. Depending on the band structure, this term can be repulsive or attractive, so that we can engineer the low-energy physics indirectly by manipulating the high-energy properties.



# Contents

<b>1</b>	<b>Introduction</b>	<b>7</b>
1.1	Constraint random phase approximation . . . . .	7
1.2	Summary . . . . .	9
<b>2</b>	<b>Path integral cRPA</b>	<b>11</b>
2.1	cRPA method 1 . . . . .	11
2.1.1	Calculating the action . . . . .	12
2.1.2	Approximating the action . . . . .	14
2.1.3	Fourier transformation of the susceptibility . . . . .	18
2.1.4	Integration . . . . .	20
2.2	cRPA method 2 . . . . .	23
2.2.1	Calculating the action . . . . .	23
2.2.2	Approximating the action . . . . .	25
2.2.3	Fourier transformation . . . . .	27
2.2.4	Integration . . . . .	29
<b>3</b>	<b>Three-band model</b>	<b>33</b>
3.1	Numerical test of cRPA method 1 . . . . .	34
3.1.1	Susceptibility . . . . .	34
3.1.2	Numerical results . . . . .	35
3.1.3	Problems of cRPA method 1 . . . . .	36
3.2	Numerical test of cRPA method 2 . . . . .	40
3.2.1	Susceptibility . . . . .	41
3.2.2	Numerical results . . . . .	43
3.3	cRPA and ctQMC study . . . . .	45
3.3.1	Continuous time Quantum Monte Carlo . . . . .	46
3.3.2	Dynamical screening . . . . .	50
3.3.3	Engineering effective models . . . . .	52
3.3.4	ctQMC results . . . . .	55
<b>4</b>	<b>Conclusion</b>	<b>59</b>
<b>A</b>	<b>Detailed calculations</b>	<b>61</b>
A.1	Commutation of $\hat{n}_n(\mathbf{q})$ . . . . .	61
A.2	Commutation of the integration sequence . . . . .	62
A.3	Commutation of $\hat{n}_\alpha(\mathbf{q})$ . . . . .	64
A.4	Effective interaction using cRPA method 2 . . . . .	65

## Contents

---

<b>B Deutsche Zusammenfassung</b>	<b>67</b>
<b>C Bibliography</b>	<b>71</b>
<b>D Danksagungen</b>	<b>75</b>
<b>E Eidesstattliche Erklärung</b>	<b>77</b>

# 1 Introduction

Humans have always been interested in understanding their environment. Driven by curiosity and the hope for advancements made by their discoveries, they have tried to comprehend the phenomena and matters surrounding them. In the course of time, the growing human knowledge has given rise to more and more sophisticated instruments. With regard to the theoretical study of solids, the current research focuses on applications of quantum mechanics and challenges the problem of many-body systems. In combination with the quantum mechanical behavior, the interacting nature of the electrons leads to a rich variety of physics which is a possible basis for innovative devices [1].

Many physical properties are governed by electrons energetically close to the Fermi level, compared to the interaction strength. Hence, it makes sense to focus on these electrons. However, the influence of the remaining high-energy bands, the so-called host bands, should not be neglected completely. A possible method includes the host bands on the level of a random phase approximation (RPA), whereas the low-energy bands, the so-called target bands, are studied using a more accurate method [2]. This combined method, which has been successfully applied to iron based superconductors [3] and 3*d* transition metals [4, 5], is called constraint RPA (cRPA). In this work, two cRPA methods are introduced and used to study one-dimensional systems. A possible application of this procedure to real materials would be the atomic gold chains which have been grown on germanium by Claessen et al. [6, 7]. Besides, the cRPA might be suitable for further analysis of graphene nanoribbons. Theoretical [8, 9] and experimental studies [10] found low-energy states located at the edges and studied the magnetic properties [11, 12].

## 1.1 Constraint random phase approximation

The basic idea of the cRPA is the systematic construction of low-energy effective models starting from the consideration of a much wider energy range. Ideally, the parameters of this effective model are calculated from first principles with high accuracy, so that it generates an even quantitatively correct physical picture. The complete cRPA procedure consists of three steps [13]: Firstly, the computation of the global band structure, secondly, the downfolding of the high-energy degrees of freedom, i.e. the states related to the host bands, using a renormalization procedure and thirdly, the solution of the remaining low-energy effective model. Since a primary aim of this thesis is the introduction of an alternative method for the second step, we present the common method for this step in more detail. The following discussion is based on [13] and [2]. At first, the full Hamiltonian is split into three parts, according to the energy range of the involved operators:

$$\hat{H} = \hat{H}_L + \hat{H}_H + \hat{H}_{HL} \quad (1.1)$$

The indices  $L$ ,  $H$  and  $HL$  denote the low-energy, high-energy and the coupling part, respectively. Similarly, this distinction can be used for the traces appearing in the partition function  $Z$ :

$$Z = \text{Tr}(\exp(-S)) = \text{Tr}_L \text{Tr}_H(\exp(-S)), \quad (1.2)$$

where  $S$  denotes the action. Performing the partial trace over the high-energy parts, we obtain the low-energy action  $S_L$ :

$$S_L = -\log(\text{Tr}_H \exp(-S)) \quad (1.3)$$

This expression may be used to define a low-energy Hamiltonian  $\hat{H}'_L$ . Notice that due to the renormalization by the high-energy parts,  $\hat{H}'_L$  is not equal to  $\hat{H}_L$ : The electrons of the target bands are dressed by the high-energy excitations, the original target band interaction is screened. In order to perform the partial trace  $\text{Tr}_H$  over the high-energy operators, the high-energy Hilbert space has to be distinguished from the low-energy Hilbert space. For this purpose, one can use Wannier functions, for example the maximally localized Wannier functions, or Wannier orbitals. If the target and host bands are entangled, the implementation of this step has to be done more carefully [5]. For the calculation of the screened interaction, we need the polarization  $P$ . However, for the downfolding we only take the part of  $P$  into consideration which is not generated by low-energy degrees of freedom:

$$P = P_L + P_H \quad (1.4)$$

$P_L$  exclusively contains the low-energy contributions, whereas  $P_H$  contains all the rest, i.e. purely high-energy and mixed contributions. Standard RPA is used to calculate  $P_H$ , but not the complete polarization  $P$ , which is why the method is called constraint RPA. If we apply the RPA method to  $P$  starting from an original interaction strength  $v$ , the screened interaction  $W$  has the following form:

$$W = \frac{v}{1 - vP} \quad (1.5)$$

Expressing this result with the two different contributions  $P_L$  and  $P_H$ , we get:

$$W = \frac{v}{1 - vP_H - vP_L} = \frac{v}{(1 - vP_H)(1 - vP_L(1 - P_H)^{-1})} = \frac{W_H}{1 - W_H P_L} \quad (1.6)$$

Here, we have defined

$$W_H = \frac{v}{1 - vP_H}. \quad (1.7)$$

This result shows that we can interpret the influence of the host bands as an effective screening of the interaction  $v$ , which can be separated from the screening related to the target band processes on the RPA level. This additionally motivates the cRPA method, where we use  $W_H$  as the effective interaction for the low-energy model. Note that due to the dependence of the polarization  $P_H$  on the frequency, the new interaction parameter  $W_H$  is frequency dependent, too. This downfolding procedure is the standard scheme for the cRPA, but extensions to a functional renormalization group scheme have already been proposed [14].



## 1.2 Summary

The cRPA scheme presented in this thesis adopts the central concept of the standard cRPA: We develop two cRPA methods using path integration and combine them with the continuous time Quantum Monte Carlo (ctQMC) method as the solver for the low-energy effective model. Both procedures for the downfolding step are described in chapter 2. Bearing in mind the localized bands of the graphene ribbons, the first cRPA method is based on localization, whereas the second method does not require this condition. As a consequence, it can be applied to more general band structures, but the split-up into target and host bands has to be possible in both cases. In chapter 3, both cRPA methods are tested numerically on a three-band model. This test reveals serious problems of the first method which are explained subsequently. The second method is not affected by these difficulties, we therefore use this for further studies. After the RPA conversion of the three-band model into a low-energy effective model, we obtain a  $t$ - $V$  model with an additional effective interaction. We present the solution of this model and particularly discuss the influence of the host band on the results.



## 2 Path integral cRPA

The two cRPA methods which we developed in order to derive one-dimensional effective low-energy models are quite similar and use the same starting point. As already mentioned, the first attempt, which will be called cRPA method 1 in the following, turns out to be problematic, since it cannot capture the high-energy processes correctly. However, due to the similarity to the second method, which we call cRPA method 2, and the relative simplicity, it will be described in detail. We hope that the discussion of its failure can be instructive for future attempts.

The common idea of both models is as follows: We start with the partition function and treat  $\beta$  as imaginary time, which is then separated into  $M$  discrete time steps  $\Delta\tau$  [15]:

$$Z = \text{Tr} \left( e^{-\beta\hat{H}} \right) = \text{Tr} \left( \left( e^{-\Delta\tau\hat{H}_0(\tau) - \Delta\tau\hat{H}_I(\tau)} \right)^M \right) + \mathcal{O}(\Delta\tau) \quad (2.1)$$

with  $\hat{H}_0$  and  $\hat{H}_I$  being the non-interacting and interacting part of the full Hamiltonian  $\hat{H}$ . The latter contains square terms of bosonic operators  $\hat{B}_i$  for which we can use the Hubbard-Stratonovich transformation [16, 17]

$$e^{\hat{B}_i^2} = \frac{1}{\sqrt{2\pi}} \int_{-\infty}^{\infty} d\phi_i e^{-\frac{\phi_i^2}{2} - \sqrt{2}\phi_i\hat{B}_i} \quad (2.2)$$

in order to simplify this part. Our concept presented in the subsequent sections is the following: After a Taylor expansion of the exponent up to second order around the paramagnetic solution, we will be able to evaluate the partial trace over the high-energy operators  $\hat{B}_{\text{high}}$ . We can integrate out the corresponding  $\phi_{\text{high}}$  and obtain the desired effective model, which only contains the low-energy operators  $\hat{B}_{\text{low}}$ .

### 2.1 cRPA method 1

The first method is based on the assumption that we only have one low-energy target band and that this band is localized. We express the Hamiltonian by Wannier operators  $c^\dagger, c$ , since we can relate the low-energy regime to one set of Wannier operators  $c_{1,k}^\dagger, c_{1,k}$ .

The system under consideration is a ribbon of finite width in  $x$ -direction and with periodic boundary conditions in  $y$ -direction. The interaction strength can in principle depend on all four spatial coordinates  $n, m, n'$  and  $m'$  of the involved operators, therefore we denote it as  $v_{nmn'm'}$ . If in  $y$ -direction only the spatial difference  $\Delta y$  is relevant, that means

$v_{nmn'm'} = v_{nm, n'-m'}$ , we can rewrite  $\hat{H}_I$  starting from a usual Coulomb-like expression

$$\begin{aligned}
 H_I &= \sum_{n,n'} \sum_{m,m'} \frac{v_{nmn'm'}}{2} c_{n,n'}^\dagger c_{n,n'} c_{m,m'}^\dagger c_{m,m'} \\
 &= \frac{1}{2L^2} \sum_{n,n'} \sum_{m,m'} \sum_{k,k'} \sum_{q,q'} v_{nm, n'-m'} c_{n,k}^\dagger c_{n,k+q} c_{m,k'}^\dagger c_{m,k'-q} e^{i(n'q-m'q')} \\
 &= \frac{1}{2L^2} \sum_{n,m} \sum_{k,k'} \sum_{q,q'} \sum_{n',\tilde{n}} v_{nm, \tilde{n}} c_{n,k}^\dagger c_{n,k+q} c_{m,k'}^\dagger c_{m,k'-q} e^{i\tilde{n}q'} e^{in'(q-q')} \\
 &= \frac{1}{2L} \sum_{n,m} \sum_{k,k'} \sum_q v_{nm}(q) c_{n,k}^\dagger c_{n,k+q} c_{m,k'}^\dagger c_{m,k'-q} \\
 &= \frac{1}{2} \sum_{n,m,q} v_{nm}(q) \hat{n}_n(q) \hat{n}_m(-q)
 \end{aligned} \tag{2.3}$$

with

$$\hat{n}_n(q) = \frac{1}{\sqrt{L}} \sum_k c_{n,k}^\dagger c_{n,k+q} \tag{2.4}$$

and

$$v_{nm}(q) = \sum_{\tilde{n}} v_{nm, \tilde{n}} e^{iq\tilde{n}}. \tag{2.5}$$

Due to the hermiticity of the Hamiltonian  $v_{nmn'm'} = v_{mnm'n'}$  has to be fulfilled for real values of the interaction strength. This implies  $v_{nm}(q) = v_{mn}(-q)$  and we obtain therefore

$$\begin{aligned}
 H_I &= \frac{1}{2} \sum_{n,m} \sum_q v_{nm}(q) \hat{n}_n(q) \hat{n}_m(-q) \\
 &= \frac{1}{2} \sum_{n,m} \sum_{q>0} (v_{nm}(q) \hat{n}_n(q) \hat{n}_m(-q) + v_{nm}(-q) \hat{n}_n(-q) \hat{n}_m(q)) \\
 &= \frac{1}{2} \sum_{n,m} \sum_{q>0} (v_{nm}(q) \hat{n}_n(q) \hat{n}_m(-q) + v_{mn}(q) \hat{n}_m(q) \hat{n}_n(-q)) \\
 &= \sum_{n,m} \sum_{q>0} v_{nm}(q) \hat{n}_n(q) \hat{n}_m(-q).
 \end{aligned} \tag{2.6}$$

As it is done for the Jellium-model [18], we neglect the ( $q = 0$ )-term, since this only leads to a constant offset. Overall, the full Hamiltonian reads

$$\hat{H} = \hat{H}_0 + \hat{H}_I = \sum_{\alpha,k} E_\alpha(k) \gamma_{\alpha,k}^\dagger \gamma_{\alpha,k} + \sum_{n,m} \sum_{q>0} v_{nm}(q) \hat{n}_n(q) \hat{n}_m(-q). \tag{2.7}$$

### 2.1.1 Calculating the action

In order to be able to apply the Hubbard-Stratonovich transformation, we have to rewrite the interacting part of the Hamiltonian, which should only contain square terms according

to eq. (2.2). Since the operators  $\hat{n}_n(q)$  commute (see appendix, section A.1)

$$[\hat{n}_n(q), \hat{n}_m(q')] = 0, \quad (2.8)$$

we achieve this by using

$$\hat{H}_I = \sum_{n,m} \sum_{q>0} \frac{v_{nm}(q)}{4} ((\hat{n}_n(q) + \hat{n}_m(-q))^2 - (\hat{n}_n(q) - \hat{n}_m(-q))^2). \quad (2.9)$$

We insert this Hamiltonian in eq.(2.1) and do the Hubbard-Stratonovich transformation for every  $q$ ,  $n$ ,  $m$  and  $\tau$ , as well as for the  $+$  and  $-$ -terms:

$$Z = \text{Tr} \left( \prod_{\tau=0}^{\beta} e^{-\Delta\tau \hat{H}_0(\tau)} \int \prod_{q,m,n,\tau} \left( \frac{d\phi_{q,n,m,\tau} d\varphi_{q,n,m,\tau}}{2\pi} \right) e^{-\tilde{S}(\phi_{q,n,m,\tau}, \varphi_{q,n,m,\tau})} \right), \quad (2.10)$$

where  $\tilde{S}$  is defined by

$$\begin{aligned} \tilde{S}(\phi_{q,n,m,\tau}, \varphi_{q,n,m,\tau}) = & \\ & \sum_{n,m} \sum_{q>0} \left( \frac{\phi_{q,n,m,\tau}^2}{2} + i\phi_{q,n,m,\tau} \sqrt{\frac{\Delta\tau v_{nm}(q)}{2}} (\hat{n}_n(q) + \hat{n}_m(-q)) \right. \\ & \left. + \frac{\varphi_{q,n,m,\tau}^2}{2} + \varphi_{q,n,m,\tau} \sqrt{\frac{\Delta\tau v_{nm}(q)}{2}} (\hat{n}_n(q) - \hat{n}_m(-q)) \right). \end{aligned} \quad (2.11)$$

$\phi_{q,n,m,\tau}$  and  $\varphi_{q,n,m,\tau}$  are substituted by

$$z_{q,n,m,\tau} = \sqrt{\frac{v_{nm}(q)}{2\Delta\tau}} (\phi_{q,n,m,\tau} + i\varphi_{q,n,m,\tau}) \quad (2.12)$$

and we obtain

$$\begin{aligned} \tilde{S} = & \\ & \sum_{n,m} \sum_{q>0} \left( \frac{\phi_{q,n,m,\tau}^2}{2} + \frac{\varphi_{q,n,m,\tau}^2}{2} + \right. \\ & \left. i\sqrt{\frac{\Delta\tau v_{nm}(q)}{2}} ((\phi_{q,n,m,\tau} - i\varphi_{q,n,m,\tau})\hat{n}_n(q) + (\phi_{q,n,m,\tau} + i\varphi_{q,n,m,\tau})\hat{n}_m(-q)) \right) \\ & = \Delta\tau \sum_{n,m} \sum_{q>0} \left( \frac{|z_{q,n,m,\tau}|^2}{v_{nm}(q)} + i(\bar{z}_{q,n,m,\tau}\hat{n}_n(q) + z_{q,n,m,\tau}\hat{n}_m(-q)) \right). \end{aligned} \quad (2.13)$$

If we additionally take into account that the trace does not effect the auxiliary fields, the resulting expression for the partition function is

$$Z = \int \prod_{\tau=0}^{\beta} \prod_{q,m,n} \left( \frac{d\text{Re}(z_{q,n,m,\tau}) d\text{Im}(z_{q,n,m,\tau}) \Delta\tau}{\pi v_{nm}(q)} \right) e^{-S(z_{q,n,m,\tau}, \bar{z}_{q,n,m,\tau})}. \quad (2.14)$$

Here, we have introduced the action

$$\begin{aligned}
 S(z_{q,n,m,\tau}, \bar{z}_{q,n,m,\tau}) &= \Delta\tau \sum_{\tau,n,m} \sum_{q>0} \frac{|z_{q,n,m,\tau}|^2}{v_{nm}(q)} - \\
 \log \left( \text{Tr} \left( \prod_{\tau=0}^{\beta} \exp \left( -\Delta\tau \hat{H}_0(\tau) - i\Delta\tau \sum_{n,m} \sum_{q>0} (\bar{z}_{q,n,m,\tau} \hat{n}_n(q) + z_{q,n,m,\tau} \hat{n}_m(-q)) \right) \right) \right),
 \end{aligned} \tag{2.15}$$

which we will use as the starting point for the following approximations.

## 2.1.2 Approximating the action

Within this subsection we will use a different notation, in order to distinguish between the high- and low-energy contributions. Since  $z_{q,1,1,\tau}$  and  $\bar{z}_{q,1,1,\tau}$  only couple to the target band densities  $\hat{n}_1(q)$  and  $\hat{n}_1(-q)$ , we relate them to the low-energy processes and refer to them as

$$z_{q,1,1,\tau} = z_{q,\tau}, \quad \bar{z}_{q,1,1,\tau} = \bar{z}_{q,\tau}, \tag{2.16}$$

in contrast to the other auxiliary fields  $z_{q,n,m,\tau}$  and  $\bar{z}_{q,n,m,\tau}$  with  $n \neq 1$  or  $m \neq 1$ , which we call

$$z_{q,n,m,\tau} = \zeta_{q,n,m,\tau}, \quad \bar{z}_{q,n,m,\tau} = \bar{\zeta}_{q,n,m,\tau} \tag{2.17}$$

in the following. The idea of the upcoming calculation is to find an approximation for the action, which enables us to perform the integrations in eq. (2.14) for the partition function  $Z$ . However, we do not want to integrate out all auxiliary fields, which would simply restore the original term, but only the high-energy auxiliary fields, thus the  $\zeta$  and  $\bar{\zeta}$ . The approximation has to ensure that no operators related to the high-energy bands, so  $\hat{n}_n(q)$  and  $\hat{n}_m(-q)$  with  $n, m \neq 1$ , remain in the equations. Their influence on the target band should be contained in additional terms of computable quantities, which appear in the low-energy effective model.

We assume the interaction to mainly affect the low-energy bands, so that deviations of the high-energy bands from the paramagnetic solution  $\zeta_{q,n,m,\tau} = \bar{\zeta}_{q,n,m,\tau} = 0$  should be small. Therefore, we approximate the action  $S(z, \bar{z}, \zeta, \bar{\zeta})$  in a first step by its Taylor

expansion in  $\zeta$  and  $\bar{\zeta}$  up to second order:

$$\begin{aligned}
 & S(z, \bar{z}, \zeta, \bar{\zeta}) \approx \\
 & S(z, \bar{z}, \zeta = 0, \bar{\zeta} = 0) \\
 & + \sum_{q,n,m,\tau} \frac{\partial S}{\partial \zeta_{q,n,m,\tau}} \Big|_{\zeta=0, \bar{\zeta}=0} \zeta_{q,n,m,\tau} + \sum_{q,n,m,\tau} \frac{\partial S}{\partial \bar{\zeta}_{q,n,m,\tau}} \Big|_{\zeta=0, \bar{\zeta}=0} \bar{\zeta}_{q,n,m,\tau} \\
 & + \sum_{q,n,m,\tau} \sum_{q',n',m',\tau'} \frac{\partial^2 S}{\partial \zeta_{q,n,m,\tau} \partial \bar{\zeta}_{q',n',m',\tau'}} \Big|_{\zeta=0, \bar{\zeta}=0} \zeta_{q,n,m,\tau} \bar{\zeta}_{q',n',m',\tau'} \\
 & + \frac{1}{2} \sum_{q,n,m,\tau} \sum_{q',n',m',\tau'} \frac{\partial^2 S}{\partial \zeta_{q,n,m,\tau} \partial \zeta_{q',n',m',\tau'}} \Big|_{\zeta=0, \bar{\zeta}=0} \zeta_{q,n,m,\tau} \zeta_{q',n',m',\tau'} \\
 & + \frac{1}{2} \sum_{q,n,m,\tau} \sum_{q',n',m',\tau'} \frac{\partial^2 S}{\partial \bar{\zeta}_{q,n,m,\tau} \partial \bar{\zeta}_{q',n',m',\tau'}} \Big|_{\zeta=0, \bar{\zeta}=0} \bar{\zeta}_{q,n,m,\tau} \bar{\zeta}_{q',n',m',\tau'}. \tag{2.18}
 \end{aligned}$$

Furthermore, we assume that the interplay between high- and low-energy physics is small, which is reasonable if both energy regimes are clearly separated. This means that if the behavior of one energy regime is not very sensitive to the other one, we can approximate the first derivatives with respect to the high-energy auxiliary fields in first order by

$$\begin{aligned}
 & \frac{\partial S}{\partial \zeta_{q,n,m,\tau}} \Big|_{\zeta=0, \bar{\zeta}=0} \approx \frac{\partial S}{\partial \zeta_{q,n,m,\tau}} \Big|_{\zeta=0, \bar{\zeta}=0, z=0, \bar{z}=0} + \\
 & \sum_{q',\tau'} \left( \frac{\partial^2 S}{\partial \zeta_{q,n,m,\tau} \partial z_{q',\tau'}} \Big|_{\zeta=0, \bar{\zeta}=0, z=0, \bar{z}=0} z_{q',\tau'} + \frac{\partial^2 S}{\partial \zeta_{q,n,m,\tau} \partial \bar{z}_{q',\tau'}} \Big|_{\zeta=0, \bar{\zeta}=0, z=0, \bar{z}=0} \bar{z}_{q',\tau'} \right) \tag{2.19}
 \end{aligned}$$

$$\begin{aligned}
 & \frac{\partial S}{\partial \bar{\zeta}_{q,n,m,\tau}} \Big|_{\zeta=0, \bar{\zeta}=0} \approx \frac{\partial S}{\partial \bar{\zeta}_{q,n,m,\tau}} \Big|_{\zeta=0, \bar{\zeta}=0, z=0, \bar{z}=0} + \\
 & \sum_{q',\tau'} \left( \frac{\partial^2 S}{\partial \bar{\zeta}_{q,n,m,\tau} \partial z_{q',\tau'}} \Big|_{\zeta=0, \bar{\zeta}=0, z=0, \bar{z}=0} z_{q',\tau'} + \frac{\partial^2 S}{\partial \bar{\zeta}_{q,n,m,\tau} \partial \bar{z}_{q',\tau'}} \Big|_{\zeta=0, \bar{\zeta}=0, z=0, \bar{z}=0} \bar{z}_{q',\tau'} \right) \tag{2.20}
 \end{aligned}$$

and similarly the second derivatives in zeroth order by

$$\frac{\partial^2 S}{\partial \zeta_{q,n,m,\tau} \partial \bar{\zeta}_{q',n',m',\tau'}} \Big|_{\zeta=0, \bar{\zeta}=0} \approx \frac{\partial^2 S}{\partial \zeta_{q,n,m,\tau} \partial \bar{\zeta}_{q',n',m',\tau'}} \Big|_{\zeta=0, \bar{\zeta}=0, z=0, \bar{z}=0} \tag{2.21}$$

$$\frac{\partial^2 S}{\partial \zeta_{q,n,m,\tau} \partial \zeta_{q',n',m',\tau'}} \Big|_{\zeta=0, \bar{\zeta}=0} \approx \frac{\partial^2 S}{\partial \zeta_{q,n,m,\tau} \partial \zeta_{q',n',m',\tau'}} \Big|_{\zeta=0, \bar{\zeta}=0, z=0, \bar{z}=0} \tag{2.22}$$

$$\frac{\partial^2 S}{\partial \bar{\zeta}_{q,n,m,\tau} \partial \bar{\zeta}_{q',n',m',\tau'}} \Big|_{\zeta=0, \bar{\zeta}=0} \approx \frac{\partial^2 S}{\partial \bar{\zeta}_{q,n,m,\tau} \partial \bar{\zeta}_{q',n',m',\tau'}} \Big|_{\zeta=0, \bar{\zeta}=0, z=0, \bar{z}=0}. \tag{2.23}$$

Overall, we have to consider three types of expressions: A  $\zeta$ -independent first term, first derivatives of the action with respect to  $\zeta$  and  $\bar{\zeta}$  as well as second derivatives with respect to  $\zeta$ ,  $\bar{\zeta}$ ,  $z$  and  $\bar{z}$ .

### First term

If we simply write down the first term of the Taylor expansion by setting  $\zeta$  and  $\bar{\zeta}$  equal to zero, we obtain

$$S_0 \equiv S(z, \bar{z}, \zeta = 0, \bar{\zeta} = 0) = \sum_{\tau} \Delta\tau \sum_{q>0} \frac{|z_{q,\tau}|^2}{v_{11}(q)} - \log \left( \text{Tr} \left( \prod_{\tau=0}^{\beta} \exp \left( -\Delta\tau \hat{H}_0(\tau) - i\Delta\tau \sum_{q>0} (\bar{z}_{q,\tau} \hat{n}_1(q) + z_{q,\tau} \hat{n}_1(-q)) \right) \right) \right) \quad (2.24)$$

As we could easily confirm by reversing the Hubbard-Stratonovich transformation, this expression contains the full Hamiltonian of the target band. The influence of the high-energy bands is completely neglected, which is not surprising if we bear in mind the construction of this term. However, this is no problem, since this influence should be incorporated in the higher order terms.

### First derivatives

Previous to the calculation of the first derivatives, it is useful to introduce the quantity

$$\hat{U}(\tau_1, \tau_2) = \prod_{\tau=\tau_1}^{\tau_2} \exp \left( -\Delta\tau \hat{H}_0(\tau) - i\Delta\tau \sum_{q>0} (\bar{z}_{q,\tau} \hat{n}_1(q) + z_{q,\tau} \hat{n}_1(-q)) \right), \quad (2.25)$$

which always appears when we set  $\zeta = 0$  and  $\bar{\zeta} = 0$ . Note that  $\hat{U}(\tau_1, \tau_2)$  is simply the time evolution operator of the non-interacting system if  $z = 0$  and  $\bar{z} = 0$ .

Expressing the derivative of  $S$  with respect to  $\zeta_{q,n,m,\tau}$  by  $\hat{U}$  and explicitly writing down the time dependence of  $\hat{n}_m(-q, \tau)$ , which has been omitted so far for simplicity, we get

$$\left. \frac{\partial S}{\partial \zeta_{q,n,m,\tau}} \right|_{\zeta=0, \bar{\zeta}=0, z=0, \bar{z}=0} = \left( \frac{\Delta\tau \bar{\zeta}_{q,n,m,\tau}}{v_{nm}(q)} + \frac{i\Delta\tau}{\text{Tr}(\hat{U}(\beta, 0))} \text{Tr}(\hat{U}(\beta, \tau) \hat{n}_m(-q, \tau) \hat{U}(\tau, 0)) \right) \Big|_{\zeta=0, \bar{\zeta}=0, z=0, \bar{z}=0}. \quad (2.26)$$

The first term vanishes at  $\bar{\zeta} = 0$  and for  $z = 0$  and  $\bar{z} = 0$ , the second term is just the expectation value of the non-interacting system

$$\langle \dots \rangle_0 = \frac{1}{Z_0} \text{Tr} \left( e^{-\beta \hat{H}_0} \dots \right) \quad (2.27)$$

for  $\hat{n}_m(-q, \tau)$ . If we use the definition of  $\hat{n}_m(-q, \tau)$  (see eq. (2.4)), we have

$$\left. \frac{\partial S}{\partial \zeta_{q,n,m,\tau}} \right|_{\zeta=0, \bar{\zeta}=0, z=0, \bar{z}=0} = i\Delta\tau \langle \hat{n}_m(-q, \tau) \rangle_0 = \frac{i\Delta\tau}{\sqrt{L}} \sum_k \langle c_{m,k}^\dagger(\tau) c_{m,k-q}(\tau) \rangle_0 \quad (2.28)$$

which vanishes due to momentum conservation, since  $q > 0$ .



In the same way, we can show that the derivative of  $S$  with respect to  $\bar{\zeta}_{q,n,m,\tau}$  vanishes:

$$\frac{\partial S}{\partial \bar{\zeta}_{q,n,m,\tau}} \Big|_{\zeta=0, \bar{\zeta}=0, z=0, \bar{z}=0} = \frac{\Delta\tau \zeta_{q,n,m,\tau}}{v_{nm}(q)} \Big|_{\zeta=0, \bar{\zeta}=0, z=0, \bar{z}=0} + i\Delta\tau \langle \hat{n}_n(q, \tau) \rangle_0 = 0 \quad (2.29)$$

Since both derivatives vanish,  $\zeta_{q,n,m,\tau} = \bar{\zeta}_{q,n,m,\tau} = 0$  defines a local extremum of  $S$ , if we neglect  $z$  and  $\bar{z}$ . This reflects that  $\zeta_{q,n,m,\tau} = \bar{\zeta}_{q,n,m,\tau} = 0$  is one solution of this system, more precisely, the paramagnetic solution. The result of the above calculation is the confirmation of this solution, without proving its stability. The actual type of approximation we apply in this subsection is an expansion around the saddle point of the partition function.

## Second derivatives

Since we need the second derivatives of  $S$  with respect to every combination of  $\zeta$ ,  $\bar{\zeta}$ ,  $z$  and  $\bar{z}$  except  $z$  and  $\bar{z}$  exclusively, we have to consider seven different possibilities. The first expression we calculate is  $\frac{\partial^2 S}{\partial \zeta \partial \bar{\zeta}}$ :

$$\begin{aligned} \frac{\partial^2 S}{\partial \zeta_{q,n,m,\tau} \partial \bar{\zeta}_{q',n',m',\tau'}} \Big|_{\zeta=0, \bar{\zeta}=0, z=0, \bar{z}=0} &= \frac{\Delta\tau}{v_{n,m}(q)} \delta_{nn'} \delta_{mm'} \delta_{q,q'} \delta_{\tau\tau'} \\ &+ \Delta\tau^2 \left( \langle \hat{T} \hat{n}_m(-q, \tau) \hat{n}_{n'}(q', \tau') \rangle_0 - \langle \hat{n}_m(-q, \tau) \rangle_0 \langle \hat{n}_{n'}(q', \tau') \rangle_0 \right) = \\ &\frac{\Delta\tau}{v_{n,m}(q)} \delta_{nn'} \delta_{mm'} \delta_{q,q'} \delta_{\tau\tau'} + \Delta\tau^2 \langle \hat{T} \hat{n}_m(-q, \tau) \hat{n}_{n'}(q, \tau') \rangle_0 \delta_{qq'} \end{aligned} \quad (2.30)$$

Here, we have introduced the time ordering operator  $\hat{T}$ .  $\langle \hat{n}_m(-q, \tau) \rangle_0$  and  $\langle \hat{n}_{n'}(q', \tau') \rangle_0$  vanish because of momentum conservation, just like the first derivatives. For the same reason,  $\langle \hat{T} \hat{n}_m(-q, \tau) \hat{n}_{n'}(q', \tau') \rangle_0$  is only nonzero if  $q = q'$ . While the first term of the result simply refers to the square interaction term of  $S$ , the second one is worth being discussed in some more detail. It is responsible for the coupling between two different auxiliary fields and thus for the coupling between different bands. Since we are interested in the influence of the high-energy bands on the target band, this is exactly the effect we are looking for. Note that this coupling requires the same value of  $q$  and  $q'$ , but not the same value of the imaginary times  $\tau$  and  $\tau'$ . We use the coupling prefactor to define the generalized susceptibility

$$\chi_{0,nm}(q, \tau, \tau') \equiv \langle \hat{T} \hat{n}_n(q, \tau) \hat{n}_m(-q, \tau') \rangle_0. \quad (2.31)$$

The index 0 reminds us, that it can be calculated within the non-interacting system.  $\chi_{0,nm}(q, \tau, \tau')$  only depends on the time difference, which is easily verified by applying the invariance of the trace under cyclic permutations, assuming  $\tau > \tau'$ :

$$\chi_{0,nm}(q, \tau, \tau') = \frac{1}{Z_0} \text{Tr} \left( e^{-(\beta-\tau)\hat{H}_0} \hat{n}_n(q) e^{-(\tau-\tau')\hat{H}_0} \hat{n}_m(-q) e^{-\tau'\hat{H}_0} \right) \quad (2.32)$$

Therefore, we can write  $\chi_{0,nm}(q, \tau - \tau') \equiv \chi_{0,nm}(q, \tau, \tau')$ . Due to its dependence on  $q$  and  $\Delta\tau$ , this susceptibility contains the effects of both spatial and temporal fluctuations.

The next expression we look into is  $\frac{\partial^2 S}{\partial \zeta \partial \bar{\zeta}}$ :

$$\begin{aligned} & \left. \frac{\partial^2 S}{\partial \zeta_{q,n,m,\tau} \partial \bar{\zeta}_{q',n',m',\tau'}} \right|_{\zeta=0, \bar{\zeta}=0, z=0, \bar{z}=0} = \\ & \Delta \tau^2 \left( \langle \hat{T} \hat{n}_m(-q, \tau) \hat{n}_{m'}(-q', \tau') \rangle_0 - \langle \hat{n}_m(-q, \tau) \rangle_0 \langle \hat{n}_{m'}(-q', \tau') \rangle_0 \right) = 0 \end{aligned} \quad (2.33)$$

Again, both terms vanish because of the momentum conservation. For  $\frac{\partial^2 S}{\partial \bar{\zeta} \partial \zeta}$ , the calculation is quite similar:

$$\begin{aligned} & \left. \frac{\partial^2 S}{\partial \bar{\zeta}_{q,n,m,\tau} \partial \zeta_{q',n',m',\tau'}} \right|_{\zeta=0, \bar{\zeta}=0, z=0, \bar{z}=0} = \\ & \Delta \tau^2 \left( \langle \hat{T} \hat{n}_n(q, \tau) \hat{n}_{n'}(q', \tau') \rangle_0 - \langle \hat{n}_n(q, \tau) \rangle_0 \langle \hat{n}_{n'}(q', \tau') \rangle_0 \right) = 0 \end{aligned} \quad (2.34)$$

We still need the derivatives with respect to  $z$  and  $\bar{z}$ . Since the calculation is completely equivalent to the corresponding ones above, we can simply write down the result, using the index 1 at the appropriate places:

$$\left. \frac{\partial^2 S}{\partial \zeta_{q,n,m,\tau} \partial z_{q',\tau'}} \right|_{\zeta=0, \bar{\zeta}=0, z=0, \bar{z}=0} = 0 \quad (2.35)$$

$$\left. \frac{\partial^2 S}{\partial \zeta_{q,n,m,\tau} \partial \bar{z}_{q',\tau'}} \right|_{\zeta=0, \bar{\zeta}=0, z=0, \bar{z}=0} = \Delta \tau^2 \chi_{0,1m}(q, \tau' - \tau) \delta_{qq'} \quad (2.36)$$

$$\left. \frac{\partial^2 S}{\partial \bar{\zeta}_{q,n,m,\tau} \partial z_{q',\tau'}} \right|_{\zeta=0, \bar{\zeta}=0, z=0, \bar{z}=0} = \Delta \tau^2 \chi_{0,n1}(q, \tau - \tau') \delta_{qq'} \quad (2.37)$$

$$\left. \frac{\partial^2 S}{\partial \bar{\zeta}_{q,n,m,\tau} \partial \bar{z}_{q',\tau'}} \right|_{\zeta=0, \bar{\zeta}=0, z=0, \bar{z}=0} = 0 \quad (2.38)$$

Now we have explicit expressions for all terms that appear in the approximation scheme.

### 2.1.3 Fourier transformation of the susceptibility

Before we insert the results of the last subsection into the approximated expression of the action  $S$  and go on with the calculation of the partition function  $Z$ , we can use a property of the susceptibility in order to simplify further steps. This property is the periodicity of  $\chi_{0,nm}(q, \tau)$  with respect to  $\tau$ , which we can verify, choosing  $\tau \in ] -\beta, 0]$ :

$$\begin{aligned} \chi_{0,nm}(q, \beta + \tau) &= \langle \hat{T} \hat{n}_n(q, \tau + \beta) \hat{n}_m(-q, 0) \rangle_0 \\ &= \frac{1}{\text{Tr}(U_0(\beta, 0))} \text{Tr} \left( e^{-\beta \hat{H}_0} e^{(\tau+\beta) \hat{H}_0} \hat{n}_n(q) e^{-(\tau+\beta) \hat{H}_0} \hat{n}_m(-q) \right) \\ &= \frac{1}{\text{Tr}(U_0(\beta, 0))} \text{Tr} \left( e^{-\beta \hat{H}_0} \hat{n}_m(-q) e^{\tau \hat{H}_0} \hat{n}_n(q) e^{-\tau \hat{H}_0} \right) \\ &= \langle \hat{n}_m(-q, 0) \hat{n}_n(q, \tau) \rangle_0 = \langle \hat{T} \hat{n}_n(q, \tau) \hat{n}_m(-q, 0) \rangle_0 = \chi_{0,nm}(q, \tau) \end{aligned} \quad (2.39)$$

Due to this periodicity, it makes sense to define the Fourier transform of the susceptibility

$$\chi_{0,nm}(q, \Omega_m) = \int_0^\beta d\tau e^{i\Omega_m\tau} \chi_{0,nm}(q, \tau), \quad (2.40)$$

where  $\Omega_m = \frac{2\pi m}{\beta}$  are the bosonic Matsubara frequencies [19]. In order to distinguish both  $m$  indices, we always write sums over  $\Omega_m$  if we refer to the Matsubara frequencies in contrast to the position index  $m$ . The inverse transformation therefore is

$$\chi_{0,nm}(q, \tau) = \frac{1}{\beta} \sum_{\Omega_m} e^{-i\Omega_m\tau} \chi_{0,nm}(q, \Omega_m). \quad (2.41)$$

We now return to the previous notation using  $z_{q,n,m,\tau}$ . We can express the complete result for the second derivatives with Matsubara frequencies instead of imaginary time using  $\delta_{\tau\tau'} = \frac{1}{M} \sum_{\Omega_m} e^{-i\Omega_m(\tau'-\tau)}$ :

$$\begin{aligned} & \left. \frac{\partial^2 S}{\partial z_{q,n,m,\tau} \partial \bar{z}_{q',n',m',\tau'}} \right|_{z=0, \bar{z}=0} \\ &= \frac{\Delta\tau}{v_{nm}(q)} \delta_{nn'} \delta_{mm'} \delta_{q,q'} \delta_{\tau\tau'} + \Delta\tau^2 \langle \hat{T} \hat{n}_m(-q, \tau) \hat{n}_{n'}(q, \tau') \rangle_0 \delta_{qq'} \\ &= \Delta\tau^2 \frac{\delta_{q,q'}}{\beta} \sum_{\Omega_m} \left( \frac{\delta_{nn'} \delta_{mm'}}{v_{nm}(q)} e^{-i\Omega_m(\tau'-\tau)} + e^{-i\Omega_m(\tau'-\tau)} \chi_{0,n'm}(q, \Omega_m) \right) \end{aligned} \quad (2.42)$$

If we look at the total approximated action  $S(z, \bar{z})$ , the advantage of this procedure becomes obvious:

$$\begin{aligned} S(z, \bar{z}) &= S_0 + \sum_{q>0} \sum_{q'>0} \sum'_{n,m,n'm'} \int_0^\beta d\tau \int_0^\beta d\tau' \sum_{\Omega_m} \frac{\delta_{q,q'}}{\beta} e^{-i\Omega_m(\tau'-\tau)} \times \\ & \quad z_{q,n,m,\tau} \left( \frac{\delta_{nn'} \delta_{mm'}}{v_{nm}(q)} + \chi_{0,n'm}(q, \Omega_m) \right) \bar{z}_{q',n',m',\tau'} \\ &= S_0 + \sum_{q>0} \sum'_{n,m,n'm'} \sum_{\Omega_m} z_{q,n,m,\Omega_m} \left( \frac{\delta_{nn'} \delta_{mm'}}{v_{nm}(q)} + \chi_{0,n'm}(q, \Omega_m) \right) \bar{z}_{q,n',m',\Omega_m} \end{aligned} \quad (2.43)$$

Here, we have used

$$\sum'_{\{n_\alpha\}} : \text{sum over } \{n_\alpha\} \text{ with at least one } n_\alpha \neq 1 \quad (2.44)$$

and

$$\begin{aligned} z_{q,n,m,\Omega_m} &= \frac{1}{\sqrt{\beta}} \int_0^\beta d\tau e^{i\Omega_m\tau} z_{q,n,m,\tau} \\ \bar{z}_{q,n,m,\Omega_m} &= \frac{1}{\sqrt{\beta}} \int_0^\beta d\tau e^{-i\Omega_m\tau} \bar{z}_{q,n,m,\tau}. \end{aligned} \quad (2.45)$$

We managed to reduce the two integrations over  $\tau$  and  $\tau'$  to only one sum over  $\Omega_m$ . It is useful to sort the appearing terms according to their indices. We split up the sum, one part of the sum containing the square terms, i.e. auxiliary fields with the same indices, the other one containing the mixed terms. Furthermore, we add a term with low-energy indices  $n = 1$  and  $m = 1$  in order to omit the restriction of the sums:

$$\begin{aligned}
 S(z, \bar{z}) + \sum_{q>0} \sum_{\Omega_m} |z_{q,1,1,\Omega_m}|^2 \left( \frac{1}{v_{11}(q)} + \chi_{0,11}(q, \Omega_m) \right) = \\
 S_0 + \sum_{q>0} \sum_{\Omega_m} \left( \sum_{n,m} |z_{q,n,m,\Omega_m}|^2 \left( \frac{1}{v_{nm}(q)} + \chi_{0,nm}(q, \Omega_m) \right) \right. \\
 \left. + \sum_{n,m} \sum_{n',m' \neq n,m} z_{q,n,m,\Omega_m} \chi_{0,n'm}(q, \Omega_m) \bar{z}_{q,n',m',\Omega_m} \right) \quad (2.46)
 \end{aligned}$$

With this expression, we can continue the calculation.

## 2.1.4 Integration

The quantity from which we originally started our calculations is the partition function  $Z$ . Applying the approximations and using the results of the previous subsections, we obtain

$$\begin{aligned}
 Z = \int \prod_{q,\Omega_m} \prod_{n,m} \left( \frac{dRe(z_{q,n,m,\Omega_m}) dIm(z_{q,n,m,\Omega_m}) \Delta\tau}{\pi v_{nm}(q)} \right) e^{-S_0} \times \\
 \prod_{q,\Omega_m} \exp \left( |z_{q,1,1,\Omega_m}|^2 \left( \frac{1}{v_{11}(q)} + \chi_{0,11}(q, \Omega_m) \right) \right) \times \\
 \prod_{q,\Omega_m} \exp \left( - \sum_{n,m} |z_{q,n,m,\Omega_m}|^2 \left( \frac{1}{v_{nm}(q)} + \chi_{0,nm}(q, \Omega_m) \right) \right. \\
 \left. - \sum_{n,m} \sum_{n',m' \neq n,m} z_{q,n,m,\Omega_m} \chi_{0,n'm}(q, \Omega_m) \bar{z}_{q,n',m',\Omega_m} \right). \quad (2.47)
 \end{aligned}$$

There are two important points that we notice about this expression: Firstly, we can easily perform the integrations over the auxiliary fields, since these are all Gaussian integrations. Secondly, we can perform the integrations independently for all different values of  $q$  and  $\Omega_m$ . Therefore, we can write

$$\begin{aligned}
 Z = \int \prod_{q,\Omega_m} \left( \frac{dRe(z_{q,1,1,\Omega_m}) dIm(z_{q,1,1,\Omega_m}) \Delta\tau}{\pi v_{11}(q)} \right) \times \\
 \prod_{q,\Omega_m} \exp \left( |z_{q,1,1,\Omega_m}|^2 \left( \frac{1}{v_{11}(q)} + \chi_{0,11}(q, \Omega_m) \right) \right) e^{-S_0} \prod_{q,\Omega_m} Z_{q,\Omega_m} \quad (2.48)
 \end{aligned}$$

and with  $z_{q,n,m,\Omega_m} = x_{q,n,m,\Omega_m} + iy_{q,n,m,\Omega_m}$

$$\begin{aligned}
 Z_{q,\Omega_m} &= \int \prod'_{n,m} \left( \frac{dx_{q,n,m,\Omega_m} dy_{q,n,m,\Omega_m} \Delta\tau}{\pi v_{nm}(q)} \right) \times \\
 &\exp \left( - \sum_{n,m} \left( (x_{q,n,m,\Omega_m}^2 + y_{q,n,m,\Omega_m}^2) \left( \frac{1}{v_{nm}(q)} + \chi_{0,nm}(q, \Omega_m) \right) \right) \right) \times \\
 &\exp \left( - \sum_{n,m} \sum_{n',m' \neq n,m} \chi_{0,n'm'}(q, \Omega_m) (x_{q,n,m,\Omega_m} x_{q,n',m',\Omega_m} + y_{q,n,m,\Omega_m} y_{q,n',m',\Omega_m}) \right) \times \\
 &\exp \left( - \sum_{n,m} \sum_{n',m' \neq n,m} \chi_{0,n'm'}(q, \Omega_m) (iy_{q,n,m,\Omega_m} x_{q,n',m',\Omega_m} - ix_{q,n,m,\Omega_m} y_{q,n',m',\Omega_m}) \right).
 \end{aligned} \tag{2.49}$$

Similarly to the notation for the sums, we introduced

$$\prod'_{\{n_\alpha\}} : \text{product over } \{n_\alpha\} \text{ with at least one } n_\alpha \neq 1 \tag{2.50}$$

here. It is possible to use a matrix formulation for this integration, but since we always have to distinguish between  $x_{q,1,1,\Omega_m}$  and  $y_{q,1,1,\Omega_m}$  and the other auxiliary fields, a description of this method runs the risk of being rather confusing. We will adopt this method for the second cRPA scheme presented later. We compute the integration for the cRPA method 1 simply by performing the integrations consecutively, starting with  $x_{q,\tilde{n},\tilde{m}}(\Omega_m)$  and  $y_{q,\tilde{n},\tilde{m}}(\Omega_m)$ , with  $\tilde{n} \neq 1$  or  $\tilde{m} \neq 1$ . Since we know that the integration is the same for all  $q$  and  $\Omega_m$ , we will omit this indices for simplicity. The integration is essentially the inverse of the Hubbard-Stratonovich transformation (see eq. (2.2)), if we identify

$$\phi_x = \sqrt{\frac{2}{v_{\tilde{n}\tilde{m}}} + 2\chi_{0,\tilde{n}\tilde{m}}} x_{\tilde{n},\tilde{m}} \tag{2.51}$$

$$\begin{aligned}
 \hat{B}_x &= \sqrt{\frac{v_{\tilde{n}\tilde{m}}}{4 + 4v_{\tilde{n}\tilde{m}}\chi_{0,\tilde{n}\tilde{m}}}} \sum_{n,m \neq \tilde{n},\tilde{m}} \chi_{0,\tilde{n}m}(x_{n,m} + iy_{n,m}) + \chi_{0,n\tilde{m}}(x_{n,m} - iy_{n,m}) \\
 &= \sqrt{\frac{v_{\tilde{n}\tilde{m}}}{4 + 4v_{\tilde{n}\tilde{m}}\chi_{0,\tilde{n}\tilde{m}}}} \sum_{n,m \neq \tilde{n},\tilde{m}} (\chi_{0,\tilde{n}m} z_{n,m} + \chi_{0,n\tilde{m}} \bar{z}_{n,m})
 \end{aligned} \tag{2.52}$$

$$\phi_y = \sqrt{\frac{2}{v_{\tilde{n}\tilde{m}}} + 2\chi_{0,\tilde{n}\tilde{m}}} y_{\tilde{n},\tilde{m}} \tag{2.53}$$

$$\begin{aligned}
 \hat{B}_y &= \sqrt{\frac{v_{\tilde{n}\tilde{m}}}{4 + 4v_{\tilde{n}\tilde{m}}\chi_{0,\tilde{n}\tilde{m}}}} \sum_{n,m \neq \tilde{n},\tilde{m}} \chi_{0,\tilde{n}m}(-ix_{n,m} + y_{n,m}) + \chi_{0,n\tilde{m}}(ix_{n,m} + y_{n,m}) \\
 &= -i \sqrt{\frac{v_{\tilde{n}\tilde{m}}}{4 + 4v_{\tilde{n}\tilde{m}}\chi_{0,\tilde{n}\tilde{m}}}} \sum_{n,m \neq \tilde{n},\tilde{m}} (\chi_{0,\tilde{n}m} z_{n,m} - \chi_{0,n\tilde{m}} \bar{z}_{n,m}).
 \end{aligned} \tag{2.54}$$

Therefore, the integration of the first pair of auxiliary fields is very easy. After this integration step, we are left with

$$\begin{aligned}
 Z_{q,\Omega_m} &= \frac{1}{1 + v_{\tilde{n}\tilde{m}}\chi_{0,\tilde{n}\tilde{m}}} \Delta\tau \int \prod'_{n,m} \left( \frac{dx_{n,m} dy_{n,m} \Delta\tau}{\pi v_{nm}} \right) \times \\
 &\quad \exp \left( - \sum_{n,m} |z_{n,m}|^2 \left( \frac{1}{v_{nm}} + \chi_{0,nm} \right) - \sum_{n,m} \sum_{n',m' \neq n,m} z_{n,m} \chi_{0,n'm} \bar{z}_{n',m'} \right) \times \\
 &\quad \exp \left( \frac{v_{\tilde{n}\tilde{m}}}{1 + v_{\tilde{n}\tilde{m}}\chi_{0,\tilde{n}\tilde{m}}} \sum_{n,m} \sum_{n',m'} \chi_{0,\tilde{n}m} \chi_{0,n'\tilde{m}} z_{n,m} \bar{z}_{n',m'} \right) \\
 &= \frac{1}{1 + v_{\tilde{n}\tilde{m}}\chi_{0,\tilde{n}\tilde{m}}} \Delta\tau \int \prod'_{n,m} \left( \frac{dx_{n,m} dy_{n,m} \Delta\tau}{\pi v_{nm}} \right) \times \\
 &\quad \exp \left( - \sum_{n,m} |z_{n,m}|^2 \left( \frac{1}{v_{nm}} + \chi_{0,nm} - \frac{v_{\tilde{n}\tilde{m}}\chi_{0,n\tilde{m}}\chi_{0,\tilde{n}m}}{1 + v_{\tilde{n}\tilde{m}}\chi_{0,\tilde{n}\tilde{m}}} \right) \right) \times \\
 &\quad \exp \left( - \sum_{n,m} \sum_{n',m' \neq n,m} z_{n,m} \left( \chi_{0,n'm} - \frac{v_{\tilde{n}\tilde{m}}\chi_{0,n'\tilde{m}}\chi_{0,\tilde{n}m}}{1 + v_{\tilde{n}\tilde{m}}\chi_{0,\tilde{n}\tilde{m}}} \right) \bar{z}_{n',m'} \right), \quad (2.55)
 \end{aligned}$$

where all sums and products are restricted to  $(n, m) \neq (\tilde{n}, \tilde{m})$ . Note that no substantially new term appears, it is still a Gaussian integration. We can include the additional term in the susceptibility by defining

$$\chi'_{0,nm} = \chi_{0,nm} - \frac{v_{\tilde{n}\tilde{m}}\chi_{0,n\tilde{m}}\chi_{0,\tilde{n}m}}{1 + v_{\tilde{n}\tilde{m}}\chi_{0,\tilde{n}\tilde{m}}}. \quad (2.56)$$

This procedure is repeated for all remaining  $z_{n,m}$  except  $z_{1,1}$ . Naturally, the result has to be independent of the sequence of the integration, which is shown in the appendix, section A.2. Applying this method, the sums will get shorter in every step, but the susceptibilities will become more and more complicated, since we always have to redefine them according to eq. (2.56). In the end, we will only have to consider one auxiliary field,  $z_{1,1}$ , and therefore only one final susceptibility  $\tilde{\chi}_{0,11}$ , so

$$Z_{q,\Omega_m} \propto \exp \left( -|z_{1,1}|^2 \left( \frac{1}{v_{11}} + \tilde{\chi}_{0,11} \right) \right). \quad (2.57)$$

The contribution of the high-energy bands leads to the screening of the target band interaction  $v_{11}$ , which is the typical result of the RPA-method. If we return to the partition function, we can read off the complete expression of this screening term:

$$\begin{aligned}
 Z &\propto \int \prod_{q,\Omega_m} \left( \frac{d\text{Re}(z_{q,1,1,\Omega_m}) d\text{Im}(z_{q,1,1,\Omega_m}) \Delta\tau}{\pi v_{11}(q)} \right) \times \\
 &\quad \exp(-S_0) \prod_{q,\Omega_m} \exp \left( -|z_{q,1,1,\Omega_m}|^2 \left( \tilde{\chi}_{0,11}(q, \Omega_m) - \chi_{0,11}(q, \Omega_m) \right) \right), \quad (2.58)
 \end{aligned}$$

so we finally obtain

$$\chi_{\text{eff}}(q, \Omega_m) = \tilde{\chi}_{0,11}(q, \Omega_m) - \chi_{0,11}(q, \Omega_m). \quad (2.59)$$

We will analyze this result in section 3.1 by applying it to a simple three-band model. Before that, we will present an alternative cRPA method.

## 2.2 cRPA method 2

This second method is formulated for the more general case of a system, where no localization of the low-energy band is necessary. Without localization, we cannot work with the Wannier operators  $c^\dagger, c$ , but have to rewrite the interacting part of the Hamiltonian using the band operators  $\gamma^\dagger, \gamma$ :

$$\begin{aligned} \hat{H}_I &= \frac{1}{L} \sum_{l,l'} \sum_{k,k'} \sum_{q>0} v_{ll'}(q) c_{l,k}^\dagger c_{l,k+q} c_{l',k'}^\dagger c_{l',k'-q} \\ &= \frac{1}{L} \sum_{n,m} \sum_{n',m'} \sum_{k,k'} \sum_{q>0} v_{nmn'm'kk'}(q) \gamma_{n,k}^\dagger \gamma_{m,k+q} \gamma_{n',k'}^\dagger \gamma_{m',k'-q} \end{aligned} \quad (2.60)$$

Here, we have absorbed the transformation of the operators from  $c^\dagger, c$  to  $\gamma^\dagger, \gamma$  in the interaction strength:

$$v_{nmn'm'kk'}(q) = \sum_{l,l'} v_{ll'}(q) U_{ln}^\dagger(k) U_{ml}(k+q) U_{l'n'}^\dagger(k') U_{m'l'}(k'-q) \quad (2.61)$$

Because of the large number of indices, it is useful to abbreviate the notation by defining  $\alpha = (n, m, k)$  and  $\hat{n}_\alpha(q) = \frac{1}{\sqrt{L}} \gamma_{n,k}^\dagger \gamma_{m,k+q}$ . Therefore, the full Hamiltonian reads

$$\hat{H} = \hat{H}_0 + \hat{H}_I = \sum_{n,k} E_n(k) \gamma_{n,k}^\dagger \gamma_{n,k} + \sum_{\alpha,\alpha'} \sum_{q>0} v_{\alpha,\alpha'}(q) \hat{n}_\alpha(q) \hat{n}_{\alpha'}(-q) \quad (2.62)$$

with an arbitrary band structure expressed by  $E_n(k)$ .

### 2.2.1 Calculating the action

Just like for the first method, we start with the partition function (eq. (2.1)) and do the Hubbard-Stratonovich transformation (eq. (2.2)). For this purpose, we have to create square terms for  $\hat{H}_I$ . However, in contrast to  $\hat{n}_n(q)$ , the densities  $\hat{n}_\alpha(q)$  do not commute:

$$\begin{aligned} &[\hat{n}_\alpha(q), \hat{n}_{\alpha'}(q')] \\ &= \frac{1}{L} [\gamma_{n,k}^\dagger \gamma_{m,k+q}, \gamma_{n',k'}^\dagger \gamma_{m',k'+q'}] \\ &= \frac{1}{L} \left( \gamma_{n,k}^\dagger \gamma_{m',k'+q'} \delta_{m,n'} \delta_{k',k+q} - \gamma_{n',k'}^\dagger \gamma_{m,k+q} \delta_{m',n} \delta_{k,k'+q'} \right) \end{aligned} \quad (2.63)$$

Nevertheless, we can write  $\hat{H}_I$  as

$$\begin{aligned}\hat{H}_I &= \sum_{q>0} \sum_{\alpha, \alpha'} \frac{v_{\alpha, \alpha'}(q)}{4} \left( (\hat{n}_\alpha(q) + \hat{n}_{\alpha'}(-q))^2 - (\hat{n}_\alpha(q) - \hat{n}_{\alpha'}(-q))^2 \right) \\ &= \sum_{q>0} \sum_{\alpha, \alpha'} v_{\alpha, \alpha'}(q) \left( \hat{n}_\alpha(q) \hat{n}_{\alpha'}(-q) + \frac{1}{2} [\hat{n}_{\alpha'}(-q), \hat{n}_\alpha(q)] \right),\end{aligned}\quad (2.64)$$

since the commutation term vanishes, if we consider the sums over  $\alpha$  and  $\alpha'$  (see appendix, section A.3). The expression for the partition function we obtain after the Hubbard-Stratonovich transformation is

$$Z = \text{Tr} \left( \prod_{\tau=0}^{\beta} e^{-\Delta\tau \hat{H}_0(\tau)} \int \prod_{q, \alpha, \alpha', \tau} \left( \frac{d\phi_{q, \alpha, \alpha', \tau} d\varphi_{q, \alpha, \alpha', \tau}}{2\pi} \right) e^{-\tilde{S}(\phi_{q, \alpha, \alpha', \tau}, \varphi_{q, \alpha, \alpha', \tau})} \right) \quad (2.65)$$

with

$$\begin{aligned}\tilde{S}(\phi_{q, \alpha, \alpha', \tau}, \varphi_{q, \alpha, \alpha', \tau}) &= \sum_{\alpha, \alpha'} \sum_{q>0} \left( \frac{\phi_{q, \alpha, \alpha', \tau}^2}{2} + i\phi_{q, \alpha, \alpha', \tau} \sqrt{\frac{\Delta\tau v_{\alpha, \alpha'}(q)}{2}} (\hat{n}_\alpha(q) + \hat{n}_{\alpha'}(-q)) \right. \\ &\quad \left. + \frac{\varphi_{q, \alpha, \alpha', \tau}^2}{2} + \varphi_{q, \alpha, \alpha', \tau} \sqrt{\frac{\Delta\tau v_{\alpha, \alpha'}(q)}{2}} (\hat{n}_\alpha(q) - \hat{n}_{\alpha'}(-q)) \right).\end{aligned}\quad (2.66)$$

Again, we substitute  $\phi_{q, \alpha, \alpha', \tau}$  and  $\varphi_{q, \alpha, \alpha', \tau}$  by

$$z_{q, \alpha, \alpha', \tau} = \sqrt{\frac{v_{\alpha, \alpha'}(q)}{2\Delta\tau}} (\phi_{q, \alpha, \alpha', \tau} + i\varphi_{q, \alpha, \alpha', \tau}). \quad (2.67)$$

With this definition, we have

$$\begin{aligned}\tilde{S} &= \sum_{\alpha, \alpha'} \sum_{q>0} \left( \frac{\phi_{q, \alpha, \alpha', \tau}^2}{2} + \frac{\varphi_{q, \alpha, \alpha', \tau}^2}{2} + \right. \\ &\quad \left. i\sqrt{\frac{\Delta\tau v_{\alpha, \alpha'}(q)}{2}} \left( (\phi_{q, \alpha, \alpha', \tau} - i\varphi_{q, \alpha, \alpha', \tau}) \hat{n}_\alpha(q) + (\phi_{q, \alpha, \alpha', \tau} + i\varphi_{q, \alpha, \alpha', \tau}) \hat{n}_{\alpha'}(-q) \right) \right) \\ &= \Delta\tau \sum_{\alpha, \alpha'} \sum_{q>0} \left( \frac{|z_{q, \alpha, \alpha', \tau}|^2}{v_{\alpha, \alpha'}(q)} + i(\bar{z}_{q, \alpha, \alpha', \tau} \hat{n}_\alpha(q) + z_{q, \alpha, \alpha', \tau} \hat{n}_{\alpha'}(-q)) \right).\end{aligned}\quad (2.68)$$

The trace does not effect the auxiliary fields, so we can write

$$Z = \int \prod_{\tau=0}^{\beta} \prod_{q, \alpha, \alpha'} \left( \frac{d\text{Re}(z_{q, \alpha, \alpha', \tau}) d\text{Im}(z_{q, \alpha, \alpha', \tau}) \Delta\tau}{\pi v_{\alpha, \alpha'}(q)} \right) e^{-S(z_{q, \alpha, \alpha', \tau}, \bar{z}_{q, \alpha, \alpha', \tau})}. \quad (2.69)$$



The action  $S(z_{q,\alpha,\alpha',\tau}, \bar{z}_{q,\alpha,\alpha',\tau})$  is given by

$$S(z_{q,\alpha,\alpha',\tau}, \bar{z}_{q,\alpha,\alpha',\tau}) = \Delta\tau \sum_{\tau,\alpha,\alpha'} \sum_{q>0} \frac{|z_{q,\alpha,\alpha',\tau}|^2}{v_{\alpha,\alpha'}(q)} - \log \left( \text{Tr} \left( \prod_{\tau=0}^{\beta} \exp \left( -\Delta\tau \hat{H}_0(\tau) - i\Delta\tau \sum_{\alpha,\alpha'} \sum_{q>0} (\bar{z}_{q,\alpha,\alpha',\tau} \hat{n}_{\alpha}(q) + z_{q,\alpha,\alpha',\tau} \hat{n}_{\alpha'}(-q)) \right) \right) \right). \quad (2.70)$$

The approximation procedure for the calculation of an appropriate effective model starts from this expression.

## 2.2.2 Approximating the action

Our considerations are basically not very different from the first approximation method: Again, we assume that the interplay between high-energy and low-energy features is relatively small, so that we can split up the trace into a trace over the low-energy part  $\text{Tr}_L$  and a trace over the high-energy part  $\text{Tr}_H$ . Therefore, we can also distinguish between the low-energy and the high-energy part of the action:  $S \approx S_L + S_H$ . We use the indices  $\alpha_1$  and  $\alpha'_1$  which are defined by  $\alpha_1, \alpha'_1 = (1, 1, k)$  with arbitrary  $k$ , where index 1 again indicates the target band. The low-energy part is represented by the operators  $\hat{n}_{\alpha_1}(q)$  and  $\hat{n}_{\alpha'_1}(-q)$ , since these are the only operators that are solely related to the target band. Thus, the low-energy part of the action is

$$S_L = \Delta\tau \sum_{\tau} \sum_{\alpha_1, \alpha'_1} \sum_{q>0} \frac{|z_{q,\alpha_1, \alpha'_1, \tau}|^2}{v_{\alpha_1, \alpha'_1}(q)} - \log \left( \text{Tr}_L \left( \prod_{\tau=0}^{\beta} \exp \left( -\Delta\tau \hat{H}_{0,L}(\tau) - i\Delta\tau \sum_{\alpha, \alpha'_1} \sum_{q>0} (\bar{z}_{q,\alpha, \alpha'_1, \tau} \hat{n}_{\alpha'_1}(q) + z_{q,\alpha, \alpha'_1, \tau} \hat{n}_{\alpha'_1}(-q)) \right) \right) \right), \quad (2.71)$$

whereas the high-energy part is

$$S_H = \Delta\tau \sum_{\tau} \sum_{\alpha, \alpha'}^{\neq \alpha_1, \alpha'_1} \sum_{q>0} \frac{|z_{q,\alpha, \alpha', \tau}|^2}{v_{\alpha, \alpha'}(q)} - \log \left( \text{Tr}_H \left( \prod_{\tau=0}^{\beta} \exp \left( -\Delta\tau \hat{H}_{0,H}(\tau) - i\Delta\tau \sum_{\alpha} \sum_{\alpha'}^{\neq \alpha_1} \sum_{q>0} (\bar{z}_{q,\alpha, \alpha', \tau} \hat{n}_{\alpha}(q) + z_{q,\alpha, \alpha', \tau} \hat{n}_{\alpha}(-q)) \right) \right) \right). \quad (2.72)$$

The allocation of the square terms of the auxiliary fields is actually not necessary, but it is useful to think about the energy regime they are related to. Of course,  $z_{q,\alpha_1, \alpha'_1, \tau}$  and  $\bar{z}_{q,\alpha_1, \alpha'_1, \tau}$  are purely connected to the low-energy part, while  $z_{q,\alpha, \alpha', \tau}$  and  $\bar{z}_{q,\alpha, \alpha', \tau}$  with  $\alpha \neq \alpha_1$  and  $\alpha' \neq \alpha_1$  correspond to the high-energy part. For this reason, these auxiliary fields only appear in the low and high-energy part of the action, respectively. However, there are also fields with only one index  $\alpha_1$ . These fields are responsible for the coupling between the two energy regimes, since they couple to  $\hat{n}_{\alpha_1}(q)$  or  $\hat{n}_{\alpha_1}(-q)$  in eq. (2.71) and

to  $\hat{n}_\alpha(q)$  or  $\hat{n}_\alpha(-q)$ , with  $\alpha \neq \alpha_1$ , in eq. (2.72).  $S_L$  contains all the low-energy properties which are especially important, so we want to treat it exactly. In contrast, we have to find an appropriate approximation for  $S_H$  in order to make the calculation feasible. For this purpose, we return to the Taylor expansion around the saddle point of cRPA method 1:

$$\begin{aligned}
 S_H(z, \bar{z}) &\approx S_H(0, 0) \\
 &+ \sum_{q, \alpha, \alpha', \tau} \frac{\partial S_H}{\partial z_{q, \alpha, \alpha', \tau}} \Big|_{z=0, \bar{z}=0} z_{q, \alpha, \alpha', \tau} + \sum_{q, \alpha, \alpha', \tau} \frac{\partial S_H}{\partial \bar{z}_{q, \alpha, \alpha', \tau}} \Big|_{z=0, \bar{z}=0} \bar{z}_{q, \alpha, \alpha', \tau} \\
 &+ \sum_{q, \alpha, \alpha', \tau} \sum_{\tilde{q}, \tilde{\alpha}, \tilde{\alpha}', \tilde{\tau}} \frac{\partial^2 S_H}{\partial z_{q, \alpha, \alpha', \tau} \partial \bar{z}_{\tilde{q}, \tilde{\alpha}, \tilde{\alpha}', \tilde{\tau}}} \Big|_{z=0, \bar{z}=0} z_{q, \alpha, \alpha', \tau} \bar{z}_{\tilde{q}, \tilde{\alpha}, \tilde{\alpha}', \tilde{\tau}} \\
 &+ \frac{1}{2} \sum_{q, \alpha, \alpha', \tau} \sum_{\tilde{q}, \tilde{\alpha}, \tilde{\alpha}', \tilde{\tau}} \frac{\partial^2 S}{\partial z_{q, \alpha, \alpha', \tau} \partial z_{\tilde{q}, \tilde{\alpha}, \tilde{\alpha}', \tilde{\tau}}} \Big|_{z=0, \bar{z}=0} z_{q, \alpha, \alpha', \tau} z_{\tilde{q}, \tilde{\alpha}, \tilde{\alpha}', \tilde{\tau}} \\
 &+ \frac{1}{2} \sum_{q, \alpha, \alpha', \tau} \sum_{\tilde{q}, \tilde{\alpha}, \tilde{\alpha}', \tilde{\tau}} \frac{\partial^2 S}{\partial \bar{z}_{q, \alpha, \alpha', \tau} \partial \bar{z}_{\tilde{q}, \tilde{\alpha}, \tilde{\alpha}', \tilde{\tau}}} \Big|_{z=0, \bar{z}=0} \bar{z}_{q, \alpha, \alpha', \tau} \bar{z}_{\tilde{q}, \tilde{\alpha}, \tilde{\alpha}', \tilde{\tau}} \tag{2.73}
 \end{aligned}$$

According to this approximation method, the first derivatives should of course vanish. We will check this in the following, where we calculate all the terms appearing above.

### First term

If we set all fields equal to zero, we get

$$S_{H,0} \equiv S_H(0, 0) = -\log \left( \text{Tr}_H \left( \prod_{\tau=0}^{\beta} \exp \left( -\Delta\tau \hat{H}_{0,H}(\tau) \right) \right) \right). \tag{2.74}$$

So this term only contains the non-interacting part of the Hamiltonian for the host bands.

### First derivatives

It is again useful to define an operator

$$\begin{aligned}
 \hat{U}'(\tau_1, \tau_2) &= \\
 &\prod_{\tau=\tau_2}^{\tau_1} \exp \left( -\Delta\tau \hat{H}_{0,H}(\tau) - i\Delta\tau \sum_{\alpha} \sum_{\alpha'} \sum_{q>0}^{\neq \alpha_1} (\bar{z}_{q, \alpha, \alpha', \tau} \hat{n}_\alpha(q) + z_{q, \alpha', \alpha, \tau} \hat{n}_\alpha(-q)) \right), \tag{2.75}
 \end{aligned}$$

which becomes the time evolution operator of the non-interacting system, if the auxiliary fields vanish.

We need to calculate the first derivatives of  $S_H$  with respect to  $z_{q, \alpha, \alpha', \tau}$  with  $\alpha' \neq \alpha_1$  and with respect to  $\bar{z}_{q, \alpha, \alpha', \tau}$  with  $\alpha \neq \alpha_1$ . In the first case, the result is

$$\begin{aligned}
 \frac{\partial S_H}{\partial z_{q, \alpha, \alpha', \tau}} \Big|_{z=0, \bar{z}=0} &= \left( \frac{\Delta\tau \bar{z}_{q, \alpha, \alpha', \tau}}{v_{\alpha, \alpha'}(q)} + \frac{i\Delta\tau}{\text{Tr}(U(\beta, 0))} \text{Tr}(U(\beta, \tau) \hat{n}_{\alpha'}(-q, \tau) U(\tau, 0)) \right) \Big|_{z=0, \bar{z}=0} \\
 &= i\Delta\tau \langle \hat{n}_{\alpha'}(-q, \tau) \rangle_0 = \frac{i\Delta\tau}{\sqrt{L}} \langle \gamma_{n', k'}^\dagger(\tau) \gamma_{m', k'-q}(\tau) \rangle_0 = 0. \tag{2.76}
 \end{aligned}$$

Similarly, we get for the second case

$$\frac{\partial S_H}{\partial \bar{z}_{q,\alpha,\alpha',\tau}} \Big|_{z=0,\bar{z}=0} = \left( \frac{\Delta\tau z_{q,\alpha,\alpha',\tau}}{v_{\alpha,\alpha'}(q)} \Big|_{z=0,\bar{z}=0} + i\Delta\tau \langle \hat{n}_\alpha(q, \tau) \rangle_0 \right) = 0. \quad (2.77)$$

Thus, both derivatives vanish, just as we expected. This result confirms that the expansion around zero auxiliary fields is identical to an expansion around the saddle point.

## Second derivatives

We have to consider second derivatives of  $S_H$  with respect to combinations of  $z_{q,\alpha,\alpha',\tau}$  and  $\bar{z}_{\tilde{q},\tilde{\alpha},\tilde{\alpha}',\tilde{\tau}}$ , but only for  $\alpha' \neq \alpha_1$  or  $\tilde{\alpha} \neq \alpha_1$ . The first expression we calculate is

$$\begin{aligned} \frac{\partial^2 S_H}{\partial z_{q,\alpha,\alpha',\tau} \partial \bar{z}_{\tilde{q},\tilde{\alpha},\tilde{\alpha}',\tilde{\tau}}} \Big|_{z=0,\bar{z}=0} &= \frac{\Delta\tau}{v_{\alpha,\alpha'}(q)} \delta_{\alpha,\tilde{\alpha}} \delta_{\alpha',\tilde{\alpha}'} \delta_{q,\tilde{q}} \delta_{\tau,\tilde{\tau}} \\ &+ \Delta\tau^2 \left( \langle \hat{T} \hat{n}_{\alpha'}(-q, \tau) \hat{n}_{\tilde{\alpha}}(\tilde{q}, \tilde{\tau}) \rangle_0 - \langle \hat{n}_{\alpha'}(-q, \tau) \rangle_0 \langle \hat{n}_{\tilde{\alpha}}(\tilde{q}, \tilde{\tau}) \rangle_0 \right) \\ &= \frac{\Delta\tau}{v_{\alpha,\alpha'}(q)} \delta_{\alpha,\tilde{\alpha}} \delta_{\alpha',\tilde{\alpha}'} \delta_{q,\tilde{q}} \delta_{\tau,\tilde{\tau}} + \Delta\tau^2 \langle \hat{T} \hat{n}_{\alpha'}(-q, \tau) \hat{n}_{\tilde{\alpha}}(q, \tilde{\tau}) \rangle_0 \delta_{q,\tilde{q}}. \end{aligned} \quad (2.78)$$

The result is essentially the same as for cRPA method 1 and it motivates again to define a generalized susceptibility

$$\chi_{0,\alpha,\tilde{\alpha}}(q, \tau - \tilde{\tau}) \equiv \langle \hat{T} \hat{n}_\alpha(-q, \tau) \hat{n}_{\tilde{\alpha}}(q, \tilde{\tau}) \rangle_0. \quad (2.79)$$

As before,  $\chi_{0,\alpha,\tilde{\alpha}}$  is a property of the non-interacting system and only depends on the time difference. Note that due to our approximation scheme, there is no susceptibility with the target band related index  $\alpha_1$  in our equations.

The second derivatives  $\frac{\partial^2 S_H}{\partial z \partial z}$  and  $\frac{\partial^2 S_H}{\partial \bar{z} \partial \bar{z}}$  both vanish because of momentum conservation:

$$\begin{aligned} \frac{\partial^2 S_H}{\partial z_{q,\alpha,\alpha',\tau} \partial z_{\tilde{q},\tilde{\alpha},\tilde{\alpha}',\tilde{\tau}}} \Big|_{z=0,\bar{z}=0} &= \\ \Delta\tau^2 \left( \langle \hat{T} \hat{n}_{\alpha'}(-q, \tau) \hat{n}_{\tilde{\alpha}'}(-\tilde{q}, \tilde{\tau}) \rangle_0 - \langle \hat{n}_{\alpha'}(-q, \tau) \rangle_0 \langle \hat{n}_{\tilde{\alpha}'}(-\tilde{q}, \tilde{\tau}) \rangle_0 \right) &= 0 \end{aligned} \quad (2.80)$$

and

$$\begin{aligned} \frac{\partial^2 S_H}{\partial \bar{z}_{q,\alpha,\alpha',\tau} \partial \bar{z}_{\tilde{q},\tilde{\alpha},\tilde{\alpha}',\tilde{\tau}}} \Big|_{z=0,\bar{z}=0} &= \\ \Delta\tau^2 \left( \langle \hat{T} \hat{n}_\alpha(q, \tau) \hat{n}_{\tilde{\alpha}}(\tilde{q}, \tilde{\tau}) \rangle_0 - \langle \hat{n}_\alpha(q, \tau) \rangle_0 \langle \hat{n}_{\tilde{\alpha}}(\tilde{q}, \tilde{\tau}) \rangle_0 \right) &= 0, \end{aligned} \quad (2.81)$$

respectively. Now we have all required terms and can go on with the next steps.

### 2.2.3 Fourier transformation

It is advantageous to use the Fourier transform of  $\chi_{0,\alpha,\tilde{\alpha}}(q, \tau - \tilde{\tau})$ , as we did in the previous section. We therefore define

$$\chi_{0,\alpha,\tilde{\alpha}}(q, \tau) = \frac{1}{\beta} \sum_{\Omega_m} e^{-i\Omega_m \tau} \chi_{0,\alpha,\tilde{\alpha}}(q, \Omega_m) \quad (2.82)$$

with the bosonic Matsubara frequencies  $\Omega_m = \frac{2\pi m}{\beta}$ . We can rewrite the non-vanishing second derivatives as

$$\begin{aligned} \left. \frac{\partial^2 S_H}{\partial z_{q,\alpha,\alpha',\tau} \partial \bar{z}_{\bar{q},\bar{\alpha},\bar{\alpha}',\bar{\tau}}} \right|_{z=0,\bar{z}=0} &= \frac{\Delta\tau}{v_{\alpha,\alpha'}(q)} \delta_{\alpha,\bar{\alpha}} \delta_{\alpha',\bar{\alpha}'} \delta_{q,\bar{q}} \delta_{\tau,\bar{\tau}} + \Delta\tau^2 \langle \hat{T} \hat{n}_{\alpha'}(-q, \tau) \hat{n}_{\bar{\alpha}}(q, \bar{\tau}) \rangle_0 \delta_{q,\bar{q}} \\ &= \Delta\tau^2 \frac{\delta_{q,\bar{q}}}{\beta} \sum_{\Omega_m} \left( \frac{\delta_{\alpha,\bar{\alpha}} \delta_{\alpha',\bar{\alpha}'}}{v_{\alpha,\alpha'}(q)} e^{i\Omega_m(\bar{\tau}-\tau)} + e^{i\Omega_m(\bar{\tau}-\tau)} \chi_{0,\alpha',\bar{\alpha}}(q, \Omega_m) \right). \end{aligned} \quad (2.83)$$

In order to simplify the notation, we define the new quantity

$$\chi_{\alpha',\alpha}^0(q, \Omega_m) \equiv (1 - \delta_{\alpha,\alpha_1})(1 - \delta_{\alpha',\alpha'_1}) \chi_{0,\alpha',\alpha}(q, \Omega_m). \quad (2.84)$$

So we artificially introduce susceptibilities which contain  $\alpha_1$ , but set them equal to zero, since otherwise we had to distinguish in a complicated way between indices equal to and different from  $\alpha_1$ . Within the scope of our approximation, we can write down the complete high-energy action as

$$\begin{aligned} S_H(z, \bar{z}) &+ \sum_{\alpha_1, \alpha'_1} \sum_{q>0} \int_0^\beta d\tau \frac{|z_{q,\alpha_1, \alpha'_1, \tau}|^2}{v_{\alpha_1, \alpha'_1}(q)} \\ &= S_{H,0} + \sum_{q>0} \sum_{\tilde{q}>0} \sum_{\alpha, \alpha'} \sum_{\bar{\alpha}, \bar{\alpha}'} \int_0^\beta d\tau \int_0^\beta d\tilde{\tau} \sum_{\Omega_m} \frac{\delta_{q,\tilde{q}}}{\beta} e^{i\Omega_m(\tilde{\tau}-\tau)} \times \\ &\quad z_{q,\alpha,\alpha',\tau} \left( \frac{\delta_{\alpha,\bar{\alpha}} \delta_{\alpha',\bar{\alpha}'}}{v_{\alpha,\alpha'}(q)} + \chi_{\alpha',\bar{\alpha}}^0(q, \Omega_m) \right) \bar{z}_{\bar{q},\bar{\alpha},\bar{\alpha}',\bar{\tau}} \\ &= S_{H,0} + \sum_{q>0} \sum_{\Omega_m} \sum_{\alpha, \alpha'} \sum_{\bar{\alpha}, \bar{\alpha}'} z_{q,\alpha,\alpha',\Omega_m} \left( \frac{\delta_{\alpha,\bar{\alpha}} \delta_{\alpha',\bar{\alpha}'}}{v_{\alpha,\alpha'}(q)} + \chi_{\alpha',\bar{\alpha}}^0(q, \Omega_m) \right) \bar{z}_{\bar{q},\bar{\alpha},\bar{\alpha}',\Omega_m}. \end{aligned} \quad (2.85)$$

Here, we used the Fourier transform of  $z_{q,\alpha,\alpha',\tau}$  and  $\bar{z}_{\bar{q},\bar{\alpha},\bar{\alpha}',\bar{\tau}}$

$$\begin{aligned} z_{q,\alpha,\alpha',\Omega_m} &= \frac{1}{\sqrt{\beta}} \int_0^\beta d\tau e^{-i\Omega_m\tau} z_{q,\alpha,\alpha',\tau} \\ \bar{z}_{\bar{q},\bar{\alpha},\bar{\alpha}',\Omega_m} &= \frac{1}{\sqrt{\beta}} \int_0^\beta d\tau e^{i\Omega_m\tau} \bar{z}_{\bar{q},\bar{\alpha},\bar{\alpha}',\tau}. \end{aligned} \quad (2.86)$$

Likewise,  $\hat{n}_{\alpha_1}(q, \tau)$  and  $\hat{n}_{\alpha_1}(-q, \tau)$  have to be Fourier transformed, since they still appear in the low-energy action:

$$\begin{aligned} \hat{n}_{\alpha_1}(q, \Omega_m) &= \frac{1}{\sqrt{\beta}} \int_0^\beta d\tau e^{-i\Omega_m\tau} \hat{n}_{\alpha_1}(q, \tau) \\ \hat{n}_{\alpha_1}(-q, \Omega_m) &= \frac{1}{\sqrt{\beta}} \int_0^\beta d\tau e^{i\Omega_m\tau} \hat{n}_{\alpha_1}(-q, \tau) \end{aligned} \quad (2.87)$$

Expressed by this Fourier transformed quantities, we obtain the coupling term of the low-energy action:

$$\begin{aligned}
 & \sum_{\alpha, \alpha'} \sum_{q>0} \int_0^\beta d\tau \left( \bar{z}_{q, \alpha', \alpha, \tau} \hat{n}_{\alpha'}(q, \tau) + z_{q, \alpha, \alpha', \tau} \hat{n}_{\alpha'}(-q, \tau) \right) = \\
 & \sum_{\alpha, \alpha'} \sum_{q>0} \int_0^\beta d\tau \int_0^\beta d\tilde{\tau} \sum_{\Omega_m} \frac{1}{\beta} e^{i\Omega_m(\tilde{\tau}-\tau)} \left( \bar{z}_{q, \alpha', \alpha, \tilde{\tau}} \hat{n}_{\alpha'}(q, \tau) + z_{q, \alpha, \alpha', \tau} \hat{n}_{\alpha'}(-q, \tilde{\tau}) \right) = \\
 & \sum_{\alpha, \alpha'} \sum_{q>0} \sum_{\Omega_m} \left( \bar{z}_{q, \alpha', \alpha, \Omega_m} \hat{n}_{\alpha'}(q, \Omega_m) + z_{q, \alpha, \alpha', \Omega_m} \hat{n}_{\alpha'}(-q, \Omega_m) \right) \quad (2.88)
 \end{aligned}$$

We can now put together  $S_H$  and  $S_L$  to the total action  $S$  and separate the square terms from the mixed ones:

$$\begin{aligned}
 S = & S_{H,0} + \sum_{q>0} \sum_{\Omega_m} \sum_{\alpha, \alpha'} |z_{q, \alpha, \alpha', \Omega_m}|^2 \left( \frac{1}{v_{\alpha, \alpha'}(q)} + \chi_{\alpha', \alpha}^0(q, \Omega_m) \right) \\
 & + \sum_{q>0} \sum_{\Omega_m} \sum_{\alpha, \alpha'} \sum_{\tilde{\alpha}, \tilde{\alpha}'} (1 - \delta_{\alpha, \tilde{\alpha}} \delta_{\alpha', \tilde{\alpha}'} ) z_{q, \alpha, \alpha', \Omega_m} \chi_{\alpha', \tilde{\alpha}}^0(q, \Omega_m) \bar{z}_{q, \tilde{\alpha}, \tilde{\alpha}', \Omega_m} \\
 & - \log \left( \text{Tr}_L \left( \prod_{\Omega_m} \exp \left( -H_{0,L} - i \sum_{\alpha, \alpha'} \sum_{q>0} \left( \bar{z}_{q, \alpha', \alpha, \Omega_m} \hat{n}_{\alpha'}(q) + z_{q, \alpha, \alpha', \Omega_m} \hat{n}_{\alpha'}(-q) \right) \right) \right) \right) \quad (2.89)
 \end{aligned}$$

Comparing this expression to eq. (2.46), we find very similar terms for the high-energy auxiliary fields. However, the treatment of the target band related quantities is quite different. Here, we still have the low-energy trace  $\text{Tr}_L$  as well as the target band operators  $\hat{n}_{\alpha'}(q)$  and  $\hat{n}_{\alpha'}(-q)$ , whereas for cRPA method 1, the low-energy physics is supposed to be represented only by the low-energy auxiliary fields.

## 2.2.4 Integration

As we have seen, the approximation for the action  $S$  contains some terms that do not appear in the first method. Another difference is the presence of the target band operators. Therefore, we will choose another integration strategy: we integrate out all auxiliary fields, both of the host bands and the target band. Doing so, we will get square terms of the operators  $\hat{n}_{\alpha'}(q)$  and  $\hat{n}_{\alpha'}(-q)$ , which form the interacting part of an effective Hamiltonian.

Using eq. (2.89) we can rewrite the partition function as

$$\begin{aligned}
 Z = & \int \prod_{q, \Omega_m} \prod_{\alpha, \alpha'} \left( \frac{dRe(z_{q, \alpha, \alpha', \Omega_m}) dIm(z_{q, \alpha, \alpha', \Omega_m}) \Delta\tau}{\pi v_{\alpha, \alpha'}(q)} \right) \exp(-S) \\
 = & \exp(-S_{H,0}) \text{Tr}_L \left( \prod_{\Omega_m} e^{-H_{0,L}} \prod_q Z_{\Omega_m, q} \right). \quad (2.90)
 \end{aligned}$$

Thus, we can again take advantage of the fact that the integration can be performed independently for all  $q$  and  $\Omega_m$  and omit these indices in the following for simplicity.

In a matrix formulation, the integration, i.e. the inversion of the Hubbard-Stratonovich transformation, reads [20]

$$\int \prod_j \frac{d\phi_j}{\sqrt{2\pi}} \exp \left( -\frac{1}{2} \sum_{i,j} \phi_i A_{ij} \phi_j + \sum_j J_j \phi_j \right) = (\det A)^{-\frac{1}{2}} \exp \left( \frac{1}{2} \sum_{i,j} J_i A_{ij}^{-1} J_j \right) \quad (2.91)$$

with

$$\phi = \begin{pmatrix} x_{\alpha_1, \alpha'_1} \\ y_{\alpha_1, \alpha'_1} \\ x_{\alpha_1, \alpha'} \\ y_{\alpha_1, \alpha'} \\ x_{\alpha, \alpha'_1} \\ y_{\alpha, \alpha'_1} \\ x_{\alpha, \alpha'} \\ y_{\alpha, \alpha'} \end{pmatrix}, \quad J = \begin{pmatrix} -i \hat{n}_{\alpha_1}(q) - i \hat{n}_{\alpha'_1}(-q) \\ -\hat{n}_{\alpha_1}(q) + \hat{n}_{\alpha'_1}(-q) \\ -i \hat{n}_{\alpha_1}(q) \\ -\hat{n}_{\alpha_1}(q) \\ -i \hat{n}_{\alpha'_1}(-q) \\ \hat{n}_{\alpha'_1}(-q) \\ 0 \\ 0 \end{pmatrix}.$$

and

$$A = \begin{pmatrix} V_{\alpha_1, \alpha'_1}^{-1} & 0 & 0 & 0 & 0 & 0 & 0 & 0 \\ 0 & V_{\alpha_1, \alpha'_1}^{-1} & 0 & 0 & 0 & 0 & 0 & 0 \\ 0 & 0 & V_{\alpha_1, \alpha'}^{-1} & 0 & X_{\alpha', \alpha}^1 & -i X_{\alpha', \alpha}^1 & X_{\alpha', \alpha}^3 & -i X_{\alpha', \alpha}^3 \\ 0 & 0 & 0 & V_{\alpha_1, \alpha'}^{-1} & i X_{\alpha', \alpha}^1 & X_{\alpha', \alpha}^1 & i X_{\alpha', \alpha}^3 & X_{\alpha', \alpha}^3 \\ 0 & 0 & X_{\alpha', \alpha}^2 & i X_{\alpha', \alpha}^2 & V_{\alpha, \alpha'_1}^{-1} & 0 & X_{\alpha', \alpha}^4 & i X_{\alpha', \alpha}^4 \\ 0 & 0 & -i X_{\alpha', \alpha}^2 & X_{\alpha', \alpha}^2 & 0 & V_{\alpha, \alpha'_1}^{-1} & -i X_{\alpha', \alpha}^4 & X_{\alpha', \alpha}^4 \\ 0 & 0 & X_{\alpha', \alpha}^5 & i X_{\alpha', \alpha}^5 & X_{\alpha', \alpha}^6 & -i X_{\alpha', \alpha}^6 & V_{\alpha, \alpha'}^{-1} + X_{\alpha', \alpha}^7 & i X_{\alpha', \alpha}^7 \\ 0 & 0 & -i X_{\alpha', \alpha}^5 & X_{\alpha', \alpha}^5 & i X_{\alpha', \alpha}^6 & X_{\alpha', \alpha}^6 & -i X_{\alpha', \alpha}^7 & V_{\alpha, \alpha'}^{-1} + X_{\alpha', \alpha}^7 \end{pmatrix}$$

Note that the entries of the vector  $\phi$  are vectors itself. Their dimensions are determined by the number of different indices  $\alpha$ ,  $\alpha'$ ,  $\alpha_1$  and  $\alpha'_1$ . The entries of vector  $J$  and matrix  $A$  are vectors and matrices as well, with the appropriate dimensionality.  $V$  and  $X$  are related to the interaction terms and the susceptibility contribution, respectively. We use the inverse matrices  $V^{-1}$  to recall that the interaction prefactors of the original Hamiltonian appear in the denominator after the Hubbard-Stratonovich transformation. In order to discriminate between the matrices  $X$ , we introduce the superscript  $n = 1, 2, \dots, 7$ .

Using this notation, one immediately sees that the low-energy auxiliary fields are completely decoupled. The coupling between different auxiliary fields arises from the RPA-approximation of the high-energy fields, which did not affect  $z_{\alpha_1, \alpha'_1}$  and  $\bar{z}_{\alpha_1, \alpha'_1}$ . Actually, our approximation scheme did not change any term of the target band interaction at all. Therefore, we will just reobtain its original interaction

$$\sum_{\alpha_1, \alpha'_1} \sum_{q>0} v_{\alpha_1, \alpha'_1}(q) \hat{n}_{\alpha_1}(q) \hat{n}_{\alpha'_1}(-q). \quad (2.92)$$

The remaining integration can be simplified by a transformation of  $\phi$ :

$$\phi' = \frac{1}{\sqrt{2}} \begin{pmatrix} \bar{z}_{\alpha_1, \alpha'} \\ \bar{z}_{\alpha, \alpha'_1} \\ \bar{z}_{\alpha, \alpha'} \\ z_{\alpha_1, \alpha'} \\ z_{\alpha, \alpha'_1} \\ z_{\alpha, \alpha'} \end{pmatrix}, \quad J'_1 = \sqrt{2} \begin{pmatrix} -i \hat{n}_{\alpha_1}(q) \\ 0 \\ 0 \\ 0 \\ -i \hat{n}_{\alpha_1}(-q) \\ 0 \end{pmatrix}, \quad J'_2 = \sqrt{2} \begin{pmatrix} 0 \\ -i \hat{n}_{\alpha_1}(-q) \\ 0 \\ -i \hat{n}_{\alpha_1}(q) \\ 0 \\ 0 \end{pmatrix} \quad (2.93)$$

and

$$A' = \begin{pmatrix} A'_1 & 0 \\ 0 & A'_2 \end{pmatrix} \quad (2.94)$$

Applying this transformation, eq. (2.91) reads

$$\int \prod_j \frac{d\phi_j}{\sqrt{2\pi}} \exp \left( -\frac{1}{2} \sum_{i,j} \phi'_i A'_{ij} \bar{\phi}'_j + \frac{1}{2} \sum_j (\phi'_j J'_{1j} + J'_{2j} \bar{\phi}'_j) \right) = (\det A)^{-\frac{1}{2}} \exp \left( \frac{1}{2} \sum_{i,j} J'_{2i} A'^{-1}_{ij} J'_{1j} \right). \quad (2.95)$$

Due to the structure of  $A'$ , we only have to deal with the smaller matrices  $A'_1$  and  $A'_2$  and we can treat the upper and the lower part separately. Furthermore,  $A'_2$  is essentially the transpose of  $A'_1$ , so that the calculation is very similar for both. Therefore, we will describe the following steps in more detail only for  $A'_1$ , since this should be sufficient to understand the complete calculation. Using the notation introduced earlier, we get

$$A'_1 = \begin{pmatrix} V_{\alpha_1, \alpha'}^{-1} & 0 & 0 \\ 2X_{\alpha', \alpha}^2 & V_{\alpha, \alpha'_1}^{-1} & 2X_{\alpha', \alpha}^4 \\ 2X_{\alpha', \alpha}^5 & 0 & V_{\alpha, \alpha'}^{-1} + 2X_{\alpha', \alpha}^7 \end{pmatrix}. \quad (2.96)$$

According to eq. (2.95), we need the inverse of  $A'_1$ :

$$A'^{-1}_1 = \begin{pmatrix} V_{\alpha_1, \alpha'} & 0 & 0 \\ \tilde{A} & V_{\alpha, \alpha'_1} & -2V_{\alpha, \alpha'_1} X_{\alpha', \alpha}^4 \tilde{V}_{\alpha, \alpha'} \\ -2\tilde{V}_{\alpha, \alpha'} X_{\alpha', \alpha}^5 V_{\alpha_1, \alpha'} & 0 & V_{\alpha, \alpha'} \end{pmatrix}, \quad (2.97)$$

with

$$\tilde{V}_{\alpha, \alpha'} = (V_{\alpha, \alpha'}^{-1} + 2X_{\alpha', \alpha}^7)^{-1} \text{ and } \tilde{A} = V_{\alpha, \alpha'_1} \left( 4X_{\alpha', \alpha}^4 \tilde{V}_{\alpha, \alpha'} X_{\alpha', \alpha}^5 - 2X_{\alpha', \alpha}^2 \right) V_{\alpha_1, \alpha'}. \quad (2.98)$$

Since there is in each case only one entry in the upper part of the vectors  $J'_1$  and  $J'_2$ , we do not need the complete expression for  $A'^{-1}_1$ , but only  $\tilde{A}$ . Calculating the remaining vector-matrix multiplications, we get the additional interaction term  $v_{\text{eff}}(q, \Omega_m)$ . We will calculate this expression explicitly in section 3.2 for a model with three-bands.





### 3 Three-band model

In order to test the presented methods, we apply them to a model which is comparatively simple, but at the same time complex enough to contain the nontrivial interaction between different bands. Therefore, we consider a system consisting of three chains of atoms, neglecting the spin of the electrons. The three chains have different chemical potentials  $\mu_n$  and we allow hopping within the chains as well as between the outer chains and the middle chain, with the corresponding hopping parameters being  $t_n$  and  $t'$ , respectively. The non-interacting part of the Hamiltonian is

$$\hat{H}_0 = \sum_{n=1}^3 \sum_i \left( \mu_n c_{n,i}^\dagger c_{n,i} - t_n \left( c_{n,i}^\dagger c_{n,i+1} + h.c. \right) \right) - \sum_i t_\perp \left( c_{1,i}^\dagger c_{2,i} + c_{2,i}^\dagger c_{3,i} + h.c. \right), \quad (3.1)$$

which we can rewrite in momentum space for the  $y$ -component as

$$\hat{H}_0 = \sum_{n=1}^3 \sum_k c_{n,k}^\dagger c_{n,k} (\mu_n - 2t_n \cos(k)) - \sum_k t_\perp \left( c_{1,k}^\dagger c_{2,k} + c_{2,k}^\dagger c_{3,k} + h.c. \right) \quad (3.2)$$

using periodic boundary conditions in  $y$ -direction, parallel to the chains. Diagonalizing  $\hat{H}_0$ , we get three different bands, characterized by the dispersion relations  $E_\alpha(k)$ :

$$\hat{H}_0 = \sum_{\alpha=1}^3 \sum_k E_\alpha(k) \gamma_{\alpha,k}^\dagger \gamma_{\alpha,k} \quad (3.3)$$

If we want to be able to apply the presented cRPA methods to this model, we have to choose model parameters, which make sure that only one band  $E_2(k)$  crosses the Fermi level, whereas the other bands  $E_1(k)$  and  $E_3(k)$  lie completely below or above it. We achieve this by varying the chemical potential for the atomic chains, with negative values for  $\mu_1$ , vanishing  $\mu_2$  and positive values for  $\mu_3$ . Note that this notation differs from the one used in chapter 2, since  $\gamma_{2,k}^\dagger$  and  $\gamma_{2,k}$  correspond to the low-energy regime, while  $\gamma_{1,k}^\dagger$ ,  $\gamma_{1,k}$ ,  $\gamma_{3,k}^\dagger$  and  $\gamma_{3,k}$  correspond to higher energies.

Concerning the interacting part of the Hamiltonian  $H_I$ , we use different expressions for both cRPA methods, containing Wannier operators  $c^\dagger, c$  for cRPA method 1 and band operators  $\gamma^\dagger, \gamma$  for cRPA method 2. In principle, this is not necessary, since we know the relation between these two operators and can therefore convert the values of the interaction strength. However, if we do so, the interaction strength will depend on an additional parameter in one of both methods. By choosing two different  $H_I$ , we avoid this complication and reduce the computational effort, without vitiating the intended method test.

## 3.1 Numerical test of cRPA method 1

We will study the three-band model using first cRPA method 1. Since we implemented this method with the Wannier operators, we express the interaction term by the corresponding densities  $\hat{n}_n(q) = \frac{1}{\sqrt{L}} \sum_k c_{n,k}^\dagger c_{n,k+q}$ . We are interested in the effect of the interaction of the host bands and target bands on the interaction of the low-energy properties. Thus, we need at least

$$\begin{aligned} \hat{H}_I = & \\ & \sum_{q>0} (u(q) \hat{n}_2(q) \hat{n}_2(-q) + v(q) \hat{n}_2(q) (\hat{n}_1(-q) + \hat{n}_3(-q)) + v(q) (\hat{n}_1(q) + \hat{n}_3(q)) \hat{n}_2(-q)). \end{aligned} \quad (3.4)$$

We could as well consider interaction terms consisting only of high-energy operators, but this expression is sufficient to check the appropriateness of cRPA method 1, so we will restrict to it.

### 3.1.1 Susceptibility

In order to calculate the effective interaction, we need the susceptibility  $\chi_{0,nm}(q, \tau)$ , which is defined as (see eq. (2.31))

$$\begin{aligned} \chi_{0,nm}(q, \tau) &= \langle \hat{T} \hat{n}_n(q, \tau) \hat{n}_m(-q, 0) \rangle_0 \\ &= \frac{1}{L} \sum_{k,k'} \langle c_{n,k}^\dagger(\tau) c_{n,k+q}(\tau) c_{m,k'}^\dagger(0) c_{m,k'-q}(0) \rangle_0 \end{aligned} \quad (3.5)$$

with  $\tau > 0$ . We can evaluate the expectation value, if we substitute the Wannier operators  $c_{n,k}^\dagger, c_{n,k}$ :

$$c_{n,k}^\dagger(\tau) = \sum_{\alpha} U_{n\alpha}^\dagger(k) \gamma_{\alpha,k}^\dagger(\tau), \quad c_{n,k}(\tau) = \sum_{\alpha} \gamma_{\alpha,k}(\tau) U_{\alpha n}(k) \quad (3.6)$$

Therefore, we get

$$\begin{aligned} & \langle c_{n,k}^\dagger(\tau) c_{n,k+q}(\tau) c_{m,k'}^\dagger(0) c_{m,k'-q}(0) \rangle_0 \\ &= \sum_{\alpha,\alpha'} \sum_{\beta,\beta'} U_{n\alpha}^\dagger(k) U_{\alpha'n}(k+q) U_{m\beta}^\dagger(k') U_{\beta'm}(k'-q) \times \\ & \quad \langle \gamma_{\alpha,k}^\dagger(\tau) \gamma_{\alpha',k+q}(\tau) \gamma_{\beta,k'}^\dagger(0) \gamma_{\beta',k'-q}(0) \rangle_0 \\ &= \sum_{\alpha,\beta} \delta_{k,k'-q} U_{n\alpha}^\dagger(k) U_{\beta n}(k+q) U_{m\beta}^\dagger(k+q) U_{\alpha m}(k) \times \\ & \quad e^{\tau(E_\alpha(k) - E_\beta(k+q))} f(E_\alpha(k)) (1 - f(E_\beta(k+q))). \end{aligned} \quad (3.7)$$

This leads to the following expression for the susceptibility:

$$\begin{aligned} \chi_{0,nm}(q, \tau) = & \\ & \frac{1}{L} \sum_{k,\alpha,\beta} U_{n\alpha}^\dagger(k) U_{\beta n}(k+q) U_{m\beta}^\dagger(k+q) U_{\alpha m}(k) e^{\tau(E_\alpha(k) - E_\beta(k+q))} \frac{e^{\beta E_\beta(k+q)}}{(e^{\beta E_\alpha(k)} + 1) (e^{\beta E_\beta(k+q)} + 1)} \end{aligned} \quad (3.8)$$

According to cRPA method 1, we need the Fourier transform of  $\chi_{0,nm}(q, \tau)$ . For this transformation step, we only have to consider the time dependent part of the susceptibility:

$$\int_0^\beta d\tau e^{\tau(i\Omega_m + E_\alpha(k) - E_\beta(k+q))} = \frac{e^{\beta(i\Omega_m + E_\alpha(k) - E_\beta(k+q))} - 1}{i\Omega_m + E_\alpha(k) - E_\beta(k+q)} \quad (3.9)$$

Altogether, we get

$$\begin{aligned} & \chi_{0,nm}(q, \Omega_m) \\ &= \frac{1}{L} \sum_{k,\alpha,\beta} \frac{U_{n\alpha}^\dagger(k) U_{\beta n}(k+q) U_{m\beta}^\dagger(k+q) U_{\alpha m}(k) (e^{\beta E_\alpha(k)} - e^{\beta E_\beta(k+q)})}{(i\Omega_m + E_\alpha(k) - E_\beta(k+q)) (e^{\beta E_\alpha(k)} + 1) (e^{\beta E_\beta(k+q)} + 1)} \\ &= \frac{1}{L} \sum_{k,\alpha,\beta} U_{n\alpha}^\dagger(k) U_{\beta n}(k+q) U_{m\beta}^\dagger(k+q) U_{\alpha m}(k) \frac{f(E_\beta(k+q)) - f(E_\alpha(k))}{i\Omega_m + E_\alpha(k) - E_\beta(k+q)}. \end{aligned} \quad (3.10)$$

Depending on the properties of the non-interacting Hamiltonian,  $\chi_{0,nm}(q, \Omega_m)$  can have different symmetries. For example, in this case  $H_0$  does not only have real eigenvalues, but also real eigenvectors. Thus, we can use  $U_{n\alpha}^\dagger(k) = U_{\alpha n}(k)$ , which leads to  $\chi_{0,nm}(q, \Omega_m) = \chi_{0,mn}(q, \Omega_m)$ , according to eq. (3.10). For this reason, there are only six independent susceptibilities for this model, since  $\chi_{0,12}(q, \Omega_m) = \chi_{0,21}(q, \Omega_m)$ ,  $\chi_{0,13}(q, \Omega_m) = \chi_{0,31}(q, \Omega_m)$  and  $\chi_{0,23}(q, \Omega_m) = \chi_{0,32}(q, \Omega_m)$ .

After the calculation of the susceptibilities, we follow the procedure given by eq. (2.56) in order to obtain the effective interaction. Using the symmetry of the susceptibility discussed above and the parameter set of our model, we get

$$\tilde{\chi}_{0,22} = \frac{\chi_{0,22}}{(1 + v(\chi_{0,21} + \chi_{0,23}))^2 - v^2 \chi_{0,22}(\chi_{0,11} + \chi_{0,33} + 2\chi_{0,13})}, \quad (3.11)$$

where we omitted the dependence on momentum  $q$  and Matsubara frequency  $\Omega_m$  to abbreviate the notation. As this expressions shows,  $\tilde{\chi}_{0,22}$  does not depend on the interaction of the central band  $u(q)$ , but only on the interaction between the central band and the outer bands  $v(q)$ . Subtracting  $\chi_{0,22}(q, \Omega_m)$  from  $\tilde{\chi}_{0,22}(q, \Omega_m)$ , we finally get the effective susceptibility  $\chi_{\text{eff}}(q, \Omega_m)$  according to cRPA method 1.

### 3.1.2 Numerical results

Since we now know how to calculate the effective interaction, we can compare numerical data with our expectations. For this purpose, we do not use  $\chi_{\text{eff}}(q, \Omega_m)$  computed for the Matsubara frequencies, but for real frequencies  $\Omega$ . In our notation, the quantity we analyze is  $\chi_{\text{eff}}(q, -i\Omega)$ . It is related to  $\chi_{\text{eff}}(q, \Omega_m)$  via complex integration. We use this quantity since it directly shows at which energies the effective interaction is especially affected by particle-hole excitations. This can be related to the band structure in order to check whether the effective interaction really contains the physical processes we want to include on the RPA level.

For the numerical computation, we choose  $\mu_1 = -\mu_3 = -4$ ,  $\mu_2 = 0$ ,  $t_1 = t_3 = -0.5$ ,  $t_2 = 1$ ,  $t_\perp = 0.1$  and inverse temperature  $\beta = 10$ . Therefore, one band  $E_2(k)$  is half-filled, one band  $E_1(k)$  is completely filled and one band  $E_3(k)$  is empty (see fig. 3.1). Due to

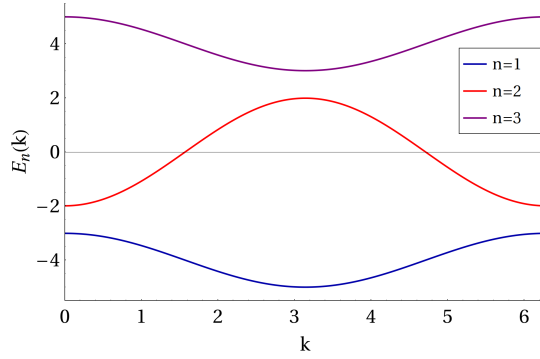


**Figure 3.1:** Band structure of the three-band model with  $\mu_1 = -\mu_3 = -4$ ,  $\mu_2 = 0$ ,  $t_1 = t_3 = -0.5$ ,  $t_2 = 1$  and  $t_\perp = 0.1$

the small value of the inter-chain hopping  $t_\perp$  compared to the differences in the chemical potentials, these bands are to a large extent localized on the chains: We can relate  $E_2(k)$  to the central chain labeled  $n = 2$ ,  $E_1(k)$  to the outer chain labeled  $n = 1$  and  $E_3(k)$  to the opposite chain labeled  $n = 3$ .

Since we did not include the low-energy auxiliary fields in the cRPA scheme, we assume that  $\chi_{\text{eff}}(q, -i\Omega)$  only contains high-energy contributions. However, the numerical result shown in fig. 3.2 disproves this expectation. The dominant contribution does not stem from excitations between the high energy bands  $E_1(k)$  and  $E_3(k)$ , but from excitations within the low-energy band  $E_2(k)$ . As the comparison with the band structure reveals, the blue structure at low frequencies is due to processes at the Fermi level. They appear at momentum  $q = 0$  and at  $q = \pi$ , since  $E_2(k)$  crosses the Fermi level at two points, with a difference in momentum of  $\Delta k = \pi$ . The red structure is even more pronounced, which can be explained by a phase space argument: The effect of particle-hole excitations is especially important if the involved parts of the band structure are parallel. Following this explanation and comparing the maximum of the red feature to the band structure, we again find that it is caused by excitations within the band  $E_2(k)$ . Energetically, an excitation from the target band to the host bands is possible. However, this structure would appear at  $q = \frac{\pi}{2}$  and  $q = \frac{3\pi}{2}$  for the lowest frequencies, but there is no structure with the appropriate properties.

At higher frequencies which exceed the bandwidth of  $E_2(k)$ , processes concerning only the target band are no longer possible. Thus, the blue feature at  $\Omega \approx 5$  and  $q \approx \pi$  is really one of the high-energy contributions we tried to capture. Apparently, the effective interaction calculated by cRPA method 1 contains the influence of the host bands, but this method is not able to isolate them from the low-energy processes.

### 3.1.3 Problems of cRPA method 1

We had to realize that we cannot use cRPA method 1 to achieve what we aimed at: It does not separate the high-energy processes from the physics of the target band. But what is the problem of this method, why does it not fulfill our expectations? Is there a

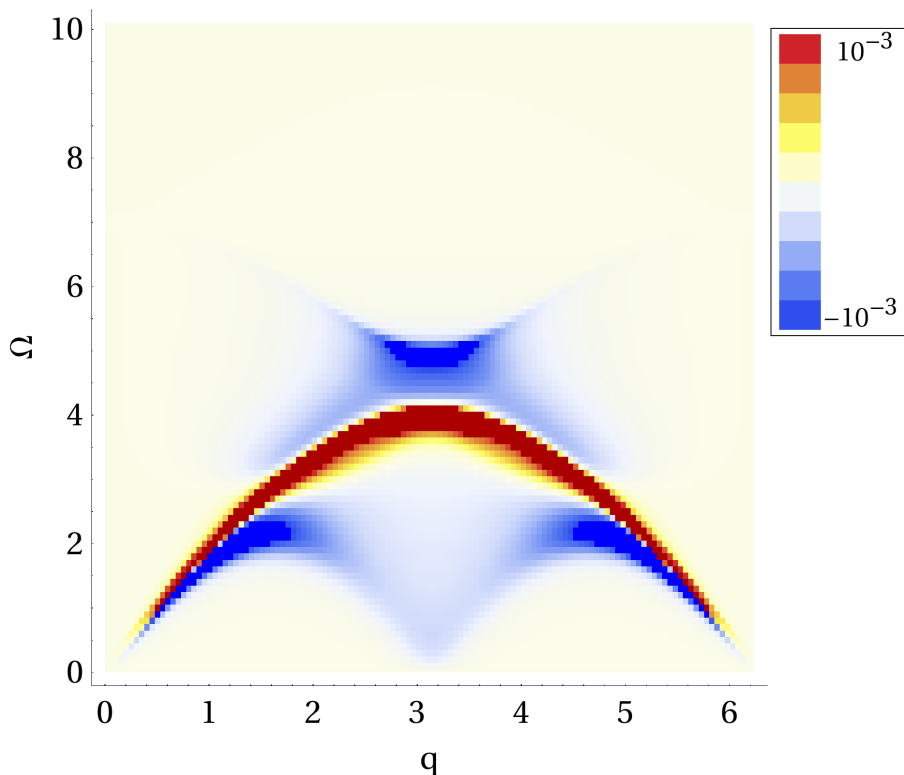


**Figure 3.2:** Imaginary part of  $\chi_{\text{eff}}(q, -i\Omega)$  for  $\mu_1 = -\mu_3 = -4$ ,  $\mu_2 = 0$ ,  $t_1 = t_3 = -0.5$ ,  $t_2 = 1$ ,  $t_{\perp} = 0.1$  and  $v(q) = 1$

general problem of our procedure, or do we still have a chance to be more successful with cRPA method 2?

In order to answer these questions, we go back to the expression for the calculation of the susceptibility in eq. (3.10). In this equation, the fraction describes the influence of particle-hole excitations. We understand this part quite well, since we can connect the band structure and the features of  $\chi_{\text{eff}}(q, -i\Omega)$ . Therefore, we turn to the prefactors stemming from the eigenvectors of the non-interacting Hamiltonian. The inter-chain hopping parameter  $t_{\perp}$  is small compared to the energy difference of the three-bands. If we neglect this parameter completely and consider the matrix which couples the Bloch operators  $c_{n,k}^{\dagger}$  and  $c_{n,k}$  in the non-interacting Hamiltonian, we find that this matrix is diagonal. Its eigenvalues and eigenvectors are given by

$$\begin{aligned}
 E_1(k) &= \mu_1 - 2t_1 \cos(k), \quad E_2(k) = \mu_2 - 2t_2 \cos(k), \quad E_3(k) = \mu_1 - 2t_3 \cos(k), \\
 v_1 &= \begin{pmatrix} 1 \\ 0 \\ 0 \end{pmatrix}, \quad v_2 = \begin{pmatrix} 0 \\ 1 \\ 0 \end{pmatrix}, \quad v_3 = \begin{pmatrix} 0 \\ 0 \\ 1 \end{pmatrix}.
 \end{aligned} \tag{3.12}$$

Since the entries of the eigenvectors determine the prefactors  $U_{\alpha n}$ , we know that  $U_{11}$ ,  $U_{22}$  and  $U_{33}$  are largest. Prefactors with two different indices scale with  $t_{\perp}$ . Using an

expansion around  $t_{\perp} = 0$  up to second order for the calculation of  $U_{\alpha n}$ , we find

$$\begin{aligned} U_{12} &= \mathcal{O}\left(\frac{t_{\perp}}{E_2 - E_1}\right), U_{13} = \mathcal{O}\left(\frac{t_{\perp}^2}{(E_2 - E_1)E_3}\right), U_{21} = \mathcal{O}\left(\frac{t_{\perp}}{E_2 - E_1}\right), \\ U_{23} &= \mathcal{O}\left(\frac{t_{\perp}}{E_3 - E_2}\right), U_{31} = \mathcal{O}\left(\frac{t_{\perp}^2}{(E_3 - E_2)E_1}\right), U_{32} = \mathcal{O}\left(\frac{t_{\perp}}{E_3 - E_2}\right). \end{aligned} \quad (3.13)$$

For simplicity, we will only write  $\tilde{t}_{\perp}$  and  $\tilde{t}_{\perp}^2$  instead of the complete arguments where a linear or square term of  $t_{\perp}$  appears. Of course, this notation is not very precise, since it makes a difference by which energy or energy difference  $t_{\perp}$  is divided. However, for this discussion, which only considers different orders of magnitudes, these differences are not important.

For the computation of the susceptibility, we multiply by four of these factors. For the different susceptibilities  $\chi_{0,nm}$  we use to calculate the effective interaction, we compare the largest contributions in terms of  $\tilde{t}_{\perp}$ . As we have seen, the value of  $\chi_{\text{eff}}(q, -i\Omega)$  is especially high, if a particle-hole excitation with frequency  $\Omega$  and momentum  $q$  is possible and we also know which of these excitation are particularly important. The main contribution to the susceptibility stems from excitation within the target band, unlike our intention. Therefore, the corresponding prefactor of  $\chi_{0,nm}$  is  $(U_{2n}U_{2m})^2$ . Using the above results, we find

$$\chi_{0,22} = \mathcal{O}(1), \chi_{0,12} \propto \chi_{0,23} = \mathcal{O}(\tilde{t}_{\perp}^2), \chi_{0,11} \propto \chi_{0,33} \propto \chi_{0,13} = \mathcal{O}(\tilde{t}_{\perp}^4). \quad (3.14)$$

Since the band  $E_2(k)$  is mainly localized on the central band, the contribution is reduced if the susceptibility is related to the outer chains  $n = 1, 3$ . With similar considerations for excitations between the target band and one of the host bands, we expect the following behavior of the susceptibilities:

$$\chi_{0,22} \propto \chi_{0,12} \propto \chi_{0,23} \propto \chi_{0,11} \propto \chi_{0,33} = \mathcal{O}(\tilde{t}_{\perp}^2), \chi_{0,13} = \mathcal{O}(\tilde{t}_{\perp}^4) \quad (3.15)$$

The band and chain indices are combined in both possible ways, so we always multiply with at least two of the small factors proportional to  $\tilde{t}_{\perp}$ . Only for  $\chi_{0,13}$ , we cannot avoid having one prefactor proportional to  $\tilde{t}_{\perp}^2$ . Finally, if both of the host bands are concerned, all susceptibilities behave similarly:

$$\chi_{0,22} \propto \chi_{0,12} \propto \chi_{0,23} \propto \chi_{0,11} \propto \chi_{0,33} \propto \chi_{0,13} = \mathcal{O}(\tilde{t}_{\perp}^4) \quad (3.16)$$

In the first instance, this might seem surprising, but it is not hard to explain: For every chain index  $n = 2$ , we will get two factors proportional to  $\tilde{t}_{\perp}$ . For chain indices  $n = 1$  or  $n = 3$ , there is one factor of order  $\mathcal{O}(1)$  and one factor of order  $\mathcal{O}(\tilde{t}_{\perp}^2)$ . Altogether, this does not make any difference, we will in any case end up with  $\tilde{t}_{\perp}^4$ .

We now have explicit expectations for the dominant contributions of the different susceptibilities and can compare them to numerical results. To obtain the numerical data, we use the same parameter set as before. Due to the symmetry of both host bands,  $\chi_{0,21}(q, -i\Omega) = \chi_{0,23}(q, -i\Omega)$  and  $\chi_{0,11}(q, -i\Omega) = \chi_{0,33}(q, -i\Omega)$ , we can restrict our discussion to four different susceptibilities.

For  $\chi_{0,22}$ , excitations within the target band are essential, since the other processes are suppressed with at least a factor of  $\tilde{t}_\perp^2$ . This picture is confirmed by fig. 3.3(a) which shows the susceptibility  $\chi_{0,22}$ . The low-energy feature is predominant, there is only a very weak signature for processes involving the host bands. As we expected, the order of magnitude of  $\chi_{0,22}$  is about 1, in contrast to the other susceptibilities. The largest contributions to

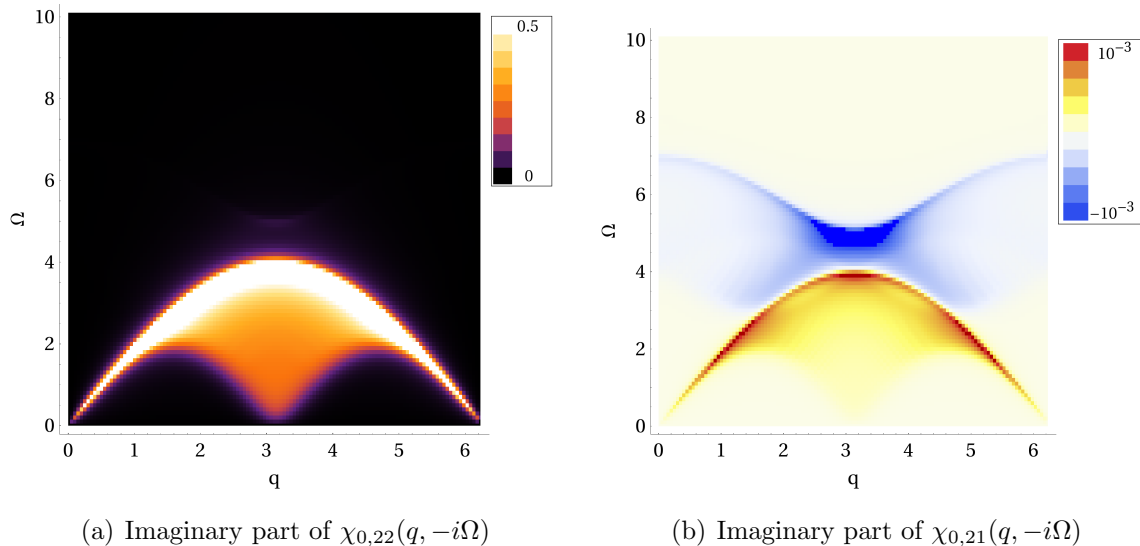


**Figure 3.3:** Contributions to the effective interaction

$\chi_{0,21}$  are of the order  $\tilde{t}_\perp^2$  and correspond to both intra-target band and target-host band excitations. Our numerical result for  $\chi_{0,21}$ , shown in fig. 3.3(b), is consistent with this description: The positive parts of  $\chi_{0,21}$  stem from processes within the target band, the negative parts stem from processes between target and host bands. For  $\chi_{0,11}$ , only the latter processes are relevant, since they give the most important contribution, proportional to  $\tilde{t}_\perp^2$ . Therefore, the order of magnitude is similar to the one of  $\chi_{0,21}$  (see fig. 3.4(a)). Finally, for  $\chi_{0,13}$  all excitations contribute with the same strength, proportional to  $\tilde{t}_\perp^4$ . Thus, this susceptibility has the smallest numerical value, but contains more features than the other ones. In fig. 3.4(b), one can see the signature of the host band excitations which is too small to be visible for the other susceptibilities. Physical processes happening on different energy scales are represented in equal measure by this single susceptibility  $\chi_{0,13}$ .

This reveals the basic problem of cRPA method 1: Identifying chain indices with band indices is not an appropriate way to separate these processes, as shown by  $\chi_{0,13}$  and  $\chi_{0,21}$ . We can try to circumvent this problem: For example, we could choose a different non-interacting Hamiltonian, which creates more overlap between the outer chains. Doing so, the high-energy feature of  $\chi_{0,13}$  corresponding to host band excitation would be enhanced. However, this would only improve the situation for  $\chi_{0,13}$  and we would lose the generality of this method. Furthermore, no such procedure is possible for  $\chi_{0,21}$ . Another possible modification is the change of the interacting part of the Hamiltonian, for example by introducing an interaction term between the outer chains. We argued that it is possible

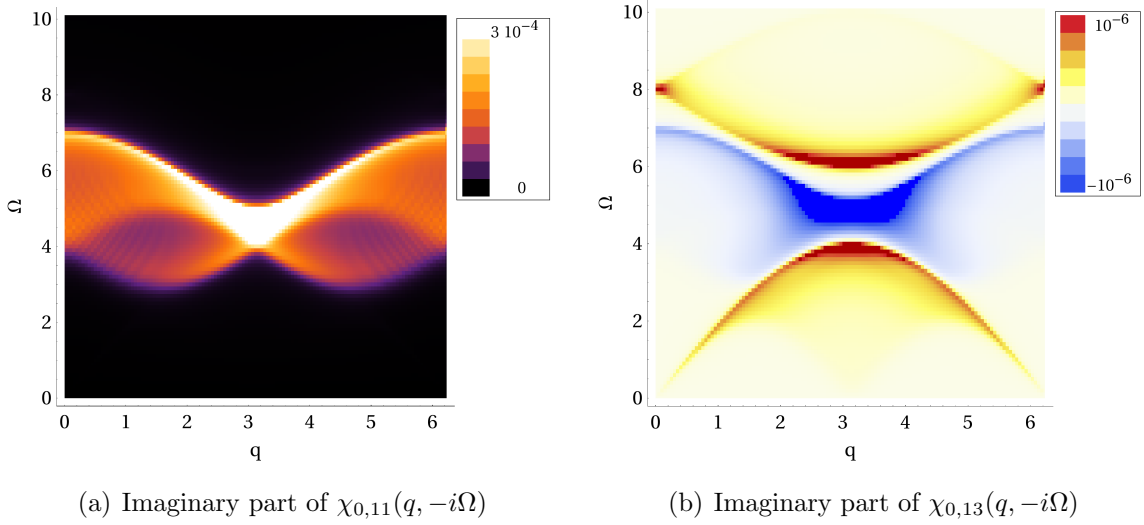


**Figure 3.4:** Contributions to the effective interaction

that the susceptibility  $\chi_{0,13}$  is mainly determined by high-energy processes. Thus, we could hope that the suggested procedure would modify  $\chi_{\text{eff}}$  (see eq. (3.11)), so that  $\chi_{0,13}$  plays the crucial role. However, there is no possibility to avoid the low-energy contributions simply because we are interested in the influence of the high-energy contributions on the target band. Therefore, even if we are able to isolate effects concerning only the host bands, we still have to connect them to the target band. Within cRPA method 1, this is only possible via the introduction of a susceptibility with chain index  $n = 2$ . As we have argued above and as it is shown exemplarily in fig. 3.3, these susceptibilities necessarily contain signatures of intra-target band excitations. Therefore, we do not see a possible solution for the problems of cRPA method 1. There is at least one positive insight, revealed by this discussion: The reason for the failure of this method, namely the identification of band and chain indices, is the particular property of this method, so we can be optimistic about cRPA method2.

## 3.2 Numerical test of cRPA method 2

For cRPA method 2, a different formulation of the interacting part of the Hamiltonian is convenient, using the operators  $\gamma_{n,k}^\dagger$  and  $\gamma_{n,k}$ . The general form of  $\hat{H}_I$  is

$$\hat{H}_I = \sum_{\alpha, \alpha'} \sum_{q>0} v_{\alpha, \alpha'}(q) \hat{n}_\alpha(q) \hat{n}_{\alpha'}(-q) \quad (3.17)$$

with  $\alpha = (n, m, k)$  and  $\hat{n}_\alpha(q) = \frac{1}{\sqrt{L}} \gamma_{n,k}^\dagger \gamma_{m, k+q}$ , as introduced in section 2.2. Again, the model we will study in the following does not have this very general form. In fact, we need a model which allows some, but not all possible high-energy processes in order to study whether these effects are captured correctly by cRPA method 2. Therefore, we can introduce some simplifications. The most important one is choosing the  $v_{\alpha, \alpha'}(q)$  to be



independent of  $k$  and  $k'$ . Doing so, we can redefine  $\alpha$  and  $\hat{n}_\alpha(q)$ :

$$\alpha = (n, m) \quad (3.18)$$

$$\hat{n}_\alpha(q) = \frac{1}{\sqrt{L}} \sum_k \gamma_{n,k}^\dagger \gamma_{m,k+q} \quad (3.19)$$

With this notation, all equations of the more general case remain valid for our toy model, but the final step of the calculation, the integration, is much easier, since the number of the integration parameters  $z_{\alpha,\alpha'}$  is reduced substantially. Furthermore, we attribute the same interaction strength to processes which are similar with respect to the involved particles, neglecting processes involving mainly particles of the host bands:

$$\begin{aligned} v_1(q) &\equiv v_{2222}(q), \\ v_2(q) &\equiv v_{222n}(q) = v_{m222}(q), \\ v'_2(q) &\equiv v_{22n2}(q) = v_{2m22}(q), \\ v_3(q) &\equiv v_{22nm}(q) = v_{n'm'22}(q), \\ v_4(q) &\equiv v_{2nm2}(q) = v_{n'22m'}(q), \\ v'_4(q) &\equiv v_{2n2m}(q) = v_{n'2m'2}(q), \\ v_{nmm'n'}(q) &= v_{2nmm'}(q) = v_{n2mm'}(q) = v_{nm2n'}(q) = v_{nmm'n'}(q) = 0 \end{aligned} \quad (3.20)$$

with  $n, m, n', m' \neq 2$ . Finally, we pay attention to the  $q$ -dependence of the interaction. Since we deal with spinless fermions, there is no on-site interaction. Within one chain, we therefore have only nearest neighbor interaction, which leads to a  $q$  dependence of the cosine-type. In contrast, interaction between different chains might affect nearest neighbors and next-nearest neighbors, so creates an additional constant term. Due to the localization of the bands,  $v_1(q)$  is determined by the interaction on the central chain, so the cosine term should be dominant. As for the other interaction parameters, both intra-chain and inter-chain interaction are relevant. Therefore, it is reasonable to choose

$$\frac{v_1(q)}{v_1} = 2 \cos(q), \quad \frac{v_2(q)}{v_2} = \frac{v'_2(q)}{v'_2} = \frac{v_3(q)}{v_3} = \frac{v_4(q)}{v_4} = \frac{v'_4(q)}{v'_4} = u + 2 \cos(q). \quad (3.21)$$

So we have one parameter  $v_n$  for each type of interaction and an additional parameter  $u$ , which controls the relative strength of the nearest neighbor interaction between different chains.

### 3.2.1 Susceptibility

Having defined the full Hamiltonian, we can calculate the effective interaction via the susceptibilities  $\chi_{0,\alpha,\alpha'}$ . Their definition differs from the one of cRPA method 1 (see eq. (2.79)):

$$\begin{aligned} \chi_{0,\alpha,\alpha'}(q, \tau) &= \frac{1}{L} \sum_{k,k'} \langle \hat{T} \gamma_{n,k}^\dagger(\tau) \gamma_{m,k-q}(\tau) \gamma_{n',k'}^\dagger(0) \gamma_{m',k'+q}(0) \rangle_0 \\ &= \frac{1}{L} \sum_k \delta_{n,m'} \delta_{m,n'} e^{\tau(E_n(k+q) - E_m(k))} f(E_n(k+q)) (1 - f(E_m(k))) \end{aligned} \quad (3.22)$$

with  $\tau > 0$ . If we do the Fourier transformation of  $\chi_{0,\alpha,\alpha'}(q, \tau)$ , we get

$$\chi_{0,\alpha,\alpha'}(q, \Omega_m) = \frac{1}{L} \sum_k \delta_{n,m'} \delta_{m,n'} \frac{f(E_m(k)) - f(E_n(k+q))}{i\Omega_m + E_n(k+q) - E_m(k)}. \quad (3.23)$$

Due to the two Kronecker deltas, most of the susceptibilities  $\chi_{0,\alpha,\alpha'}(q, \Omega_m)$  vanish. In order to only consider the non-vanishing susceptibilities, we introduce the following notation:

$$\chi_{m,n}(q, \Omega_m) = \frac{1}{L} \sum_k \frac{f(E_m(k)) - f(E_n(k+q))}{i\Omega_m + E_n(k+q) - E_m(k)} \quad (3.24)$$

Using the integration scheme of cRPA method 2, we obtain the additional effective interaction:

$$v_{\text{eff}}(q, \Omega_m) = v_2(q)^2 \tilde{\chi}_2(q, \Omega_m) + v_2(q)v'_2(q) \tilde{\chi}'_2(q, \Omega_m) + v'_2(q)^2 \tilde{\chi}''_2(q, \Omega_m) + v_3(q)^2 \tilde{\chi}_3(q, \Omega_m) \quad (3.25)$$

$$\tilde{\chi}_2(q, \Omega_m) = \frac{\chi'_{n,2}(q, \Omega_m)(1 + v_4(q)\chi'_{2,n}(q, \Omega_m))}{(1 + v_4(q)\chi'_{2,n}(q, \Omega_m))(1 + v_4(q)\chi'_{n,2}(q, \Omega_m)) - v'_4(q)^2 \chi'_{2,n}(q, \Omega_m)\chi'_{n,2}(q, \Omega_m)} \quad (3.26)$$

$$\tilde{\chi}'_2(q, \Omega_m) = \frac{-2v'_4(q)\chi'_{2,n}(q, \Omega_m)\chi'_{n,2}(q, \Omega_m)}{(1 + v_4(q)\chi'_{2,n}(q, \Omega_m))(1 + v_4(q)\chi'_{n,2}(q, \Omega_m)) - v'_4(q)^2 \chi'_{2,n}(q, \Omega_m)\chi'_{n,2}(q, \Omega_m)} \quad (3.27)$$

$$\tilde{\chi}''_2(q, \Omega_m) = \frac{\chi'_{2,n}(q, \Omega_m)(1 + v_4(q)\chi'_{n,2}(q, \Omega_m))}{(1 + v_4(q)\chi'_{2,n}(q, \Omega_m))(1 + v_4(q)\chi'_{n,2}(q, \Omega_m)) - v'_4(q)^2 \chi'_{2,n}(q, \Omega_m)\chi'_{n,2}(q, \Omega_m)} \quad (3.28)$$

$$\tilde{\chi}_3(q, \Omega_m) = \sum_{n,m}^{\neq 2} \chi_{n,m}(q, \Omega_m) \quad (3.29)$$

with  $\chi'_{2,n}(q, \Omega) = \chi_{2,1}(q, \Omega) + \chi_{2,3}(q, \Omega)$ ,  $\chi'_{n,2}(q, \Omega) = \chi_{1,2}(q, \Omega) + \chi_{3,2}(q, \Omega)$ . According to  $\hat{H}_I$ , more interaction processes are possible compared to the model we used for cRPA method 1.  $v_{\text{eff}}(q, \Omega_m)$ , which should represent all the high-energy processes, is therefore much more complicated. Nevertheless, we can understand the single contributions. Let us consider the term  $v_3(q)^2 \tilde{\chi}_3(q, \Omega_m)$  first. The interaction process represented by  $v_3(q)$  either excites an electron and a hole from the target band to the host bands or reverses such excitations. The contribution of this excitation is given by  $\tilde{\chi}_3(q, \Omega_m)$ . Thus, the complete expression  $v_3(q)^2 \tilde{\chi}_3(q, \Omega_m)$  contains the creation of this excitation, expressed by  $v_3(q)$ , the intermediate state, expressed by  $\tilde{\chi}_3(q, \Omega_m)$ , and its annihilation, expressed by  $v_3(q)$  again. This term is relatively simple, since  $\hat{H}_I$  does not allow other interactions of this particle-hole excitation. However, if the intermediate state consists of an excited electron and hole, with one of them in the target band, the situation is different. Such excitations, which are related to the interaction parameters  $v_2(q)$  and  $v'_2(q)$ , can interact with excitations of the same type via processes represented by  $v_4(q)$  and  $v'_4(q)$ . In this way, chains of interactions arise which lead to the denominators as a typical result of a RPA method. Further details of this calculation are given in the appendix, section A.4.

### 3.2.2 Numerical results

For the test of cRPA method 2, we again use the real frequencies  $\Omega$ . Compared to section 3.1, we choose a similar parameter set, but destroy the symmetry between the host bands: We set  $\beta = 10$ ,  $\mu_1 = -4$ ,  $\mu_3 = 3$ ,  $\mu_2 = 0$ ,  $t_1 = -t_3 = -0.5$ ,  $t_2 = 1$  and  $t_\perp = 0.1$ . The resulting band structure is shown in fig. 3.5. According to eq. (2.61), we can use arguments

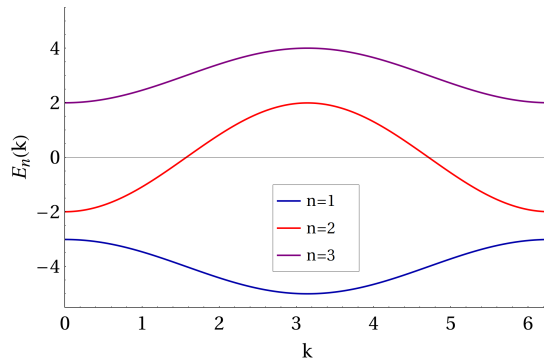


**Figure 3.5:** Band structure of the three-band model with  $\mu_1 = -4$ ,  $\mu_3 = 3$ ,  $\mu_2 = 0$ ,  $t_1 = -t_3 = -0.5$ ,  $t_2 = 1$  and  $t_\perp = 0.1$

about the orders of magnitude of the interaction parameters which are similar to our considerations on the susceptibilities in subsection 3.1.3. Let us assume that the interaction parameters originally stem from a strong nearest neighbor interaction, weak next-nearest neighbor interaction, both between different chains, and a weak nearest neighbor interaction within one chain. Therefore, it is reasonable to choose  $v_2 = 0.2$ ,  $v'_2 = 0.1$ ,  $v_3 = 0.8$ ,  $v_4 = 0.02$ ,  $v'_4 = 0.01$  and  $u = 10$  for the interaction Hamiltonian. Computing  $v_{\text{eff}}(q, -i\Omega)$  with this parameter set, we get the following result (see fig. 3.6): There are three different features, the dominant one appearing at the highest frequencies. In contrast to the effective interaction calculated by cRPA method 1, no low-energy contribution is visible. This confirms our expectation to only capture the high-energy processes concerning the host bands.

It seems plausible that the three structures of  $v_{\text{eff}}(q, -i\Omega)$  are related to the three different types of excitations, involving either the target band and one of the host bands or both host bands. We check this assumption by computing the single contributions to the effective interaction,  $\tilde{\chi}_2(q, -i\Omega)$ ,  $\tilde{\chi}'_2(q, -i\Omega)$ ,  $\tilde{\chi}''_2(q, -i\Omega)$  and  $\tilde{\chi}_3(q, -i\Omega)$ . According to the definitions of these expressions in eqs. (3.25)-(3.29),  $\tilde{\chi}_2(q, -i\Omega)$  corresponds to a particle-hole excitation of the bands  $E_2(k)$  and  $E_3(k)$ . This is in agreement with the relevant frequency range from  $\Omega = 2$  to  $\Omega = 6$  and its momentum dependence (see fig. 3.7(a)). The most important contribution between  $\Omega = 4$  and  $\Omega = 6$  is caused by excitation between parallel parts of both bands, as explained in subsection 3.1.2. If we compare  $\tilde{\chi}_2(q, -i\Omega)$  to the total effective interaction, we find that this feature appears in both cases. For  $\tilde{\chi}''_2(q, -i\Omega)$ , the situation is very similar. Here, we see the influence of excitations concerning the target band  $E_2(k)$  and the host band  $E_1(k)$ . The structure is nearly identical, but shifted by a momentum  $\Delta q = \pi$ , since  $t_1 = -t_3$ , and also shifted

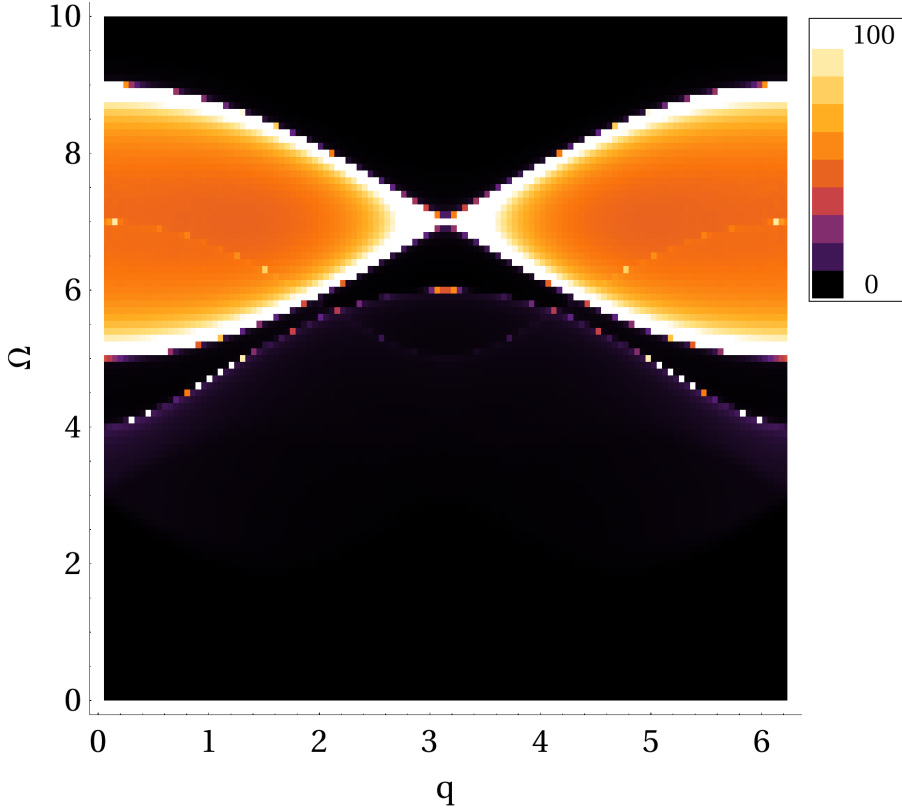


**Figure 3.6:** Imaginary part of  $v_{\text{eff}}(q, -i\Omega)$

towards higher frequencies, since  $|\mu_1| > |\mu_3|$  (see fig. 3.7(b)). Again, only the most prominent feature of  $\tilde{\chi}_2''(q, -i\Omega)$  is visible in fig. 3.6. Both possible types of processes, which involve the target band and one of the host bands, are relevant for  $\tilde{\chi}_2''(q, -i\Omega)$ . Therefore, its structure contains both of the corresponding features (see fig. 3.8(a)). The effect of the above contributions to  $v_{\text{eff}}(q, -i\Omega)$  is relatively small due to the numerical value of the corresponding interaction parameters.  $\tilde{\chi}_2(q, -i\Omega)$  and  $\tilde{\chi}_2''(q, -i\Omega)$  enter  $v_{\text{eff}}(q, -i\Omega)$  with the prefactors  $v_2(q)^2$  and  $v_2'(q)^2$ , respectively. Both are smaller than  $v_3(q)$  and since the interaction parameters have to be squared, this difference has a great influence. Therefore, the main contribution to the effective interaction stems from  $\tilde{\chi}_3(q, -i\Omega)$ . This expression which captures the excitations between both host bands is shown in fig. 3.8(b). Its maximum is at  $\Omega = 7$ , and  $q = \pi$ , since  $E_1(k)$  and  $E_3(k + \pi)$  are nearly parallel with an energy difference  $\Delta E = 7$ . Due to the bandwidth of these bands, the frequencies for possible particle-hole excitations range from  $\Omega = 5$  to  $\Omega = 9$ .

Overall, these results meet our expectations. The effective interaction calculated by cRPA method 2 really contains the high-energy processes related to the host bands. In contrast to cRPA method 1, we do not accidentally include excitations which actually concern the target band, exclusively. Additionally, we have some understanding of the correspondence between single terms of the interaction Hamiltonian and the contributions to the effective interaction. With this affirmation and this knowledge, we can use this

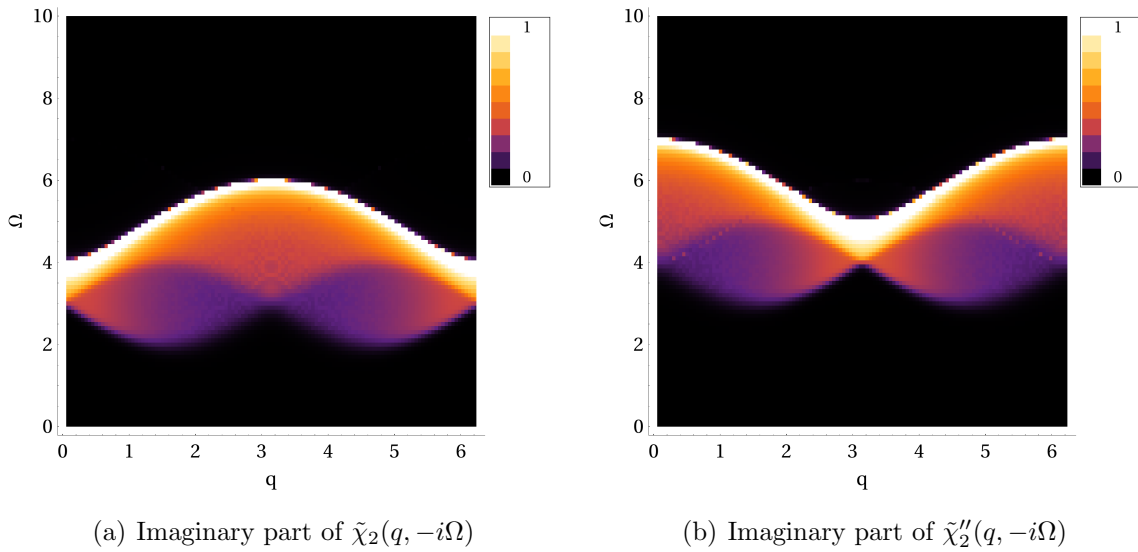


**Figure 3.7:** Contributions to the effective interaction

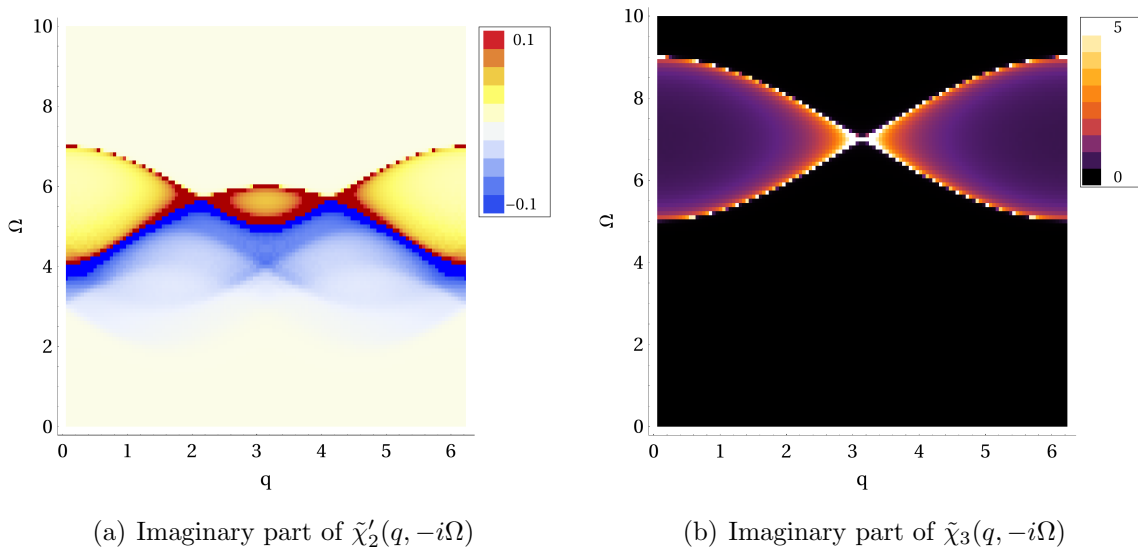


**Figure 3.8:** Contributions to the effective interaction

method to further analyze the three-band model.

### 3.3 cRPA and ctQMC study

So far, all our considerations were related to the high-energy physical processes, as it is the second step of a cRPA method to include them into an effective low-energy model. In order to study the three-band model, we need an additional method, which solves the effective low-energy model. In our case, this method is the continuous time Quantum

Monte Carlo (ctQMC), which will shortly be discussed in the following subsection.

Starting from the three-band model, the effective model generated by cRPA method 2 is a  $t$ - $V$  model with an additional interaction term

$$S = S_0 + v_1 \sum_i \int_0^\beta d\tau \hat{n}_i(\tau) \hat{n}_{i+1}(\tau) - \lambda \sum_{i,j} \int_0^\beta d\tau \int_0^\beta d\tau' \hat{n}_i(\tau) v_{\text{eff}}(i-j, \tau - \tau') \hat{n}_j(\tau'). \quad (3.30)$$

In the standard  $t$ - $V$  model,  $S_0$  is related to a hopping Hamiltonian of neighboring sites

$$\hat{H}_{tV,0} = -t \sum_i \left( c_i^\dagger c_{i+1} + c_{i+1}^\dagger c_i \right), \quad (3.31)$$

whereas in this context,  $S_0$  stems from the target band of the non-interacting Hamiltonian. The second term is just the nearest neighbor interaction of the target band, as indicated by the prefactor  $v_1$ . The last term is the additional contribution of the host bands we get from the cRPA. We introduce the prefactor  $\lambda$  in order to have a single parameter by which we can easily switch the additional effective interaction on and off. Effectively, the variation of  $\lambda$  corresponds to the variation of the interaction parameters  $v_2$ ,  $v'_2$  and  $v_3$ .

Before we present our own results of this model, which includes the effective interaction term, we shortly discuss the standard  $t$ - $V$  model. It is a well studied model, particularly as it is related to spin models [21, 22]. As long as the interaction is small, for  $|\frac{V}{t}| < 2$ , the system is a Luttinger liquid [23]. For attractive interaction, pairing fluctuations are dominant, whereas for repulsive interaction, charge fluctuations dominate. However, if the interaction is stronger than this value, different phases emerge: At  $\frac{V}{t} = -2$ , the system undergoes a first-order phase transition to a phase separated state for all band fillings, while for  $\frac{V}{t} > 2$ , the system is in a charge density wave phase [24]. So the value of the interaction parameter relative to the hopping determines the system properties and it is crucial whether the interaction corresponds to attraction or repulsion. This finding is important for our study of the three-band model, since we add effective interaction terms, which could be either attractive or repulsive.

### 3.3.1 Continuous time Quantum Monte Carlo

For the study of the low-energy effective model we use ctQMC. We briefly present the basic ideas of QMC [25] and ctQMC, following the description of Gull et al. [26]. In many cases, the central problem for the numerical calculation of physical properties is the evaluation of sums or integrals over a multidimensional phase space  $\mathcal{C}$ . For example, if we consider the partition function, we have to deal with an expression

$$Z = \int_{\mathcal{C}} d\mathbf{x} p(\mathbf{x}) \quad (3.32)$$

with  $p(\mathbf{x})$  being the Boltzmann weight of a certain configuration  $\mathbf{x} \in \mathcal{C}$ . Similarly, the expectation value of an observable  $\mathcal{O}$  is

$$\langle \mathcal{O} \rangle = \frac{1}{Z} \int_{\mathcal{C}} d\mathbf{x} \mathcal{O}(\mathbf{x}) p(\mathbf{x}). \quad (3.33)$$

In a Monte Carlo simulation, only  $M$  states  $\mathbf{x}_n$  of the full configuration space  $\mathcal{C}$  are selected, each with probability  $\frac{p(\mathbf{x}_n)}{Z}$ :

$$\langle \mathcal{O} \rangle_{\text{MC}} \equiv \frac{1}{M} \sum_{n=1}^M \mathcal{O}(\mathbf{x}_n) \quad (3.34)$$

Due to the central limit theorem, the Monte Carlo result approximates the exact value for large  $M$  [27]. The sampling of the integrals is performed using the configurations  $\mathbf{x}_n$  generated by a Markov process. The probability of a direct transition from configuration  $\mathbf{x}$  to configuration  $\mathbf{y}$  is denoted by  $W_{\mathbf{xy}}$ , all these probabilities of all transitions form the transition matrix. Since  $W_{\mathbf{xy}}$  are the transition probabilities, they have to fulfill

$$\sum_{\mathbf{y}} W_{\mathbf{xy}} = 1. \quad (3.35)$$

Furthermore, there are two necessary properties of the Markov process: Firstly, it has to be ergodic, which means that any configuration  $\mathbf{y}$  can be reached starting from any other configuration  $\mathbf{x}$  in a finite number of steps. Secondly, stationarity of the distribution  $p(\mathbf{x})$  requires balance, i.e.

$$\int_{\mathcal{C}} d\mathbf{x} W_{\mathbf{xy}} p(\mathbf{x}) = p(\mathbf{y}) \quad (3.36)$$

As an alternative sufficient, but not necessary condition, one commonly uses the detailed balance condition:

$$\frac{W_{\mathbf{xy}}}{W_{\mathbf{yx}}} = \frac{p(\mathbf{y})}{p(\mathbf{x})} \quad (3.37)$$

In order to satisfy detailed balance, the Metropolis-Hastings algorithm distinguishes between the proposal and acceptance of a transition from state  $\mathbf{x}$  to state  $\mathbf{y}$ :

$$W_{\mathbf{xy}} = W_{\mathbf{xy}}^{\text{prop}} W_{\mathbf{xy}}^{\text{acc}} \quad (3.38)$$

Detailed balance is satisfied, if the acceptance probability is taken as

$$W_{\mathbf{xy}}^{\text{acc}} = \min \left[ 1, \frac{p(\mathbf{y}) W_{\mathbf{yx}}^{\text{prop}}}{p(\mathbf{x}) W_{\mathbf{xy}}^{\text{prop}}} \right]. \quad (3.39)$$

If the proposed configuration  $\mathbf{y}$  is rejected,  $\mathbf{x}$  is used again, otherwise we switch to  $\mathbf{y}$ . Repeating this procedure of proposing an update, accepting or rejecting it and measuring the observables, we get the Monte Carlo expectation value.

After this outline of the essential ideas of the Monte Carlo method, we present the corresponding properties of ctQMC method we used. The general form of the partition function

$$\begin{aligned} Z &= \text{Tr} \left( \hat{T} e^{-\beta \hat{H}_A} \exp \left( - \int_0^\beta d\tau \hat{H}_B(\tau) \right) \right) \\ &= \sum_n (-1)^n \int_0^\beta d\tau_1 \dots \int_{\tau_{n-1}}^\beta d\tau_n \text{Tr} \left( e^{-\beta \hat{H}_A} \hat{H}_B(\tau_n) \times \dots \times \hat{H}_B(\tau_1) \right) \end{aligned} \quad (3.40)$$

is a useful starting point for ctQMC. The convergence of the series is guaranteed by the finiteness of the number of states, which is a particular property of fermionic systems [28]. We can apply the Monte Carlo method to eq. 3.40, by identifying the configurations  $\mathbf{x}$  of eq. (3.32) with  $\mathbf{x} = (n, (\tau_1, \dots, \tau_n), \gamma)$ . This means, we sample over all expansion orders  $n$ , all times  $\tau_1, \dots, \tau_n$  and all possible diagrams formed by the  $n$  vertices related to  $\hat{H}_B$ , which is denoted by  $\gamma$ . Therefore,  $\gamma$  can include the topology of a diagram as well as other discrete variables like spin, orbital or lattice indices. In our case,  $\hat{H}_B$  is the interaction part of the Hamiltonian. However, eq. (3.40) contains a possible problem, namely the factor  $(-1)^n$ : Up to now, we assumed that we sum and integrate probabilities, which means positive numbers. Here, we see that this is not the case for all contributions. In fact, negative signs appear frequently for fermionic systems, since fermionic operators anticommute. Sampling over the absolute value and reweighing the measurements according to this new probability distribution does not solve the sign problem. The crucial point is the possible counterbalance of positive and negative terms which leads to exponentially growing errors. In our case, we can solve the problem by introducing an auxiliary Ising spin field  $s$ . Apart from a trivial constant, we do not change the action which enters the partition function, if we rewrite eq. (3.30) as

$$\begin{aligned}
 S = S_0 + \sum_{i,s} \int_0^\beta d\tau \frac{v_1}{2} \left( \hat{n}_i - \frac{1}{2} - s\delta \right) \left( \hat{n}_{i+1} - \frac{1}{2} + s\delta \right) \\
 - \sum_{i,j,s} \int_0^\beta d\tau \int_0^\beta d\tau' \frac{U_{\text{eff}}}{2} p(i-j, \tau - \tau') I_{i-j, \tau - \tau'} \times \\
 \left( \hat{n}_i(\tau) - \frac{1}{2} + I_{i-j, \tau - \tau'} s\delta \right) \left( \hat{n}_j(\tau') - \frac{1}{2} + s\delta \right) \quad (3.41)
 \end{aligned}$$

with

$$U_{\text{eff}} = \lambda \sum_i \int_0^\beta d\tau |v_{\text{eff}}(i, \tau)|, \quad p(i, \tau) = \lambda \frac{|v_{\text{eff}}(i, \tau)|}{U_{\text{eff}}} \quad \text{and} \quad I_{i, \tau} = \text{sgn}(v_{\text{eff}}(i, \tau)). \quad (3.42)$$

Using  $\delta > \frac{1}{2}$  and assuming  $v_1 > 0$ , the sign problem is absent: For the first term, the product containing the densities is always negative, independent of the actual occupation and the Ising spin  $s$ . The negative sign cancels the global minus sign of the action. As for the second term, the argument is the same for negative  $I_{i-j, \tau - \tau'}$ , whereas for positive  $I_{i-j, \tau - \tau'}$ , both density terms have the same sign.

The quantities we measure in the ctQMC simulation are the density-density correlation functions

$$N(q) = \sum_r e^{iqr} \langle \hat{n}_r \hat{n}_0 \rangle \quad (3.43)$$

and the pairing correlation functions,

$$P(q) = \sum_r e^{iqr} \langle \Delta_r^\dagger \Delta_0 \rangle \quad (3.44)$$

with  $\Delta_r^\dagger = c_r^\dagger c_{r+1}^\dagger$ . This enables us to study the charge and pairing fluctuations which react to the repulsive or attractive effect of the effective interaction. This definition of



$N(q)$  and  $P(q)$  is similar to the usual one, but there is one difference: Since we deal with spinless fermions, we use neighboring electrons instead of electrons on the same site with opposite spin [29].

In order to satisfy the ergodicity condition, we need two different types of updates which increase or decrease the order  $n$ , i.e. add or remove a vertex, respectively. In principle, additional update rules can be used which may improve the efficiency of the method, but they are not necessary. Since we have two different interaction terms, the target band interaction and the effective interaction, we need updates for both of the corresponding vertices. The proposition probability for the addition of a vertex related to target band interaction is  $p_1$  and  $p_2 = 1 - p_1$  for an effective interaction vertex. The complete proposition probability for a special vertex of the first type is

$$W_{\Gamma_n \Gamma_{n+1}}^{\text{prop}} = p_1 \frac{d\tau_{n+1}}{2L\beta}. \quad (3.45)$$

Here, we have the factors 2 for the Ising spin,  $L$  for the lattice site and  $\frac{\beta}{d\tau_{n+1}}$  for the point in imaginary time. For the inverse process, so the removal of a vertex, we only have to choose one of the  $n + 1$  existing vertices, so the proposition probability is

$$W_{\Gamma_{n+1} \Gamma_n}^{\text{prop}} = \frac{1}{n + 1}. \quad (3.46)$$

In order to calculate the acceptance probability, we need the ratio of the weight of both configurations, with and without the additional vertex. This ratio is given by

$$\frac{p(\Gamma_{n+1})}{p(\Gamma_n)} = \frac{v_1 d\tau_{n+1} \det(M(\Gamma_{n+1}))}{2 \det(M(\Gamma_n))}, \quad (3.47)$$

since the calculation of the trace leads to the determinant of matrices  $M$  containing Green's functions of the non-interacting system, which depend on the time indices given by the vertices [30]. Using these expressions and eq. (3.39), we obtain the acceptance probability:

$$W_{\Gamma_n \Gamma_{n+1}}^{\text{acc}} = \min \left[ 1, \frac{L\beta v_1 \det(M(\Gamma_{n+1}))}{p_1(n + 1) \det(M(\Gamma_n))} \right] \quad (3.48)$$

In particular, this result shows that the infinitesimal formulation of the procedure, which is due to the continuity of the imaginary time, does not create problems: The infinitesimal time steps appearing in the proposition probability are cancelled by the additional infinitesimal of the configuration weight. For the inverse process, we only have to interchange the configuration indices. Therefore, the acceptance probability of a removal process is

$$W_{\Gamma_{n+1} \Gamma_n}^{\text{acc}} = \min \left[ 1, \frac{p_1(n + 1) \det(M(\Gamma_n))}{L\beta v_1 \det(M(\Gamma_{n+1}))} \right]. \quad (3.49)$$

Similar considerations are necessary for the second possible vertex, the effective interaction term. For the proposition of a special vertex, the spatial and temporal difference of the

interacting density operators has to be chosen. With this additional probability factor  $p(i - j, \tau - \tau')$ , the complete proposition probability reads

$$W_{\Gamma_n \Gamma_{n+1}}^{\text{prop}} = p_2 \frac{d\tau_{n+1}}{2L\beta} p(i - j, \tau - \tau'). \quad (3.50)$$

The proposition probability for the vertex removing update is again given by eq. (3.46), since we did not specify the type of the removed vertex. The ratio of the weight for the configuration before and after the vertex addition is given by

$$\frac{p(\Gamma_{n+1})}{p(\Gamma_n)} = \frac{U_{\text{eff}} p(i - j, \tau - \tau') d\tau_{n+1} \det(M(\Gamma_{n+1}))}{2 \det(M(\Gamma_n))}. \quad (3.51)$$

If we bring together all these terms, we get the acceptance probability for adding an effective interaction vertex:

$$W_{\Gamma_n \Gamma_{n+1}}^{\text{acc}} = \min \left[ 1, \frac{L\beta U_{\text{eff}} \det(M(\Gamma_{n+1}))}{p_2(n+1) \det(M(\Gamma_n))} \right] \quad (3.52)$$

In order to calculate the acceptance probability of the corresponding removal update, we again only need the inverse of the fracture. Having defined all the proposition and acceptance probabilities, we have all necessary information for the implementation of the ctQMC code.

### 3.3.2 Dynamical screening

Before we present our results of the three-band model, we discuss in some more detail which effects can be expected. In particular, the sign structure of the effective interaction is important for the ctQMC simulation. Moreover, we know that the solution of the  $t$ - $V$  model depends on the attractive or repulsive character of the interaction. Therefore, the central question is, whether the additional interaction term is an effective attraction or repulsion. In order to answer this question, we consider an effective interaction

$$v_{\text{eff}}(q, \tau) = \frac{1}{\beta} \sum_{\Omega_m} e^{i\Omega_m \tau} \int d\Omega \frac{N(q, \Omega)}{\Omega - i\Omega_m} \quad (3.53)$$

which is determined by excitations of the following form:

$$N(q, \Omega) = \delta(\Omega(q) - \Omega) - \delta(-\Omega(q) - \Omega), \quad \Omega(q) = \sqrt{w^2(1 - \cos(q - Q_0)) + \Delta^2} \quad (3.54)$$

Similar to the  $v_{\text{eff}}$  we computed in subsection 3.2.2, we have a dominant structure depending on momentum  $q$  and energy  $\Omega$ . The lowest energy at which excitation can happen is given by  $\Delta$ , the corresponding momentum transfer is  $Q_0$ . With these specifications, we

calculate the effective interaction in real space for  $0 < \tau < \beta$ :

$$\begin{aligned}
 v_{\text{eff}}(r, \tau) &= \frac{1}{N} \sum_q e^{-iqr} v_{\text{eff}}(q, \tau) \\
 &= \frac{1}{N\beta} \sum_{q, \Omega_m} e^{-iqr+i\Omega_m\tau} \left( \frac{1}{\Omega(q) - i\Omega_m} + \frac{1}{\Omega(q) + i\Omega_m} \right) \\
 &= \frac{1}{N} \sum_q e^{-iqr} \left( \frac{e^{\Omega(q)\tau}}{e^{\beta\Omega(q)} - 1} - \frac{e^{-\Omega(q)\tau}}{e^{-\beta\Omega(q)} - 1} \right) \\
 &= \frac{1}{N} \sum_q e^{-iqr} \left( \frac{e^{-\Omega(q)(\beta-\tau)}}{1 - e^{-\beta\Omega(q)}} + \frac{e^{-\Omega(q)\tau}}{1 - e^{-\beta\Omega(q)}} \right)
 \end{aligned} \tag{3.55}$$

Since  $\Omega(q)$  is always positive, the denominators are approximately equal to 1 for reasonably large  $\beta$  and the main contributions for  $\tau > \frac{\beta}{2}$  stem from the first term, for  $\tau < \frac{\beta}{2}$  from the second one. Let us consider the latter case, with  $\tau$  being not too small, so roughly  $1 < \tau < \frac{\beta}{2}$ . Within this range, the contributions with the lowest values of  $\Omega(q)$  are dominant, due to the exponential functions. We therefore apply a Taylor expansion of  $\Omega(q)$  around  $Q_0$  up to second order:

$$\Omega(q) \approx \Delta + \frac{w^2(q - Q_0)^2}{4\Delta} \tag{3.56}$$

Using this expansion to calculate  $v_{\text{eff}}(r, \tau)$ , we can extend the integration over  $q$  in order to finally obtain a Gaussian integral. Doing so, we get the approximate relation

$$v_{\text{eff}}(r, \tau) \propto \exp \left( iQ_0 r - \tau\Delta - \frac{r^2\Delta}{\tau w^2} \right). \tag{3.57}$$

This result yields several predictions concerning the effective interaction. The most remarkable one is that the momentum transfer of the excitation at the lowest energy determines its sign: For  $Q_0 = 0$ , we expect  $v_{\text{eff}}(r, \tau)$  to be generally attractive, whereas for  $Q_0 = \pi$ , we expect it to be repulsive for odd neighbors, but attractive for even ones. Particularly, this affects the nearest neighbor interaction, which determines the behavior of the original model. As a consequence, the system can be driven towards one or the opposite phase in the phase diagram, depending on  $Q_0$ . Of course, there is some uncertainty of this conclusion: The approximation is not valid for small  $\tau$  and if  $\tau$  and  $r$  are large,  $v_{\text{eff}}(r, \tau)$  is quite small, which is also indicated by eq. (3.57). It is therefore only in the intermediate range where our finding plays an important role.

In order to check whether the indicated dependence of the system on  $Q_0$  holds in spite of these objections, we solved the  $t$ - $V$  model using the above effective interaction  $v_{\text{eff}}(r, \tau)$  with  $t = 1$ ,  $v_1 = 1$ ,  $w = 1$ ,  $\Delta = 1$  and  $\beta = 10$  at half filling, both for  $Q_0 = 0$  and  $Q_0 = \pi$ . Comparing the results for both cases, we actually find opposite effects on the original model (see fig. 3.9). For  $Q_0 = \pi$ , the density-density correlation function  $N(q)$  has a very explicit peak at  $q = \pi$ , which is a sign that the system is driven towards the formation of a charge density wave. In contrast, the maximum is less pronounced for  $Q_0 = 0$  than for the case without the effective interaction.  $Q_0 = \pi$  and  $Q_0 = 0$  also have opposed

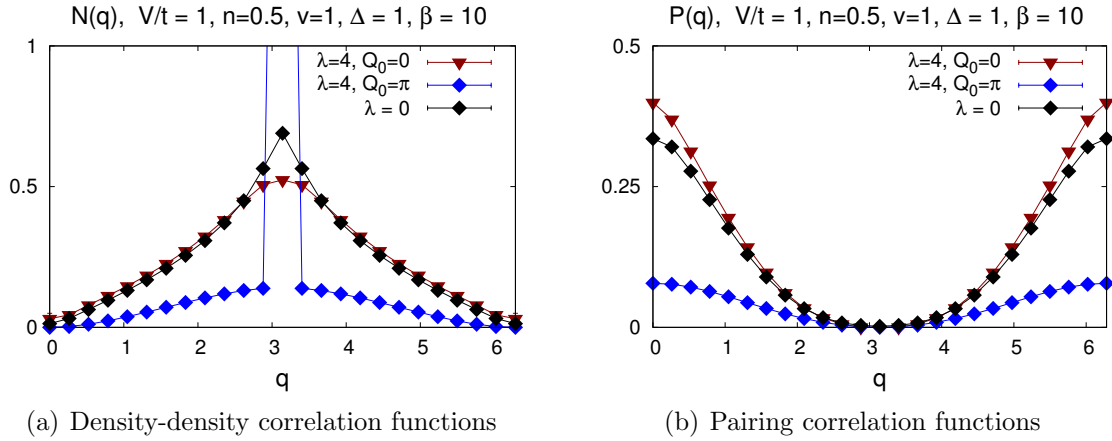


**Figure 3.9:** Simulation of the  $t$ - $V$  model with the additional effective interaction  $v_{\text{eff}}$ . Black diamonds denote the original model without  $v_{\text{eff}}$ , while red triangles and blue diamonds denote  $v_{\text{eff}}$  with  $Q_0 = 0$  and  $Q_0 = \pi$ , respectively.

effects if we compare the results of the pairing correlation function  $P(q)$ : There is a clear decrease in the first case, whereas  $P(q)$  is slightly increased in the second case. This confirms our expectations about the influence of  $Q_0$ . Since  $v_{\text{eff}}$  has a structure similar to the effective interaction we calculated numerically, we should find it in the results of the three-band model as well. As we have already shown, we understand the relation between the band structure and the effective interaction fairly well. As a consequence, we can use the dependence on  $Q_0$  in order to consciously influence the results of the  $t$ - $V$  model by the application of different band structures. In connection with real materials, this means that we would be able to change the properties of one chain of atoms via the interaction with additional chains, if these have appropriate properties and our cRPA description turns out to be correct. This imaginable procedure is what we call engineering effective models.

### 3.3.3 Engineering effective models

With regard to a theoretical model, our understanding of the  $t$ - $V$  model and the cRPA contribution of the host bands enables us to modify the physics of the target band without changing the corresponding target band parameters directly. In this sense, engineering an effective model means that we move the target band in one or the other direction of the phase diagram by varying the interaction between host and target band or the structure of the host bands. As we have seen, the momentum transfer  $Q_0$  of the excitation at lowest energy is crucial. We again choose interaction parameters that are dominated by host band excitations, whereas excitations that involve the target band play a minor role. Therefore, we compare two different band structures: For the first one, we get  $Q_0 = \pi$ , since the minimum and the maximum of the host bands have this momentum difference. For the second one, both host bands have two different minima and maxima, so we have two possible values of  $Q_0$ ,  $Q_0 = 0$  and  $Q_0 = \pi$  (see fig. 3.10). We will refer to them as

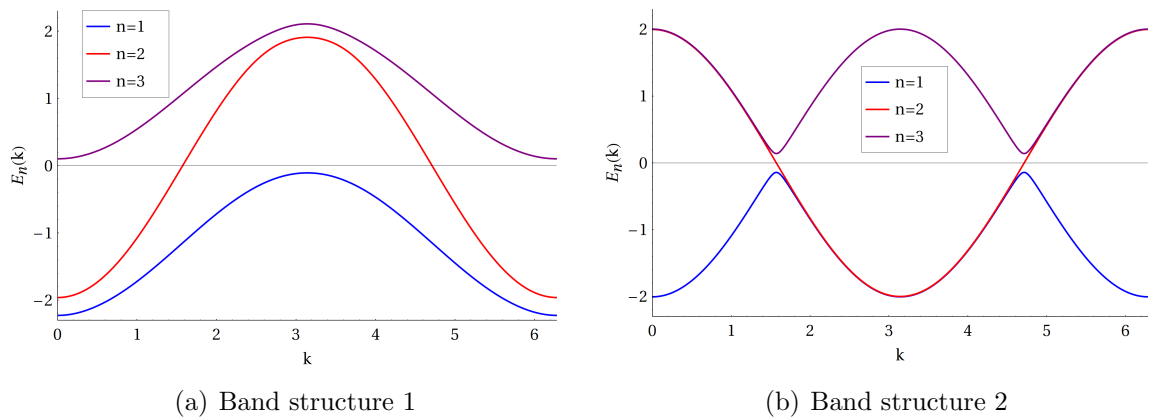


**Figure 3.10:** Band structures which allow lowest energy excitations with  $Q_0 = \pi$ , exclusively, and with both  $Q_0 = \pi$  and  $Q_0 = 0$

band structure 1 and band structure 2, respectively. Starting from the three-band model, we get band structure 1 by choosing the hopping parameters  $t_1 = 0.52$ ,  $t_2 = 1$ ,  $t_3 = 0.48$ ,  $t_\perp = 0.1$  and the chemical potentials  $\mu_1 = -1.14$ ,  $\mu_2 = 0$  and  $\mu_3 = 1.06$ . Due to the difference of the chemical potentials and the small inter-chain hopping parameter  $t_\perp$ , all bands are nearly sinusoidal and the energy gap between the host bands is about 0.2. For band structure 2, we set  $t_1 = -t_2 = t_3 = -1$ ,  $t_\perp = 0.1$  and  $\mu_1 = \mu_2 = \mu_3 = 0$ . Due to this specific choice, there is an explicit analytical expression for the bands:

$$E_1(k) = -\sqrt{\cos(k)^2 + 2t_\perp^2}, \quad E_2(k) = \cos(k), \quad E_3(k) = \sqrt{\cos(k)^2 + 2t_\perp^2} \quad (3.58)$$

So the target band is exactly sinusoidal and the energy gap between the host bands is  $2\sqrt{2}t_\perp$ . Consequently, the target band structure is very similar in both cases, aside from a phase shift of  $\pi$ . The energy range of the host bands is also comparable.

While the parameters of the non-interacting Hamiltonian have to be very different in order to create the two different band structures, we choose the same interaction parameters in order to be able to compare the results. We adopt the values of subsection 3.2.2  $v_2 = 0.2$ ,  $v'_2 = 0.1$ ,  $v_3 = 0.8$ ,  $v_4 = 0.02$  and  $v'_4 = 0.01$ , since we argued that they are quite reasonable. Furthermore, we choose again  $u = 10$  for band structure 1, but  $u = 2$  for band structure 2. The parameter  $u$  determines the relative strength of the nearest neighbor interaction between different chains, so one could imagine that its value is varied in real systems, for example by changing the geometry. The reason why we use different values of  $u$  here is that due to the momentum dependence of the interaction parameters  $u + 2\cos(q)$ , contributions at  $q = \pi$  can be weakened. For the first band structure we do not want this to happen, since this is the only possible type of low-energy excitation. However, for the second band structure, this weakening is rather helpful, since the contrast between both cases should be enhanced, if we suppress the  $q = \pi$  excitations here.

The numerical results of the effective interaction using these parameters and inverse temperature  $\beta = 20$  are shown in fig. 3.11. We again use real frequencies  $\Omega$  and consider the effective interaction in momentum space, since this enables us to easily connect its features to the respective band structure. As we intended,  $v_{\text{eff}}(q, -i\Omega)$  of band structure 1

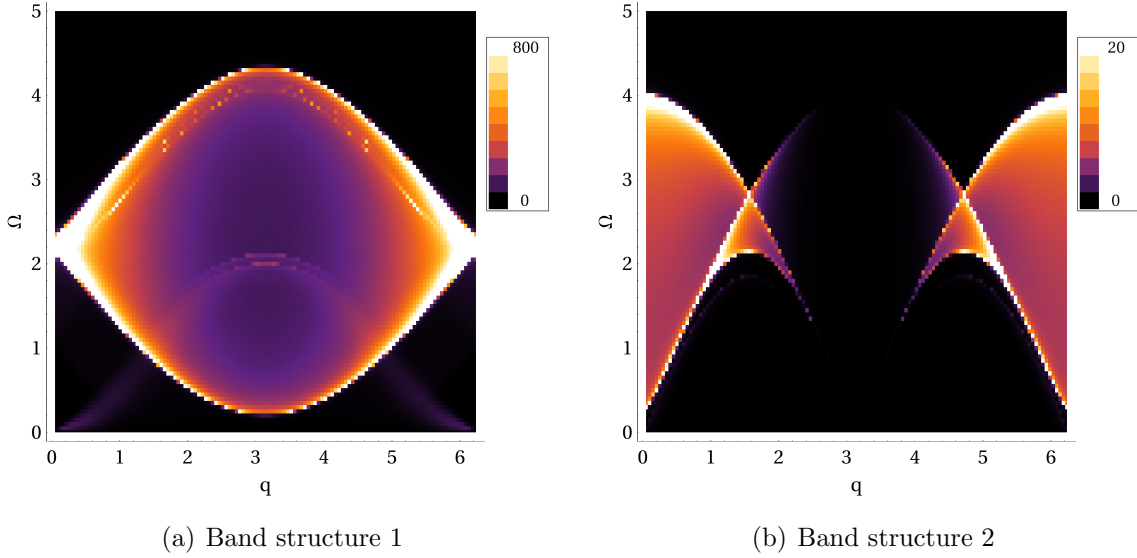


**Figure 3.11:** Effective interaction  $v_{\text{eff}}(q, -i\Omega)$  at  $\beta = 20$

has a low lying peak at  $q = \pi$ . Comparing  $v_{\text{eff}}(q, -i\Omega)$  to the band structure, we again find, that the dominant contribution stems from excitation between the host bands. However, there are some features which are due to other processes: At higher frequencies there are two curves we can ascribe to excitations involving the target band and one host band. Besides, there are two additional feature at low frequencies. They can be attributed to thermal effects of the host bands, since the energy distance to the Fermi level is relatively small at  $\beta = 20$ . If we go to lower temperatures, these features disappear and the peak at  $q = \pi$  is the only remaining low-energy feature.

For band structure 2,  $v_{\text{eff}}(q, -i\Omega)$  is rather different, but it can be explained using the same arguments as before.  $v_{\text{eff}}(q, -i\Omega)$  has the intended low-energy peak at  $q = 0$ , whereas the second peak at  $q = \pi$  is clearly suppressed by the cosine term of the interaction. Again, there is a faint feature at low frequencies, which stems from thermal excitations of the host bands. It is less clear than the corresponding feature for band structure 1, since the distance to the Fermi level is larger. The magnitude of  $v_{\text{eff}}(q, -i\Omega)$  differs as well, but this effect can be attributed to the smaller value of  $u$ .

Studying the effective interaction as a function of real frequencies  $\Omega$  and momentum  $q$  can help to identify the essential physical processes. However, it is  $v_{\text{eff}}(r, \tau)$  which enters the ctQMC calculation and in addition,  $v_{\text{eff}}(r, \tau)$  directly shows the attractive or repulsive effect. As it was indicated by eq. (3.57), a low lying  $q = \pi$  excitation leads to alternating sign of the interaction, whereas a low-energy  $q = 0$  peak leads to attraction. The numerical results of  $v_{\text{eff}}(r, \tau)$  for band structure 1 and 2 with system size  $N = 24$  confirms this expectation (see fig. 3.12). For  $\tau \approx 0$  and  $\tau \approx \beta$ , eq. (3.57) is not a good approximation, since in these cases, high-energy contributions are nearly as important as low-energy contributions. Therefore, the momentum dependence of the effective interaction does not stem from the band structure but from the momentum dependence of the interaction parameters, which is given by  $u + 2 \cos(q)$ . According to eq. (3.25), we always have to

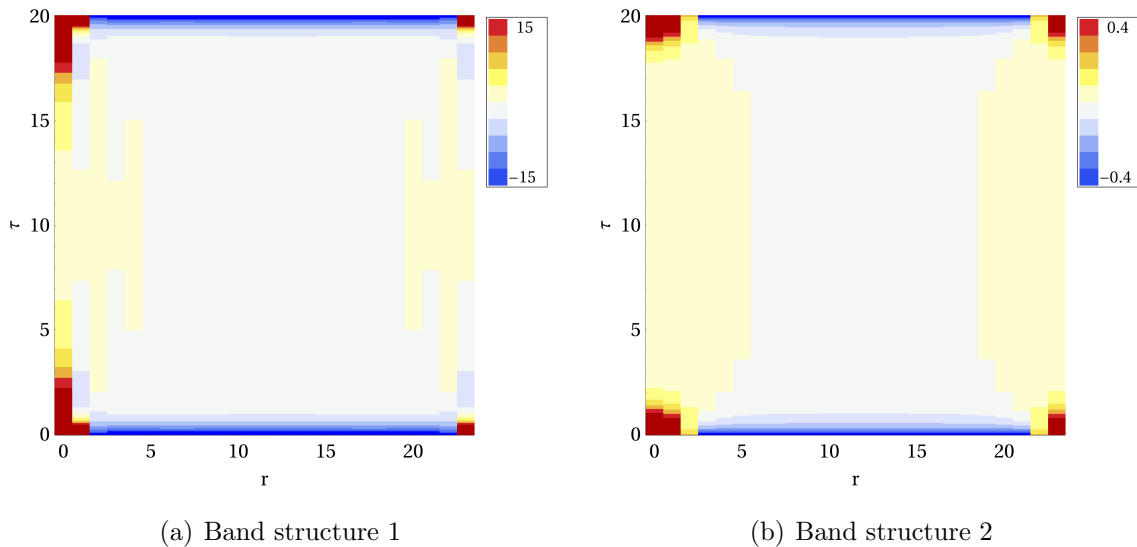


**Figure 3.12:** Effective interaction  $v_{\text{eff}}(r, \tau)$  at  $\beta = 20$  with system size  $N = 24$

deal with square interaction terms as prefactors to the effective interaction. Thus, we approximately get  $v_{\text{eff}}(r = 0, \tau = 0) \propto u^2 + 2$ ,  $v_{\text{eff}}(r = 1, \tau = 0) \propto 2u$  and likewise for  $\tau = \beta$  and  $r = 23$ , respectively. These contributions dominate, especially for the on-site interaction at  $r = 0$ . The effective interaction is slightly negative for all sites with a larger distance than the next-nearest neighbor, since we omit the addition of the constant  $q = 0$  term, according to our model Hamiltonian. These observations hold for  $v_{\text{eff}}(r, \tau)$  of both band structures. However, the most important insight we get from fig. 3.12 is the confirmation that  $v_{\text{eff}}(r, \tau)$  can either be basically attractive or have alternating sign. This behavior is restricted to intermediate time differences  $\tau$  and to sufficiently near neighbors. In this case, the maximal distance is about  $r = 5$ . The influence of the nearest neighbors is essential, so the effects we found in the previous subsection should reappear for the three-band model, even though they might be weakened as a consequence of this restrictions.

### 3.3.4 ctQMC results

In the previous subsection, we saw how different host band structures translate into different effective interactions  $v_{\text{eff}}(r, \tau)$ . Now, we use the resulting  $v_{\text{eff}}(r, \tau)$  to analyze the behavior of the three-band model with the ctQMC method. First, we consider band structure 1 again with the same interaction parameters. However, since the absolute value of the effective interaction gets quite large, which handicaps the ctQMC code, we choose the prefactor  $\lambda = 0.25$ , to scale down the complete effective interaction term. The results of the density-density correlation functions  $N(q)$  and the pairing correlation functions  $P(q)$  for inverse temperatures  $\beta = 10$  and  $\beta = 20$  are shown in fig. 3.13: Similar to the idealized case in subsection 3.3.2 the maximum of  $N(q)$  at  $q = \pi$  is increased, though not as dramatically. Additionally, this effect is enhanced if the temperature is lowered. We can ascribe this to the thermal effects we observed in fig. 3.11. Due to the relatively

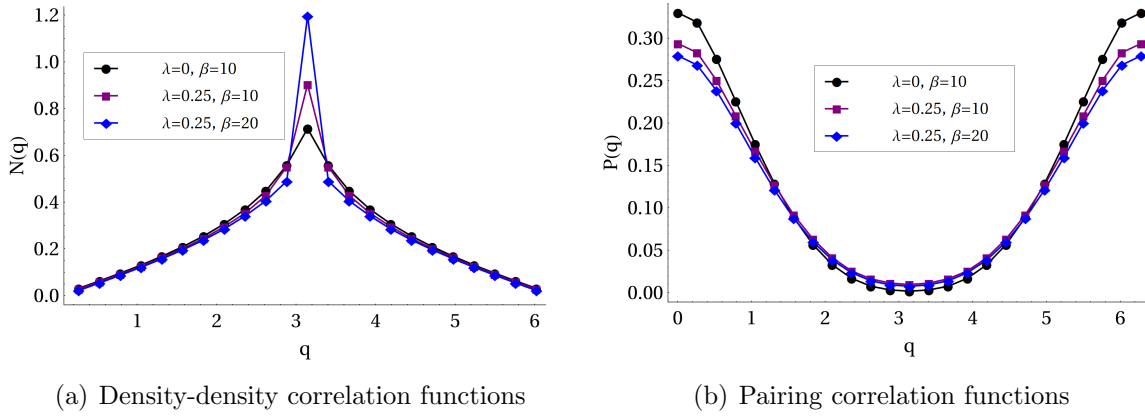


**Figure 3.13:** ctQMC results for band structure 1 without effective interaction (black) and with effective interaction at  $\beta = 10$  (purple) and  $\beta = 20$  (blue)

small energy distance of the host bands to the Fermi level, intra-host band excitations are possible. These lead to additional low-energy features of the effective interaction at  $q = 0$ . As a consequence, the repulsive effect of the  $q = \pi$  excitations is weakened. For lower temperatures, these thermal contributions are less important and the repulsive effect gets clearer. The same consideration holds for the pairing correlation functions  $P(q)$ : As expected, the high values of the pairing correlation functions around  $q = 0$  are lowered. Again, the effect is stronger for lower temperatures. Overall, these results indicate that the system is driven towards the charge density wave phase.

If we try to amplify the influence of the host bands, one method is to lower the temperature. However, this would increase the numerical effort to solve the model. Furthermore, this procedure should lead to a saturation when the temperature is low enough, so that thermal effects are negligible. We therefore choose another method, namely reducing the energy gap between the host bands. According to eq. (3.57), the damping of the effective interaction for high  $\tau$  and  $r$  is less important for smaller band gaps  $\Delta$ . Another consequence of a smaller band gap is the enhancement of the thermal excitations. For this reason, we cannot see the strongest possible effect of reducing  $\Delta$ , since this would require very low temperatures. For the band structure we use now and which we call band structure 3, we choose the chemical potentials  $\mu_1 = -1.09$ ,  $\mu_2 = 0$ ,  $\mu_3 = 1.01$  and the same hopping parameters as for band structure 2, i.e.  $t_1 = 0.52$ ,  $t_2 = 1$ ,  $t_3 = 0.48$  and  $t_\perp = 0.1$ . The band structure is very similar to band structure 1, except for the energy gap between the host bands, which is about 0.1 here (see fig. 3.14). For the interaction terms, we again use  $v_2 = 0.2$ ,  $v'_2 = 0.1$ ,  $v_3 = 0.8$ ,  $v_4 = 0.02$ ,  $v'_4 = 0.01$ ,  $u = 10$  and  $\lambda = 0.25$ . The corresponding ctQMC results are shown in fig. 3.15 for  $\beta = 10$  and  $\beta = 20$ . Both the density-density correlation function  $N(q)$  and the pairing correlation function indicate an effective increase of the repulsive interaction. Comparing fig. 3.13 and fig. 3.15, the enhancement of the host band influence due to the reduced band gap is visible. The differences from the  $\lambda = 0$  case, i.e. the simple  $t$ - $V$  model are larger for band structure 3. Furthermore, lowering the temperature has a stronger effect for a smaller band gap, since the suppression of thermal excitations is more important in this case. As a consequence,



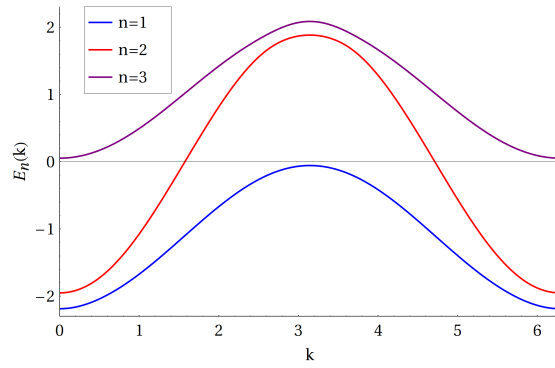


**Figure 3.14:** Band structure 3, with  $\mu_1 = -1.09$ ,  $\mu_2 = 0$ ,  $\mu_3 = 1.01$ ,  $t_1 = 0.52$ ,  $t_2 = 1$ ,  $t_3 = -0.48$  and  $t_{\perp} = 0.1$

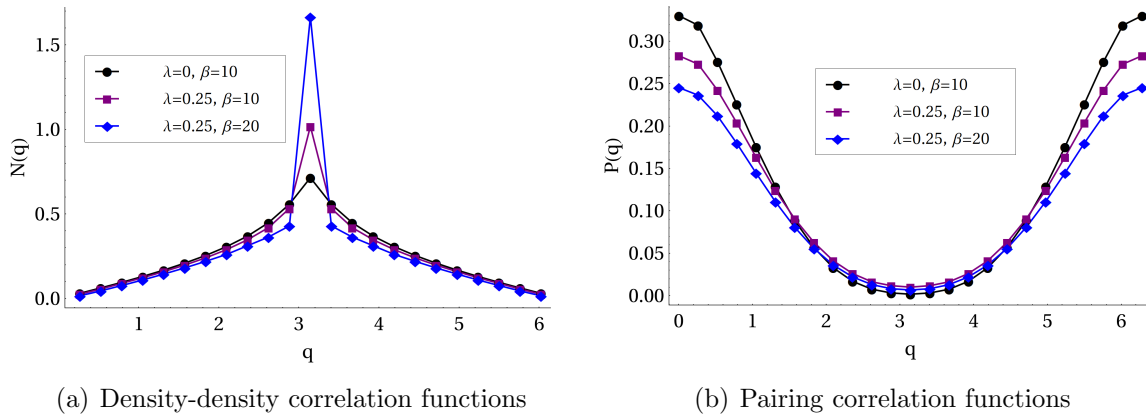


**Figure 3.15:** ctQMC results for band structure 3 without effective interaction (black) and with effective interaction at  $\beta = 10$  (purple) and  $\beta = 20$  (blue)

we expect a much higher effect for even lower temperatures.



## 4 Conclusion

We presented and tested two different cRPA schemes based on a path integral method. The basic ideas of the cRPA is the transformation of a multi-band model to a low-energy effective model. The first scheme, cRPA method 1, uses the localization of bands. After the Hubbard-Stratonovich transformation of the partition function we expand the action around the saddle point up to second order. This procedure eliminates all density operators  $\hat{n}$  and is equivalent to the RPA method. Subsequently, we integrated out the auxiliary fields related to high-energy processes and identified the effective interaction as coupling of the remaining low energy auxiliary fields. However, for cRPA method 1 two problems turned out to create objectionable low-energy contributions: In the model we used, the localization is not perfect and generally, we always need an overlap with the target band. Therefore, target band interaction is always reincluded through the back door within this formulation.

For cRPA method 2, we again used the Hubbard-Stratonovich transformed partition function as a starting point. In order to not include target band processes, we decoupled them from the high-energy processes involving host bands before we expanded the action. According to our experience with cRPA method 1, we based the attribution to high-energy or low-energy processes on the density operators  $\hat{n}$  instead of using the auxiliary fields. The decoupling is no exact property of the considered models, so we introduced a second approximation additional to the RPA of the host bands. This method turned out to avoid the problems of cRPA method 1, so we used it for our further studies.

We considered a model describing three atom chains. Using cRPA method 2, this model is transformed to a  $t$ - $V$  model with an additional effective interaction. This effective interaction contains both temporal and spacial fluctuation and we were able to explain its dominant features by the structure of the host bands. We found that a low-energy excitation leads to an additional repulsion of nearest neighbors if the momentum transfer is  $q = \pi$ , whereas vanishing momentum transfer leads to an effective attraction. This enables us to "design" an effective interaction of the target band by the manipulation of the host band structure, a procedure we called "engineering effective models".

In order to solve the low-energy model, we used a ctQMC method. We focused on the influence of the low energy  $q = \pi$  excitations and confirmed their anti-screening effect. We found that the influence of the host bands is increased if they come closer to the Fermi level, but further studies would be required in order to find out the relevant energy scale for this behavior. Another important issue for future work is a test of accuracy of the presented cRPA method. There are two possible error sources: Firstly, the RPA of the high-energy bands, which is a well-known and widely used method, and secondly, the decoupling of the high-energy processes from low-energy processes. If the distance of the band gaps from the Fermi level is large, these approximations should be irrelevant, since this improves the decoupling and diminishes the contribution of the host band interaction. However,

in the considered models the host bands are energetically close to the Fermi level, so it is still necessary to check the appropriateness of the cRPA method. For this purpose, it would be useful to compare our results to exact solutions of the three-band model. Further question of future studies arise from the application of this cRPA method to more realistic models. Within this work, we used model parameters, which we assumed to be reasonable, but it is possible to compute them for real materials from first principles. In particular, the interaction term can be calculated starting from the Coulomb interaction expression. Using such realistic models, one could study the prospects and limitations of the proposed engineering procedure for real materials. Furthermore, an extension of the cRPA scheme and the three-band model in order to include the spin would be desirable.

# A Detailed calculations

## A.1 Commutation of $\hat{n}_n(q)$

We prove the commutation of densities  $\hat{n}_n(q)$  using their definition, given in eq. (2.4), and the transformation of the Wannier operators, given in eq. (3.6):

$$\begin{aligned}
[\hat{n}_n(q), \hat{n}_m(q')] &= \frac{1}{L} \sum_{k, k'} [c_{n, k}^\dagger c_{n, k+q}, c_{n, k'}^\dagger c_{n, k'+q'}] \\
&= \frac{1}{L} \sum_{k, k'} \sum_{\alpha, \alpha'} \sum_{\beta, \beta'} U_{n\alpha}^\dagger(k) U_{\alpha'n}(k+q) U_{m\beta}^\dagger(k') U_{\beta'm}(k'+q') [\gamma_{\alpha, k}^\dagger \gamma_{\alpha', k+q}, \gamma_{\beta, k'}^\dagger \gamma_{\beta', k'+q'}] \\
&= \frac{1}{L} \sum_{\alpha, \alpha'} \left( \sum_{k, \beta'} U_{n\alpha}^\dagger(k) U_{\alpha'n}(k+q) U_{m\alpha'}^\dagger(k+q) U_{\beta'm}(k+q+q') \gamma_{\alpha, k}^\dagger \gamma_{\beta', k+q+q'} \right. \\
&\quad \left. - \sum_{k', \beta} U_{n\alpha}^\dagger(k'+q') U_{\alpha'n}(k'+q'+q) U_{m\beta}^\dagger(k') U_{\alpha m}(k'+q') \gamma_{\beta, k'}^\dagger \gamma_{\alpha', k'+q'+q} \right) \\
&= \frac{1}{L} \sum_{k, \alpha, \beta} \left( \delta_{nm} U_{n\alpha}^\dagger(k) U_{\beta m}(k+q+q') \gamma_{\alpha, k}^\dagger \gamma_{\beta, k+q+q'} \right. \\
&\quad \left. - \delta_{nm} U_{\alpha n}(k+q'+q) U_{m\beta}^\dagger(k) \gamma_{\beta, k}^\dagger \gamma_{\alpha, k+q'+q} \right) \\
&= \frac{1}{L} \delta_{nm} \sum_k (c_{n, k}^\dagger c_{m, k+q+q'} - c_{m, k}^\dagger c_{n, k+q'+q}) = 0 \tag{A.1}
\end{aligned}$$

## A.2 Commutation of the integration sequence

We want to show that we can change the sequence of the auxiliary field integration without affecting the result of the effective interaction. As we have seen in subsection 2.1.4, one integration step leads to a prefactor and an effective renormalization of the remaining susceptibilities (see eq. (2.56)). In order to compare the different integration sequences, we introduce a new notation: We write  $\chi_{nm}^{(n'm', \tilde{n}\tilde{m})}$  to indicate that  $z_{n', m'}$ ,  $\bar{z}_{n', m'}$  and  $z_{\tilde{n}, \tilde{m}}$ ,  $\bar{z}_{\tilde{n}, \tilde{m}}$  have already been integrated out. Every further integration step is denoted by the corresponding pair of indices of the auxiliary field being integrated out. We consider the susceptibility  $\chi_{nm}^{(\alpha)}$ , where an arbitrary combination of integrations has already been performed, as indicated by  $\alpha$ . If we now integrate  $z_{n', m'}$ ,  $\bar{z}_{n', m'}$  and subsequently  $z_{\tilde{n}, \tilde{m}}$ ,  $\bar{z}_{\tilde{n}, \tilde{m}}$ , we get the following prefactors:

$$\begin{aligned}
& \left( \frac{1}{1 + v_{n'm'} \chi_{n'm'}^{(\alpha)}} \right) \left( \frac{1}{1 + v_{\tilde{n}\tilde{m}} \chi_{\tilde{n}\tilde{m}}^{(\alpha, n'm')}} \right) \\
&= \frac{1}{\left(1 + v_{n'm'} \chi_{n'm'}^{(\alpha)}\right) \left(1 + v_{\tilde{n}\tilde{m}} \chi_{\tilde{n}\tilde{m}}^{(\alpha)}\right) - v_{\tilde{n}\tilde{m}} v_{n'm'} \chi_{\tilde{n}\tilde{m}}^{(\alpha)} \chi_{n'm'}^{(\alpha)}} \\
&= \left( \frac{1}{1 + v_{\tilde{n}\tilde{m}} \chi_{\tilde{n}\tilde{m}}^{(\alpha)}} \right) \left( \frac{1}{1 + v_{n'm'} \chi_{n'm'}^{(\alpha, \tilde{n}\tilde{m})}} \right) \tag{A.2}
\end{aligned}$$

This proves that we obtain the same prefactor if the integration sequence is interchanged. Let us check whether this commutation is also possible for the second term, the redefined susceptibility  $\chi_{nm}^{(\alpha, n'm', \tilde{n}\tilde{m})}$ :

$$\begin{aligned}
\chi_{nm}^{(\alpha, n'm', \tilde{n}\tilde{m})} &= \chi_{nm}^{(\alpha, n'm')} - \frac{v_{\tilde{n}\tilde{m}} \chi_{\tilde{n}\tilde{m}}^{(\alpha, n'm')} \chi_{nm}^{(\alpha, n'm')}}{1 + v_{\tilde{n}\tilde{m}} \chi_{\tilde{n}\tilde{m}}^{(\alpha, n'm')}} = \chi_{nm}^{(\alpha)} - \frac{v_{n'm'} \chi_{nm'}^{(\alpha)} \chi_{n'm}^{(\alpha)}}{1 + v_{n'm'} \chi_{n'm'}^{(\alpha)}} \\
&\quad - \frac{v_{\tilde{n}\tilde{m}} \chi_{\tilde{n}\tilde{m}}^{(\alpha)} \chi_{\tilde{n}\tilde{m}}^{(\alpha)} \left(1 + v_{n'm'} \chi_{n'm'}^{(\alpha)}\right)^2 + v_{\tilde{n}\tilde{m}} v_{n'm'}^2 \chi_{nm'}^{(\alpha)} \chi_{n'm}^{(\alpha)} \chi_{\tilde{n}\tilde{m}}^{(\alpha)} \chi_{n'm}^{(\alpha)}}{\left(\left(1 + v_{\tilde{n}\tilde{m}} \chi_{\tilde{n}\tilde{m}}^{(\alpha)}\right) \left(1 + v_{n'm'} \chi_{n'm'}^{(\alpha)}\right) - v_{\tilde{n}\tilde{m}} v_{n'm'} \chi_{n'm}^{(\alpha)} \chi_{\tilde{n}\tilde{m}}^{(\alpha)}\right) \left(1 + v_{n'm'} \chi_{n'm'}^{(\alpha)}\right)} \\
&\quad + \frac{v_{\tilde{n}\tilde{m}} v_{n'm'} \left(\chi_{nm'}^{(\alpha)} \chi_{n'm}^{(\alpha)} \chi_{\tilde{n}\tilde{m}}^{(\alpha)} + \chi_{n\tilde{m}}^{(\alpha)} \chi_{\tilde{n}m'}^{(\alpha)} \chi_{n'm}^{(\alpha)}\right) \left(1 + v_{n'm'} \chi_{n'm'}^{(\alpha)}\right)}{\left(\left(1 + v_{\tilde{n}\tilde{m}} \chi_{\tilde{n}\tilde{m}}^{(\alpha)}\right) \left(1 + v_{n'm'} \chi_{n'm'}^{(\alpha)}\right) - v_{\tilde{n}\tilde{m}} v_{n'm'} \chi_{n'm}^{(\alpha)} \chi_{\tilde{n}\tilde{m}}^{(\alpha)}\right) \left(1 + v_{n'm'} \chi_{n'm'}^{(\alpha)}\right)} \\
&= \chi_{nm}^{(\alpha)} - \frac{v_{n'm'} \chi_{nm'}^{(\alpha)} \chi_{n'm}^{(\alpha)} + v_{\tilde{n}\tilde{m}} \chi_{\tilde{n}\tilde{m}}^{(\alpha)} \chi_{\tilde{n}\tilde{m}}^{(\alpha)}}{\left(1 + v_{\tilde{n}\tilde{m}} \chi_{\tilde{n}\tilde{m}}^{(\alpha)}\right) \left(1 + v_{n'm'} \chi_{n'm'}^{(\alpha)}\right) - v_{\tilde{n}\tilde{m}} v_{n'm'} \chi_{n'm}^{(\alpha)} \chi_{\tilde{n}\tilde{m}}^{(\alpha)}} \\
&\quad - \frac{v_{n'm'} v_{\tilde{n}\tilde{m}} \left(\chi_{nm'}^{(\alpha)} \chi_{n'm}^{(\alpha)} \chi_{\tilde{n}\tilde{m}}^{(\alpha)} + \chi_{n\tilde{m}}^{(\alpha)} \chi_{\tilde{n}m'}^{(\alpha)} \chi_{n'm}^{(\alpha)}\right)}{\left(1 + v_{\tilde{n}\tilde{m}} \chi_{\tilde{n}\tilde{m}}^{(\alpha)}\right) \left(1 + v_{n'm'} \chi_{n'm'}^{(\alpha)}\right) - v_{\tilde{n}\tilde{m}} v_{n'm'} \chi_{n'm}^{(\alpha)} \chi_{\tilde{n}\tilde{m}}^{(\alpha)}} \\
&\quad + \frac{v_{n'm'} v_{\tilde{n}\tilde{m}} \left(\chi_{nm'}^{(\alpha)} \chi_{n'm}^{(\alpha)} \chi_{\tilde{n}\tilde{m}}^{(\alpha)} + \chi_{n\tilde{m}}^{(\alpha)} \chi_{\tilde{n}m'}^{(\alpha)} \chi_{n'm}^{(\alpha)}\right)}{\left(1 + v_{\tilde{n}\tilde{m}} \chi_{\tilde{n}\tilde{m}}^{(\alpha)}\right) \left(1 + v_{n'm'} \chi_{n'm'}^{(\alpha)}\right) - v_{\tilde{n}\tilde{m}} v_{n'm'} \chi_{n'm}^{(\alpha)} \chi_{\tilde{n}\tilde{m}}^{(\alpha)}} \tag{A.3}
\end{aligned}$$

This expression stays exactly the same, if we interchange the indices  $n', m'$  and  $\tilde{n}, \tilde{m}$ . Therefore, we can conclude

$$\chi_{nm}^{(\alpha, n' m', \tilde{n} \tilde{m})} = \chi_{nm}^{(\alpha, \tilde{n} \tilde{m}, n' m')}. \quad (\text{A.4})$$

For both terms, the integration sequence is commutative, as expected. Though there are many ways of implementing our integration scheme, its result is unambiguous.

### A.3 Commutation of $\hat{n}_\alpha(q)$

We have to show that

$$\sum_{\alpha, \alpha'} v_{\alpha, \alpha'}(q) [\hat{n}_\alpha(q), \hat{n}_{\alpha'}(-q)] = 0. \quad (\text{A.5})$$

This means that the sum over all densities commutes, although the single densities  $\hat{n}_\alpha(q)$  in general do not, according to eq. (2.63). In order to prove this, we need eq. (2.63) and the definition of  $v_{\alpha, \alpha'}(q)$ , given in eq. (2.61):

$$\begin{aligned} & L \sum_{\alpha, \alpha'} v_{\alpha, \alpha'}(q) [\hat{n}_\alpha(q), \hat{n}_{\alpha'}(-q)] \\ &= \sum_{n, m, k} \sum_{n', m', k'} v_{nmn'm'kk'}(q) (\gamma_{n, k}^\dagger \gamma_{m', k} \delta_{m, n'} \delta_{k', k+q} - \gamma_{n', k'}^\dagger \gamma_{m, k} \delta_{m', n} \delta_{k, k'-q}) \\ &= \sum_{l, n, m} \sum_{k, l', m'} v_{l, l'}(q) U_{ln}^\dagger(k) U_{ml}(k+q) U_{l'm}^\dagger(k+q) U_{m'l'}(k) \gamma_{n, k}^\dagger \gamma_{m', k} \\ &\quad - \sum_{l, n, m} \sum_{k, l', n'} v_{l, l'}(q) U_{ln}^\dagger(k) U_{ml}(k+q) U_{l'n'}^\dagger(k+q) U_{nl'}(k) \gamma_{n', k+q}^\dagger \gamma_{m, k+q} \\ &= \sum_{l, n, m'} \sum_k v_{l, l'}(q) U_{ln}^\dagger(k) U_{m'l}(k) \gamma_{n, k}^\dagger \gamma_{m', k} \\ &\quad - \sum_{l, m, n'} \sum_k v_{l, l'}(q) U_{ml}(k+q) U_{ln'}^\dagger(k+q) \gamma_{n', k+q}^\dagger \gamma_{m, k+q} \\ &= 0 \end{aligned} \quad (\text{A.6})$$



## A.4 Effective interaction using cRPA method 2

In subsection 3.2.1, we briefly discussed the analytical expression of the effective interaction  $v_{\text{eff}}(q, \Omega_m)$  (see eq. (3.25)-(3.29)). Here, we will justify this result more explicitly. We have seen that the additional terms leading to the effective interaction have the following structure: Starting from the target band, an interaction process causes an excited state. This state can be excited again by a subsequent interaction process to a new state, and so forth. Finally, we have to end up on the target band again. These processes generate all contributions taken into account by the RPA scheme. In order to get  $v_{\text{eff}}(q, \Omega_m)$ , we simply multiply the factors  $v_{\alpha, \alpha'}(q)$  corresponding to the interactions and  $\chi_{\alpha\alpha'}(q, \Omega_m)$  corresponding to the intermediate excited states and sum up the contributions of all possible processes with the correct sign. Since this procedure leads to infinite sums over equal processes, geometrical series appear and we can use [31]

$$\sum_{i=0}^{\infty} x^i = \frac{1}{1-x}. \quad (\text{A.7})$$

Here, we consider the first term of  $v_{\text{eff}}(q, \Omega_m)$ , given in eq. (3.26). All contributions of this term contain two interaction processes corresponding to  $v_2(q)$ . Bearing in mind the definition of  $v_2(q)$ , we conclude that this contribution consists of all processes, where the first interaction creates a hole in the target band and an electron in the host band, whereas the last interaction has the inverse effect. In order to get  $\tilde{\chi}_2$ , we have to sum up all possible processes that can take place in between. The first possible process is the creation of a different electron and a different hole, related to the interaction parameter  $v_4(q)$ . The second possible process is the annihilation of the hole and the electron, together with the creation of an electron in the target band and a hole in a host band. For this process, the corresponding interaction parameter is  $v'_4(q)$ . However, since the type of the last interaction is given by  $v_2(q)$ , this process has to be reversed, before all electrons and holes are annihilated. Both types of processes can happen infinitely often and since every interaction leads to an additional minus sign, the full expression for  $\tilde{\chi}_2$  reads

$$\begin{aligned} \tilde{\chi}_2 = & \\ & \chi'_{n,2} \sum_{i_1=0}^{\infty} (-v_4 \chi'_{n,2})^{i_1} \sum_{i_0=0}^{\infty} \left( (-v'_4 \chi'_{2,n}) \left( \sum_{i_2=0}^{\infty} (-v_4 \chi'_{2,n})^{i_2} \right) (-v'_4 \chi'_{n,2}) \left( \sum_{i_3=0}^{\infty} (-v_4 \chi'_{n,2})^{i_3} \right) \right)^{i_0}. \end{aligned} \quad (\text{A.8})$$

Using the formula for geometrical series, we get:

$$\begin{aligned} \tilde{\chi}_2 &= \frac{\chi'_{n,2}}{1 + v_4 \chi'_{n,2}} \sum_{i_0=0}^{\infty} \left( \frac{v_4'^2 \chi'_{2,n} \chi'_{n,2}}{(1 + v_4 \chi'_{2,n}) (1 + v_4 \chi'_{n,2})} \right)^{i_0} \\ &= \frac{\chi'_{n,2}}{1 + v_4 \chi'_{n,2}} \frac{(1 + v_4 \chi'_{2,n}) (1 + v_4 \chi'_{n,2})}{(1 + v_4 \chi'_{2,n}) (1 + v_4 \chi'_{n,2}) - v_4'^2 \chi'_{2,n} \chi'_{n,2}} \\ &= \frac{\chi'_{n,2} (1 + v_4 \chi'_{2,n})}{(1 + v_4 \chi'_{2,n}) (1 + v_4 \chi'_{n,2}) - v_4'^2 \chi'_{2,n} \chi'_{n,2}} \end{aligned} \quad (\text{A.9})$$

This is exactly the expression of  $\tilde{\chi}_2$  in eq. (3.26). The calculation for  $\tilde{\chi}'_2$  and  $\tilde{\chi}''_2$  is very similar, whereas the last term is a simple special case due to our choice of the interaction parameters, as we already mentioned in subsection 3.2.1.

## B Deutsche Zusammenfassung

In dieser Masterarbeit stellen wir zwei auf Pfadintegralen basierende cRPA-Methoden vor, welche wir anschließend zur Lösung eines Drei-Band-Modells nutzen. Die Grundidee der cRPA-Methode ist folgende: Für Korrelationseffekte besitzen die Beiträge der niederenergetischen Bänder eine größere Relevanz als die der hochenergetischen Bänder, aber dennoch sollen letztere nicht komplett vernachlässigt werden. Daher ist es sinnvoll eine aufwendige, aber genaue Lösungsmethode für die niederenergetischen Bänder zu verwenden, während die hochenergetischen Bänder nur unter Anwendung einer vergleichsweise groben Näherung berücksichtigt werden. Dazu wird die Lösung eines Modells in drei Schritte zerlegt: Erstens, die Berechnung der vollständigen Bandstruktur, zweitens, die Vereinfachung des ursprünglichen Modells zu einem effektiven Modell für die niederenergetischen Bänder, das den Einfluss der hochenergetischen Bänder in Form eines zusätzlichen Wechselwirkungsterms beinhaltet, und drittens, das Lösen des so erhaltenen effektiven Modells.

Die Herangehensweise, die wir in dieser Arbeit verfolgen, ist ganz analog: Die Ausgangsbandstruktur ergibt sich aus dem wechselwirkungsfreien Teil des Hamiltonoperators und das effektive Modell lösen wir mit einer ctQMC-Methode. Für den dazwischenliegenden Schritt, die Reduzierung des vollständigen Modells auf das effektive Modell, präsentieren wir zwei Möglichkeiten. Die erste Methode ist konstruiert für Systeme, die lokalisierte Bänder besitzen. Wir nutzen die Lokalisierung, indem wir die Zuordnung der Bänder zum hochenergetischen oder niederenergetischen Bereich auf Grundlage der räumlichen Indizes treffen. Nach der Hubbard-Stratonovich-Transformation der Zustandssumme und anschließender Taylor-Entwicklung der Wirkung bis zu zweiter Ordnung um den paramagnetischen Sattelpunkt integrieren wir diejenigen Hilfsfelder aus, die wir dem Hochenergiebereich zuordnen. Dem übrig bleibenden Ausdruck können wir daraufhin den zusätzlichen Wechselwirkungsterm des effektiven Modells entnehmen. Es zeigt sich jedoch, dass diese Vorgehensweise ungeeignet ist, weil sie dazu führt, dass die effektive Wechselwirkung auch niederenergetische Anteile enthält, die folglich zweimal im effektiven Modell berücksichtigt werden. Dies liegt in der mangelhaften Zuschreibung der Größen zum entsprechenden Energiebereich begründet, was einerseits der unvollständigen Lokalisierung der Bänder im untersuchten Modell, andererseits der Betrachtung der Hilfsfelder anstelle der Dichteoperatoren zuzuschreiben ist.

Dieser Mangel wurde in der Ausgestaltung der zweiten cRPA-Methode behoben. Wir beginnen wieder mit der Hubbard-Stratonovich-Transformation der Zustandssumme, doch zerlegen diesmal die Wirkung anhand der Bandindizes der Dichteoperatoren in einen niederenergetischen und einen hochenergetischen Anteil. Dadurch führen wir eine weitere Näherung ein, die jedoch gerechtfertigt ist, solange die Energiedifferenz zwischen beiden Energiebereichen ausreichend groß ist. Anschließend verwenden wir erneut die Taylor-Entwicklung um den paramagnetischen Sattelpunkt, allerdings nur für den hochenergeti-

schen Teil der Wirkung. Das Resultat ist wieder ein Gaußscher Ausdruck, sodass die Hubbard-Stratonovich-Transformation einfach rückgängig gemacht werden kann. Diese Vorgehensweise garantiert, dass das Ergebnis der Rücktransformation nur noch Operatoren enthält, die dem niederenergetischen Band zuordenbar sind. Die Operatoren stammen aus dem niederenergetischen Anteil der Wirkung, der die ursprüngliche Wechselwirkung dieses Bandes exakt reproduziert. Dies ist nicht überraschend, da wir an ihm keine weiteren Näherungen vorgenommen haben. Zusätzlich beinhaltet dieser Anteil aber auch die Kopplung der niederenergetischen Dichteoperatoren an Hilfsfelder, die eine Verbindung zu den hochenergetischen Prozessen herstellen, welche im hochenergetischen Anteil der Wirkung enthalten sind und aufgrund unserer Näherungen auf dem RPA-Niveau berücksichtigt werden. Durch die Integration der Hilfsfelder entsteht aus diesen Beiträgen erneut ein zusätzlicher Wechselwirkungsterm, der sowohl vom räumlichen Abstand als auch der Differenz der imaginären Zeit der wechselwirkenden Fermionen abhängt. Im Gegensatz zur vorangegangenen Methode ergeben sich hier keine Probleme durch die unbeabsichtigte Einbindung von niederenergetischen Beiträgen in diese effektive Wechselwirkung.

Wir wenden die zweite cRPA-Methode auf ein Modell für spinlose Fermionen auf drei Atomketten an. Hierbei besitzt jede Kette ein eigenes chemisches Potential und wir erlauben Hüpfen auf den Ketten ebenso wie Hüpfen zwischen den äußeren Ketten und der mittleren Kette. Indem wir das chemische Potential für die äußeren Atomketten ausreichend positiv beziehungsweise ausreichend negativ und für die mittlere Atomkette gleich Null wählen, stellen wir sicher, dass nur ein Band das Fermi-Niveau schneidet. Damit sind die Bänder zudem weitgehend auf den entsprechenden Atomketten lokalisiert. Zusätzlich berücksichtigen wir eine Wechselwirkung, die im Wesentlichen nächste Nachbar- und übernächste Nachbar-Prozesse umfasst und hauptsächlich, aber nicht ausschließlich, das niederenergetische Band betrifft. Unter Verwendung der cRPA-Methode berechnen wir aus diesem Modell das effektive Modell, also die zusätzliche, effektive Wechselwirkung. Das resultierende Modell ist das bereits bekannte  $t$ - $V$ -Modell, ergänzt um den effektiven Wechselwirkungsterm. Dieses Modell führt für schwache Wechselwirkung auf eine Luttinger-Flüssigkeit, für stärkere, repulsive Wechselwirkung gibt es einen Peierls-Übergang zu einer Ladungsdichtewelle. Um den Einfluss der effektiven Wechselwirkung auf dieses System herauszufinden, untersuchen wir zunächst deren Zusammenhang mit der Ausgangsbandstruktur. Es zeigt sich, dass wir diesen Zusammenhang unter Berücksichtigung der möglichen Teilchen-Loch-Anregungen gut verstehen können. Außerdem ergeben theoretische Betrachtungen, dass zwei Fälle zu unterscheiden sind: Für Bandstrukturen, die eine niederenergetische Anregung mit einem Impulsübertrag  $q = 0$  ermöglichen, ist ein attraktiver Beitrag durch die effektive Wechselwirkung zu erwarten, was dem gewöhnlichen Abschirmungseffekt entspricht. Wird durch die Bandstruktur hingegen eine niederenergetische Anregung mit einem Impulsübertrag  $q = \pi$  bevorzugt, ist dieser Beitrag repulsiv, die Wechselwirkung wird durch den Einfluss der hochenergetischen Bänder also sogar verstärkt. Die ctQMC-Resultate für das effektive Modell bestätigen diese Erwartung: Im ( $q=\pi$ )-Fall finden wir deutliche Hinweise für eine verstärkte Tendenz des Systems hin zur Ladungsdichtewelle. Dieser Effekt nimmt zu, wenn die Energielücke zwischen den hochenergetischen Bändern verringert wird, wird aber durch thermische Anregungen in diesen Bändern abgeschwächt, falls diese dem Fermi-Niveau zu nahe kom-

---

men.

Das bemerkenswerte Ergebnis, dass durch die Wahl der Bandstruktur sowohl Abschirmung als auch der gegenteilige Effekt, sozusagen Anti-Abschirmung, verursacht werden können, deutet darauf hin, dass eine willkürliche Einflussnahme auf die Wechselwirkung des niederenergetischen Bandes möglich ist. Im betrachteten eindimensionalen Fall könnte so etwa durch Hinzufügen von äußeren Atomketten mit passenden Eigenschaften bewusst auf das physikalische Verhalten der mittleren Kette zugegriffen werden. Um die Realisierbarkeit dieser Vorstellung zu prüfen, muss sich die Eignung unserer cRPA-Methode für realistische Systeme noch weiter bestätigen. Zu diesem Zweck wäre eine Erweiterung der Methode und des Modells auf Fermionen mit Spin wünschenswert. Weiterhin könnte im Rahmen der cRPA-Methode ein realistischerer Wechselwirkungsterm direkt aus einem Coulomb-Ausdruck berechnet werden, um damit zu prüfen, ob dieser zu einer Favorisierung der Abschirmung oder der Anti-Abschirmung führt. Schließlich ist auch die Genauigkeit der cRPA-Methode zu klären, denn um einen deutlichen Einfluß der effektiven Wechselwirkung zu erhalten müssen die hochenergetischen Bänder relativ nahe am Fermi-Niveau liegen. Dadurch ist allerdings die Angemessenheit der Aufteilung in hochenergetische und niederenergetische Prozesse nicht mehr garantiert. Eine exakte Lösung des Drei-Band-Modells zum Vergleich mit den cRPA-Resultaten wäre hierfür aufschlussreich.



## C Bibliography

- [1] Gabriel Kotliar and Dieter Vollhardt. Strongly Correlated Materials: Insights From Dynamical Mean-Field Theory. *Physics Today*, 57(3):53–59, 2004.
- [2] F. Aryasetiawan, M. Imada, A. Georges, G. Kotliar, S. Biermann, and A. I. Lichtenstein. Frequency-dependent local interactions and low-energy effective models from electronic structure calculations. *Phys. Rev. B*, 70:195104, Nov 2004.
- [3] Takashi Miyake, Kazuma Nakamura, Ryotaro Arita, and Masatoshi Imada. Comparison of *Ab initio* Low-Energy Models for LaFePO, LaFeAsO, BaFe<sub>2</sub>As<sub>2</sub>, LiFeAs, FeSe, and FeTe: Electron Correlation and Covalency. *Journal of the Physical Society of Japan*, 79(4):044705, 2010.
- [4] Takashi Miyake and F. Aryasetiawan. Screened Coulomb interaction in the maximally localized Wannier basis. *Phys. Rev. B*, 77:085122, Feb 2008.
- [5] Takashi Miyake, Ferdi Aryasetiawan, and Masatoshi Imada. *Ab initio* procedure for constructing effective models of correlated materials with entangled band structure. *Phys. Rev. B*, 80:155134, Oct 2009.
- [6] J. Schäfer, C. Blumenstein, S. Meyer, M. Wisniewski, and R. Claessen. New Model System for a One-Dimensional Electron Liquid: Self-Organized Atomic Gold Chains on Ge(001). *Phys. Rev. Lett.*, 101:236802, Dec 2008.
- [7] C. Blumenstein, J. Schäfer, S. Mietke, S. Meyer, A. Dollinger, M. Lochner, X. Y. Cui, L. Patthey, R. Matzdorf, and R. Claessen. Atomically controlled quantum chains hosting a Tomonaga-Luttinger liquid. *Nat Phys*, 7:776–780, Oct 2011.
- [8] Mitsutaka Fujita, Katsunori Wakabayashi, Kyoko Nakada, and Koichi Kusakabe. Peculiar Localized State at Zigzag Graphite Edge. *Journal of the Physical Society of Japan*, 65(7):1920–1923, 1996.
- [9] Young-Woo Son, Marvin L. Cohen, and Steven G. Louie. Energy Gaps in Graphene Nanoribbons. *Phys. Rev. Lett.*, 97:216803, Nov 2006.
- [10] M. F. Crommie. Spatially Resolving Spin-split Edge States of Chiral Graphene Nanoribbons. In *APS March Meeting Abstracts*, page 2002, March 2011.
- [11] Katsunori Wakabayashi, Manfred Sigrist, and Mitsutaka Fujita. Spin Wave Mode of Edge-Localized Magnetic States in Nanographite Zigzag Ribbons. *Journal of the Physical Society of Japan*, 67(6):2089–2093, 1998.

- [12] H el ene Feldner, Zi Yang Meng, Thomas C. Lang, Fakher F. Assaad, Stefan Wessel, and Andreas Honecker. Dynamical Signatures of Edge-State Magnetism on Graphene Nanoribbons. *Phys. Rev. Lett.*, 106:226401, May 2011.
- [13] Masatoshi Imada and Takashi Miyake. Electronic Structure Calculation by First Principles for Strongly Correlated Electron Systems. *Journal of the Physical Society of Japan*, 79(11):112001, 2010.
- [14] C. Honerkamp. Effective interactions in multi-band systems from constrained summations. *ArXiv e-prints*, December 2011.
- [15] N. Nagaoa. *Quantum field theory in condensed matter physics*. Springer, Berlin, Heidelberg, 1999.
- [16] J. Hubbard. Calculation of Partition Functions. *Phys. Rev. Lett.*, 3:77–78, Jul 1959.
- [17] J. E. Hirsch. Discrete Hubbard-Stratonovich transformation for fermion lattice models. *Phys. Rev. B*, 28:4059–4061, Oct 1983.
- [18] W. Nolting. *Grundkurs Theoretische Physik 7: Viel-Teilchen-Theorie*. Springer, Berlin, Heidelberg, 2005.
- [19] Gerald D. Mahan. *Many-particle physics*. Kluwer Academic/Plenum Publishers, New York, 2000.
- [20] John W. Negele and Henri Orland. *Quantum many-particle systems*. Advanced book classics. Westview, Boulder, CO, 1988. Addison-Wesley edition.
- [21] A. Luther and I. Peschel. Calculation of critical exponents in two dimensions from quantum field theory in one dimension. *Phys. Rev. B*, 12:3908–3917, Nov 1975.
- [22] F. F. Assaad and D. W urtz. Charge and spin structures in the one-dimensional  $t - J$  model. *Phys. Rev. B*, 44:2681–2696, Aug 1991.
- [23] F. D. M. Haldane. General Relation of Correlation Exponents and Spectral Properties of One-Dimensional Fermi Systems: Application to the Anisotropic  $S = \frac{1}{2}$  Heisenberg Chain. *Phys. Rev. Lett.*, 45:1358–1362, Oct 1980.
- [24] J. E. Hirsch, R. L. Sugar, D. J. Scalapino, and R. Blankenbecler. Monte Carlo simulations of one-dimensional fermion systems. *Phys. Rev. B*, 26:5033–5055, Nov 1982.
- [25] W. M. C. Foulkes, L. Mitas, R. J. Needs, and G. Rajagopal. Quantum Monte Carlo simulations of solids. *Rev. Mod. Phys.*, 73:33–83, Jan 2001.
- [26] Emanuel Gull, Andrew J. Millis, Alexander I. Lichtenstein, Alexey N. Rubtsov, Matthias Troyer, and Philipp Werner. Continuous-time Monte Carlo methods for quantum impurity models. *Rev. Mod. Phys.*, 83:349–404, May 2011.



- [27] H. Fehske, R. Schneider, and A. Weiße, editors. *Computational Many-Particle Physics*. Number 739 in Lecture Notes in Physics. Springer, Berlin, Heidelberg, 2008.
- [28] A. N. Rubtsov, V. V. Savkin, and A. I. Lichtenstein. Continuous-time quantum Monte Carlo method for fermions. *Phys. Rev. B*, 72:035122, Jul 2005.
- [29] F. F. Assaad. Spin, charge, and single-particle spectral functions of the one-dimensional quarter filled Holstein model. *Phys. Rev. B*, 78:155124, Oct 2008.
- [30] F. F. Assaad and T. C. Lang. Diagrammatic determinantal quantum Monte Carlo methods: Projective schemes and applications to the Hubbard-Holstein model. *Phys. Rev. B*, 76:035116, Jul 2007.
- [31] Ilja N. Bronstein, Konstantin A. Semendjajew, Gerhard Musiol, and Heiner Mühlig. *Taschenbuch der Mathematik*. Harri Deutsch, Frankfurt, 2000.



## D Danksagungen

Ich danke Prof. Fakher Assaad für die zahlreichen Denkanstöße und seine wertvollen Beiträge zu dieser Arbeit, sowie allen aus der Arbeitsgruppe für die vielen hilfreichen Gespräche und die angenehme Arbeitsatmosphäre. Weiterhin bedanke mich bei den an der Fehlerreduzierung Beteiligten für ihre direkte und indirekte Mitwirkung. Geistig-moralische Unterstützung verdanke ich den vielen freundlichen Menschen, die man in der Mensa und der Cafeteria trifft. Weiteren Dank schulde ich meinen Eltern, Maria und Gott. Das reiche hin.



# **E Eidesstattliche Erklärung**

Hiermit bestätige ich, Michael Seißinger, dass ich die vorliegende Arbeit selbstständig und nur mit den angegebenen Quellen und Hilfsmitteln erstellt habe und dass ich sie bisher oder gleichzeitig keiner anderen Prüfungsbehörde zur Erlangung eines Abschlusses oder einer benoteten Leistung vorgelegt habe.

Ort und Datum:

Unterschrift: